Type I and II IFNs modify the proteome of bacterial vacuoles to restrict infections via IRG1

Dissertation

zur Erlangung des akademischen Grades

Doctor rerum naturalium
(Dr. rer. nat.)

eingereicht an der

Lebenswissenschaftlichen Fakultät
der Humboldt Universität zu Berlin

von

Diplom - Biologe Jan Naujoks

Präsident
der Humboldt Universität zu Berlin

Prof. Dr. Jan-Hendrik Olbertz

Dekan
der Lebenswissenschaftlichen Fakultät

Prof. Dr. Richard Lucius

Gutachter

1. Prof. Dr. Bastian Opitz
2. Prof. Dr. Thomas F. Meyer
3. Prof. Dr. Bernd Lepenies

Tag der mündlichen Prüfung: 30.10.2015

ACKNOWLEDGEMENTS

The successful completion of a PhD project requires a high level of motivation, endless work and especially endurance. However, it is never the work of just someone itself but involves the hard work, creativity and strong support of many people on a work-related scientific level but also in a social context. Herewith I would like to express my deepest gratitude to all those people who directly and indirectly contributed to my work and supported me as a researcher and a person during the last years.

A PhD thesis needs a project and a place to realize it. Therefore I first of all would like to thank my supervisor, Prof. Bastian Opitz. I was fascinated by the project from the first day we met and he supported me wherever possible, was available at all times and promoted me with many challenging discussions and several opportunities to present my work at international conferences. Moreover, I would like to thank Prof. Norbert Suttorp for giving me the opportunity to perform my PhD work in the inspiring environment of the Department for Infectious Diseases and Pulmonary Medicine. I further would like to thank Prof. Thomas F. Meyer and Prof. Bernd Lepenies for agreeing to be part of my thesis committee and Prof. Andreas Herrmann for agreeing to preside over my thesis defense. I wish to acknowledge also the support I received from the International Max Planck Research School for Infectious Diseases and Immunology as part of the ZIBI Graduate School by funding me, enabling the participation in numerous interesting courses and providing an excellent framework for successfully completing a PhD project. Especially I would like to thank the former and current coordinators Dr. Susann Beetz, Dr. Martina Sick, Dr. Andreas Schmidt and Dr. Juliane Kofer for creating a familiar and welcoming atmosphere and being available and helpful at all times.

Several parts of my work required the expertise of experts in many different fields and were done in close and fruitful collaborations. I am therefore eternally grateful to Dr. Christoph Tabeling, Mareike Kunze, Andrea Peter, Dr. Stefan Kempa, Dr. Hans-Joachim Mollenkopf, Dr. Anca Dorhoi, Dr. Olivia Kershaw and Prof. Achim Gruber in Berlin, Germany, Dr. Brian Dill and PD Dr. Matthias Trost in Dundee, UK, Andrew Brown, Dr. Sammy Bedoui, Prof. Elizabeth Hartland and

Prof. Ian van Driel in Melbourne, Australia, and Dr. Christine Hoffmann and Prof. Hubert Hilbi in Munich, Germany. Furthermore I would like to thank Dr. Leif Sander for his inspiring discussions, creative ideas and encouraging support during the last years. Moreover I would like to thank all former and current members of the Opitz lab, namely Anett, Anne, Catherine, Claudia, Elena, Juan, Julia, Juliane, Oliver, Phillip, Uwe, Vincent, and Werner for scientific but also moral support, I enjoyed working in this lab at all times. Last but not least I would like to thank Birgitt, Doris and Janine for their great willingness to help wherever possible and whenever needed.

Finally, keeping up motivation and occasional distraction from every-day lab routine are inevitable to survive a PhD. Thus I most of all would like to express my deep gratitude to my dear family, Andrea and all my dear friends for always believing in me and for endless support and encouragement.

Thanks!

SUMMARY

Efficient innate defense mechanisms are the key to fight an invading pathogen early. Intracellular pathogens such as *Legionella pneumophila* have developed sophisticated mechanisms to manipulate these host cell processes and establish an intracellular niche for survival and replication. To overcome these microbial threats, host cells and host organisms as a whole have evolved a large repertoire of defense mechanisms. The balance between bacterial virulence strategies and defense pathways of the host finally determines the outcome of such bacterial encounters, resulting in microbial clearance or, in case of *L. pneumophila*, establishment of Legionnaires' disease. Much progress has been made in order to understand the initial pathogen recognition. However, the effector mechanisms that finally lead to killing of *L. pneumophila*, and other intracellular bacteria are poorly characterized.

The study presented here systemically examines the innate immune response against *L. pneumophila* on whole organism level as well as on a molecular level within macrophages, *L. pneumophila*s' host cell. *In vivo* transcriptome analyses identify type I and II interferons (IFNs) as master regulators of the early pulmonary gene expression during *L. pneumophila* infection. Infection experiments in wild-type mice and mice lacking type I and/or II IFN signaling reveal a severe defect of antibacterial defense when IFN signaling is absent. $CD11c^+$ cells were found to be the main targets of IFNs to restrict infection in the lung, and IFNs inhibited bacterial growth in $CD11c^+$ alveolar macrophages *ex vivo*. Subcellular quantitative mass spectrometry shows that both IFNs substantially modify the protein composition of *Legionella*-containing vacuoles. Comparative network analysis, combining these proteome data with transcriptome data as well as public database data reveals distinct subsets of transcriptionally regulated IFN-stimulated genes (ISGs) on the one hand, but interestingly also exclusively spatially IFN-regulated vacuolar proteins. Among IFN-regulated vacuolar proteins, Immunoresponsive gene 1 (IRG1) was identified as a central effector that restricts growth of *L. pneumophila* through production of the antibacterial metabolite itaconic acid in macrophages.

Collectively, this study provides a comprehensive resource of IFN-mediated effects on gene expression and the bacterial vacuolar proteome, and uncovers a cell-autonomous defense pathway against *L. pneumophila*, which is mediated by IFNs, IRG1 and itaconic acid.

ZUSAMMENFASSUNG

Effiziente Mechanismen der angeborenen Immunabwehr sind der Schlüssel zur schnellen Bekämpfung von eindringenden Pathogenen. Intrazelluläre Pathogene, wie z. B. *Legionella pneumophila* haben ausgefeilte Mechanismen entwickelt, um Wirtszellprozesse zu manipulieren und hierdurch eine intrazelluläre Nische zum Überleben und für ihre Replikation zu schaffen. Im Gegenzug haben Wirtszellen und Wirtsorganismen ein großes Repertoire an Abwehrmechanismen entwickelt, um sich vor intrazellulären Infektionen zu schützen. Die Balance zwischen bakterieller Virulenzstrategie und der Immunabwehr des Wirts entscheidet letztlich über den Ausgang einer solchen Infektion, was entweder zur erfolgreichen Beseitigung der Pathogene oder, im Falle von *L. pneumophila*, zur Manifestation der Infektion als Legionärskrankheit führt. Für das Verständnis der initialen Mechanismen der Pathogenerkennung wurden bereits große Fortschritte gemacht. Im Gegensatz dazu sind die Effektormechanismen, die letztlich zur Abtötung von *L. pneumophila* sowie anderer intrazellulärer Bakterien führen, unzureichend verstanden.

Die hier vorgestellte Studie untersucht systematisch die angeborene Immunabwehr gegen *L. pneumophila* auf Ebene des gesamten Wirtsorganismus, sowie auf molekularer Ebene in Alveolar- und Knochenmarksmakrophagen. Mittels *in vivo* Transkriptomanalysen werden Typ I und II Interferone (IFN) als Hauptregulatoren der frühen pulmonalen Genexpression in der *L. pneumophila*-Infektion identifiziert. Infektionsexperimente in Wildtyp- und IFN-Rezeptor-defizienten Tieren offenbaren, dass Typ I und II IFNe maßgeblich die antibakterielle Abwehr gegen *L. pneumophila* vermitteln. Für die Bekämpfung der Infektion in der Lunge werden $CD11c^+$ Zellen als wichtigste Empfänger der IFN-Signale identifiziert. Des Weiteren wird durch Behandlung von $CD11c^+$ Alveolarmakrophagen mit IFNen *ex vivo* das intrazelluläre bakterielle Wachstum inhibiert. Mittels subzellulärer quantitativer Massenspektrometrie wird gezeigt, dass die Proteinkomposition der Legionellen-enthaltenden Vakuole substanziell durch beide IFNe modifiziert wird. In einer vergleichenden Netzwerkanalyse werden diese Proteomdaten mit eigenen und öffentlich zugänglichen Transkriptomdaten verglichen. Hierdurch können klar abgegrenzte Untergruppen von einerseits transkriptionell durch IFN-regulierten Proteinen sowie andererseits ausschließlich räumlich IFN-regulierten Proteinen unterschieden werden. Unter den durch IFN an der Vakuole angereicherten Proteinen wird *Immunoresponsive gene 1* (IRG1) als zentraler Effektor identifiziert, welcher das

Wachstum von *L. pneumophila* durch die Produktion des antibakteriellen Metaboliten Itaconsäure inhibiert.

Zusammenfassend stellt diese Studie eine umfassende Ressource von IFN-vermittelten Effekten auf die Genexpression sowie auf das Proteom der bakteriellen Vakuole dar und deckt einen zellautonomen Abwehrmechanismus gegen *L. pneumophila* auf, welcher durch die IRG1-abhängige Produktion von Itaconsäure vermittelt wird.

CONTENT

1 INTRODUCTION

1.1 Legionella pneumophila – *an accidental pathogen*

1.1.1 History, epidemiology and biology

In late July 1976 several veterans became sick with flu-like symptoms, including fever, chest pains, lung congestion, and tiredness, after they had attended the annually American Legion convention at the Bellevue-Stratford Hotel in Philadelphia, Pennsylvania. Within the next weeks a total of 182 cases were reported of which 147 had to be hospitalized and 29 died [1]. No laboratory test could determine the cause of the mysterious illness, which quickly became known as the Legionnaires' disease. It took more than half a year of intensive investigations until the causative agent was described as a Gram-negative bacillus finally termed *Legionella pneumophila*, reflecting its victims as well as the primarily caused disease, a severe pneumonia [2,3]. Since then lots of outbreaks had been reported with high fatality rates of up to 32%. Many of these outbreaks were associated with contaminated cooling towers, hot and cold water systems, and whirlpool spas [4]. Besides these point source outbreaks *L. pneumophila* becomes more and more recognized as one of the most common pathogens to cause community-acquired pneumonia [5–7]. Risk factors associated with *Legionella*-infection include older age, solid organ transplantation, smoking, a history of cancer or hematologic malignancies, steroid therapy, other immunosuppressive treatments, and diabetes mellitus [8]. The numbers of patients with those risk factors as well as the number of reported cases of legionellosis are increasing [9–11].

In the environment *L. pneumophila* has been detected in virtually all sources of freshwater, including lakes, ponds, and rivers. Here the facultative intracellular bacterium persists and replicates as a parasite of freshwater protozoans [12,13]. In man-made water systems *L. pneumophila* almost exclusively exists within biofilms [14], were its ability to replicate seems to also depend on the presence of a protozoan host, while they are dispensable for *L. pneumophila* persistence [15]. Human infection develops following inhalation of *L. pneumophila*-contaminated aerosols into the lung, phagocytic uptake of the bacteria and subsequent intracellular growth in permissive alveolar macrophages (Figure 1.1). Since person-to-person-transmission has never been reported, human infection is a dead end for *L. pneumophila*, a therefore accidental pathogen [3,16].

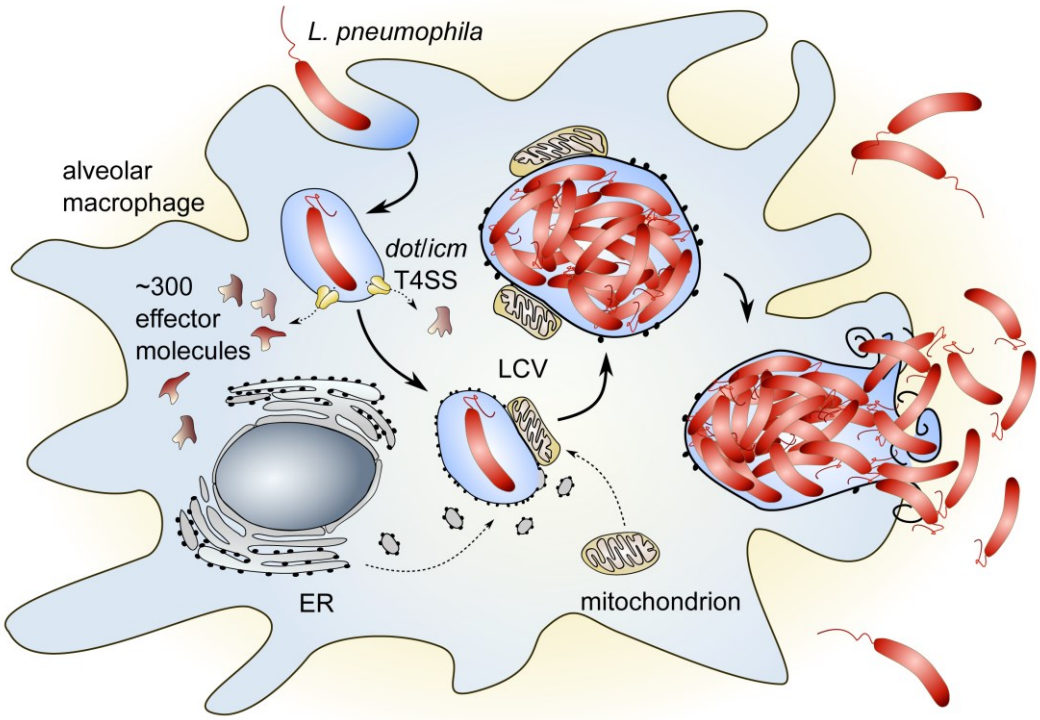

Figure 1.1 Intracellular life cycle of *L. pneumophila*. See text for detailed description.

1.1.2 The *Legionella*-containing vacuole

Most phagocytosed microorganisms are trapped within phagosomes that mature into digestive vacuoles along the endocytic pathway, a process characterized by phagolysosomal fusion, acidification and finally degradation of the vacuolar content [17]. Hallmarks of this process are the acquisition of the early and late endosomal markers Rab5 and Rab7, respectively, and finally the accumulation of further late endosomal proteins like lysosome-associated membrane glycoprotein (LAMP)-1 and cathepsin D [18–20]. *L. pneumophila*-containing phagosomes in contrast bypass this phagolysosomal pathway by utilizing a type IV secretion system (T4SS) encoded by *dot*/*icm* genes to secrete ca. 300 effector molecules into the host cell [21]. By manipulating the endolysosomal pathway and recruitment of ER-derived vesicles *L. pneumophila* creates a unique replication vacuole known as the *Legionella*-containing vacuole (LCV; Figure 1.1) [12,13,22,23]. Early recruitment of the small GTPase Rab1 and the SNARE protein Sec22b, both known to be involved in fusion events of ER-derived vesicles, as well as the appearance of resident ER proteins like calnexin are key features of the LCV establishment [24,25]. Electron microscopic studies revealed the association and fusion of ER-derived vesicles with the LCV within minutes upon phagocytosis. The LCV membrane becomes thinner

to resemble that of the closely attached ER vesicles. More and more ribosomes decorate the LCV membrane which appears to be completely comprised of rough ER within 4 to 6 h [22,26]. Remarkably, a large proportion of vacuoles were found to be close and tightly associated with mitochondria. Their function at the LCV remains, however, unknown [22,26]. The bacteria persist within this modified phagosome for 4 to 10 h without lysosomal fusion and acidification, before they start to replicate [26–29]. Until 24 h post phagocytosis *L. pneumophila* can increase in number up to 100-fold within a single large LCV (Figure 1.1 ,Figure 1.2a, b) before lysis of the host cell is initiated (Figure 1.2c) to start a new round of infection [3,22,26,30].

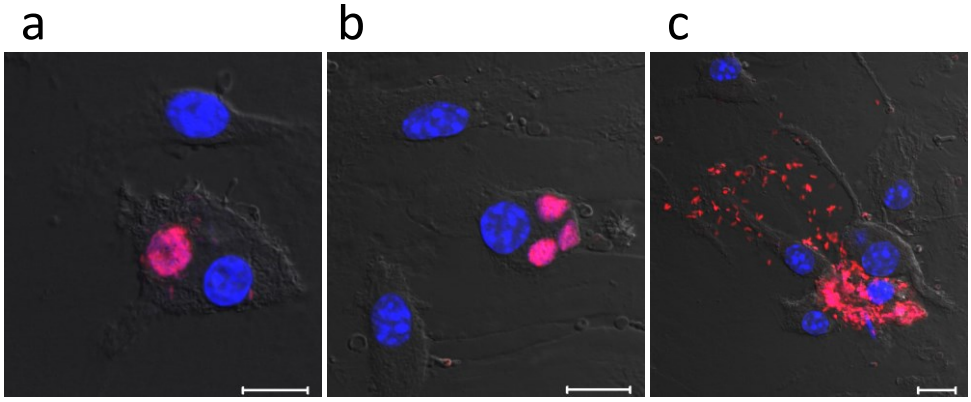

Figure 1.2 Fluorescent images of *Legionella*-containing vacuoles 24 h post infection. Bone marrow-derived macrophages (BMMs) were infected with DsRed-expressing *L. pneumophila* (red) for 24 h, fixed and nuclei stained with DAPI (blue). Cell borders were visualized by DIC microscopy (grey background). (a) A cell with a single large vacuole containing a large amount of bacteria is depicted. (b) Three individual vacuoles have formed within one single cell. (c) A large vacuole has disrupted and bacteria are released from the infected cell. Scale bar indicates 10 µm.

While intracellular pathogens such as *L. pneumophila* manipulate host cell processes in order to establish an intracellular niche for survival and replication, host cells and host organisms as a whole have evolved defense mechanisms to restrict infection. Among them, intracellular defense pathways appear to be of particular importance for fighting *L. pneumophila* pneumonia (see chapter 1.3 "Immune defense against *L. pneumophila* infection", p. 19). The balance between bacterial virulence strategies and defense pathways of the host finally determines the outcome of such bacterial encounters, resulting in microbial clearance or establishment of Legionnaires' disease.

1.2 The immune system

Multicellular organisms are continuously in close contact with microorganisms like viruses and bacteria. Many of these close associations are of benefit for both sides, like the microbiota within the human gut, providing habitat and nutrient supply to the microorganisms on the one side, and support of digestion as well as vitamin supply for the host on the other side [31]. In contrast, several other microorganisms shift this balanced co-existence in order to exploit and thereby impair the host and are therefore defined as pathogens. To counteract this process and defend themselves, multicellular organisms have evolved strategies and mechanisms to discriminate between self and non-self and to distinguish - to some extend - beneficial symbionts from pathogenic threats. In vertebrates there are two types of interconnected defense systems, the innate and the adaptive immunity. Key distinguishing feature between both are the employed types of receptors to detect the pathogen. While the innate defense relies on germ line-encoded pattern recognition receptors (PRRs) with broad specificity for highly conserved microbial patterns [32], the adaptive defense makes use of extremely diverse, randomly generated but highly specific antigen receptors [33]. Historically both types of the immune system have been viewed as an evolutionary old and primitive innate immune system and a highly developed and specified adaptive immune system. However, this might have been oversimplified since an increasing amount of data demonstrates a high degree of interdependence between both parts as well as a high level of regulatory networks to control and direct each other [34–38].

1.2.1 The innate immune system

After overcoming the host protecting mucosal barriers, invading pathogens are typically confronted with the innate immune system. Serving as the first line of defense the innate immune response is characterized by a fast initiation and comprises a collection of features, including tightly controlled antimicrobial effector-molecules that directly target and kill pathogenic microorganisms. A fundamental aspect of the innate immune system is the ability to detect molecular structures unique to microorganisms, and thereby enabling a self vs. non-self-discrimination. This recognition relies on the ability of PRRs to detect so-called pathogen-associated molecular patterns (PAMPs), although the term pathogen-

associated is in some way misleading since many PAMPs are not unique to pathogens but also common to non-pathogenic microorganisms. PAMPs are defined by three main criteria: (i) they are invariant among microorganisms of a given class, ensuring the recognition of a wide range of microbes, (ii) they are products of pathways unique to microorganisms (with few exceptions, see below) rendering them optimal for self vs. non-self-discrimination, and (iii) they have essential roles within the microbial physiology and are indispensable for their survival, limiting the ability to modify or change their characteristics in order to evade the innate immune recognition [32]. Typical bacterial PAMPs include cell wall components like lipopolysaccharide (LPS), and peptidoglycan. Nucleic acids are another group of PAMPs important for viral and bacterial detection. However, since nucleic acids *per se* are not unique to microorganisms the indispensable self vs. non-self-discrimination here is based on chemical modifications within microbial nucleic acids [39–41] or the cellular non-physiological localization of nucleic acids, e.g. within the cytosol. However, since this system is not free of mistakes, autoimmune diseases can develop when it is miss-regulated [42]. Rapidly upon host cell-pathogen contact, the PRR-PAMP interaction induces a wide variety of protective antimicrobial responses, including cell-autonomous, host cell-intrinsic mechanisms, as well as recruitment and activation of innate effector cells like neutrophils and NK cells [43–45].

Central players within the innate immune system are professional phagocytes, including macrophages, neutrophils and dendritic cells (DCs). Phagocytosis describes the process of uptake of large solid particles, including microorganisms into intracellular membrane-bound vacuoles known as phagosomes [46] and is the crucial direct and indirect first step for many innate and adaptive, respectively, immune functions. Resident macrophages serve as sentinel cells, e.g. in brain (microglia), skin (Langerhans cells), liver (Kupffer cells) and lung (alveolar macrophages) and are often the first immune cells that get into contact with invading microbes. Their primary role is to find and remove pathogens via phagocytosis followed by intracellular degradation, as well as secretion of cytokines, signaling molecules that guide the way for other immune cells to the site of infection [47–49]. Among these recruited immune cells, neutrophils are the first to arrive in large numbers. They are professional killers especially of extracellular

bacteria and fungi [50] and further amplify and modify the immune response by additional secretion of cytokines [51–54]. Besides neutrophils, monocytes are also recruited to the site of infection and are essential mediators of protective immune defense against a wide range of microbes [55]. Upon arrival they can differentiate into various macrophage or DC subsets depending on the cytokine milieu and the surrounding tissue, thereby replenishing the tissue resident cell populations and/or directly contributing to microbial clearance [55]. DCs finally link the innate and adaptive immune system and guard against infections in virtually all tissues [34]. By presenting pathogen-derived antigens in the context of major histocompatibility complex (MHC) molecules, they activate and regulate the subsequent adaptive immune response, thereby fulfilling a second highly important function of the innate immune system [35,44].

1.2.1.1 Innate detection mechanisms – inevitable first step for efficient immune responses

The key for initiation of an appropriate and efficient immune response is an early and sensitive detection of the invading microbial threat. This is achieved by a limited number of germ line-encoded receptors, the PRRs, which detect a broad spectrum of unique microbial signature molecules, known as PAMPs [43,44].

Toll-like receptors

The first identified and therefore best understood group of PRRs are the Toll-like receptors (TLRs) [56]. Belonging to the group of membrane-bound PRRs they are localized within the plasma- or endosomal membrane, thereby surveilling the cell surface as well as the phagocytosed content of endo- and phagosomes. Their respective ligands cover a broad spectrum of PAMPs ranging from LPS (TLR4) and flagellin (TLR5) to RNA (TLR3, TLR7, TLR8) and DNA (TLR9), enabling them to recognize viruses, bacteria, fungi and parasites. Upon PAMP recognition TLRs initiate a downstream signaling cascade via the adapter molecules MyD88 or TRIF and induce via the transcription factors NF-κB or IRF3 the expression of proinflammatory cytokines and type I IFNs [57].

Nod-like receptors

The second group of PRRs comprises the nucleotide-binding, oligomerization domain (NOD)-like receptors (NLRs). NLRs are a large group of PRRs defined by

a common C-terminal leucine-rich repeat (LRR) domain, a central NOD domain and an N-terminal protein interaction domain. The latter is used to further subdivide the NLRs in the five subfamilies NLRA (with an acidic transactivation domain), NLRB (with a baculovirus inhibitor of apoptosis repeat (BIR) domain), NLRC (with a caspase activation and recruitment domain (CARD)), NLRP (with a pyrin domain (PYD)) and NLRX (with an unknown domain) [58]. NLRs are cytosolic PRRs, with the mitochondrial membrane-localized NLRX1 being the only exception. Many NLRs are poorly characterized, however, the few well studied NLRs reveal already a broad spectrum of ligands and modes of action [45,58].

Among the best-understood NLRs are NOD1 and NOD2, both belonging to the NLRC subfamily. While NOD1 detects meso-diaminopimelic acid found primarily in the cell wall of Gram-negative bacteria, NOD2 recognizes the muramyl dipeptide (MDP) MurNAc-L-Ala-D-isoGln, which is conserved in peptidoglycans of Gram-positive and Gram-negative bacteria. Both subsequently signal via RIP2 and NF-kB to induce proinflammatory cytokines. Additionally, NOD1 and NOD2 were recently indicated to activate type I IFNs via the transcription factors IRF7 and IRF3, respectively, in some specific situations [58].

A further well studied and important member of the NLRs is NLRP3. NLRP3 is probably the PRR with the widest spectrum of activators ranging from PAMPs like microbial RNA and certain forms of DNA, bacterial pore-forming toxins, and the peptidoglycan derivative MDP to molecules like ATP, gout-associated uric acid crystals, aluminum salts and silica crystals [45,59]. In contrast to NOD1, NOD2 and the TLRs, NLPRP3 activation does not cause a transcriptional response but rather leads to the assembly and activation of a large hetero-multimeric protein complex called inflammasome. Besides a receptor molecule such as NLRP3, this complex often contains the adapter molecule apoptosis-associated speck-like protein containing a carboxy-terminal CARD (ASC) and the caspase-1 [60]. Activation of canonical inflammasomes culminates in the caspase-1-dependent proteolytic processing of NF-κB-dependently produced proIL-1β and proIL-18 into the mature and secreted cytokines IL-1β and IL-18, respectively. Additionally caspase-1 activation can also lead to pyroptosis, a highly inflammatory form of programmed cell death [59].

Another inflammasome depends on NLRC4, which also leads to casspase-1 activation and IL-1β secretion as well as pyroptosis. The role of ASC in this setting, however, remains elusive, since NLRC4 possesses an own CARD domain, making it possible to directly interact with caspase-1, independently of ASC [58]. Consistent with this, there had been described two modes of action for NLRC4 inflammasomes. While IL-1β processing and secretion is strongly ASC-dependent, pyroptosis is not [58]. Only recently it was demonstrated that members of the NLR family, apoptosis inhibitory protein (NAIP) gene family are necessary to confer ligand specificity to the NLRC4 inflammasome [61].

RIG-I-like receptors

The RIG-I-like receptors (RLRs) comprise only three members, retinoic acid-inducible gene I (RIG-I), melanoma differentiation-associated gene-5 (MDA-5) and laboratory of genetics and physiology 2 (LGP2), which are all cytosolic RNA sensors [62,63]. However, while RIG-I and MDA5 primarily activate the adaptor molecule mitochondrial antiviral signaling (MAVS) and subsequently the transcription factors IRF3/7 to stimulate type I IFN expression, LGP2 appears to act as a modulator of RIG-I and MDA5. RLRs play a pivotal role in detection of RNA viruses and can also contribute to the detection of AT-rich cytosolic DNA, a mechanism which involves the RNA polymerase III dependent transcription of DNA into the RIG-I ligand 5'-triphosphate-dsRNA [62].

Cytosolic DNA sensors

Cytosolic DNA sensors can be classified as a fourth group of PRRs that is defined rather by its recognized ligand than by structural similarities. Basically all members of this relatively new group of PRRs have been identified within the last 5 – 6 years, with ZBP1/DAI being an exception. Common to several of the members is the ability to induce type I IFNs via the central adapter and sensor molecule stimulator of interferon genes (STING) and the transcription factor IRF3 [64,65].

Recently, cGAS a fascinating new player of the intracellular DNA sensing has been identified [66]. Upon DNA binding cGAS (cGAMP synthase) synthesizes a cyclic dinucleotide called cGAMP (cyclic-GMP-AMP), which in turn serves as a direct ligand for STING to activate downstream signaling [67]. Besides STING-dependent type I IFN induction, other signaling pathways are also activated upon cytosolic

DNA detection. absent in melanoma 2 (AIM2), for example, forms together with ASC and caspase-1 an inflammasome to regulate IL-1β and IL-18 production as well as pyroptosis [64,68,69].

1.2.1.2 IFNs and their downstream signaling

Type I IFNs

Type I IFNs comprise a family of several subtypes of IFNα, IFNβ as well as some further, less well characterized IFNs and can be produced by basically all cell types. All type I IFNs share the same receptor, the ubiquitously expressed IFNα/β receptor (IFNAR), composed of the IFNAR1 and IFNAR2 subunits [70–73]. The canonical IFNAR signaling relies on the JAK-STAT pathway. Receptor binding activates Janus kinase 1 (JAK1) and tyrosine kinase 2 (TYK2) by autophosphorylation and subsequently leads to tyrosine phosphorylation of signal transducer and activator of transcription (STAT) family members, including STAT1, 2, 3, 5 in virtually all cells, as well as STAT4 and 6 in lymphocytes [71,74]. The classical IFNAR signaling pathway leads to formation of a heterotrimeric complex consisting of STAT1, STAT2 and IRF9 called IFN–stimulated gene factor 3 (ISGF3). Upon formation, ISGF3 translocates into the nucleus to bind to specific IFN-stimulated response element (ISRE) sites within the promoter region of so-called interferon stimulated genes (ISGs) and induce their expression [74,75]. IFNAR activation can also lead to the formation of STAT1 homodimers (also known as gamma-activated factor, GAF), which bind to IFNγ activated sites (GAS) within ISG promoter regions [71,74,76,77]. Additionally, STAT3 or STAT4 homodimers can mediate alternative, not-ISG-inducing signaling events downstream of IFNAR [74]. Notably, a recent report showed that a subset of ISGs can also be induced by an IFNAR2-independent binding of IFNβ to IFNAR1 alone [78] (Figure 1.3).

Type II IFN

While type I IFNs comprise a family of different IFNs, IFNγ is the only type II IFN, which is, in contrast to type I IFNs, produced only by few specialized cell types, such as NK cells and T cells [79]. It binds to the IFNγ receptor (IFNGR), a heterotetrameric complex consisting of two chains of IFNGR1 and two chains of IFNGR2 [80,81]. IFNγ-IFNGR binding activates JAK1 and JAK2, leading to

phosphorylation of STAT1, which subsequently forms a homodimeric complex known as GAF and translocates into the nucleus [79]. Here GAF binds to GAS sites in the promoter region of ISGs and induces their expression [79,82]. The potential of IFNγ to induce via IFNGR-mediated signaling the formation of ISGF3 and thereby genes possessing only an ISRE but no GAS site is, however, controversial [71,74,79] (Figure 1.3).

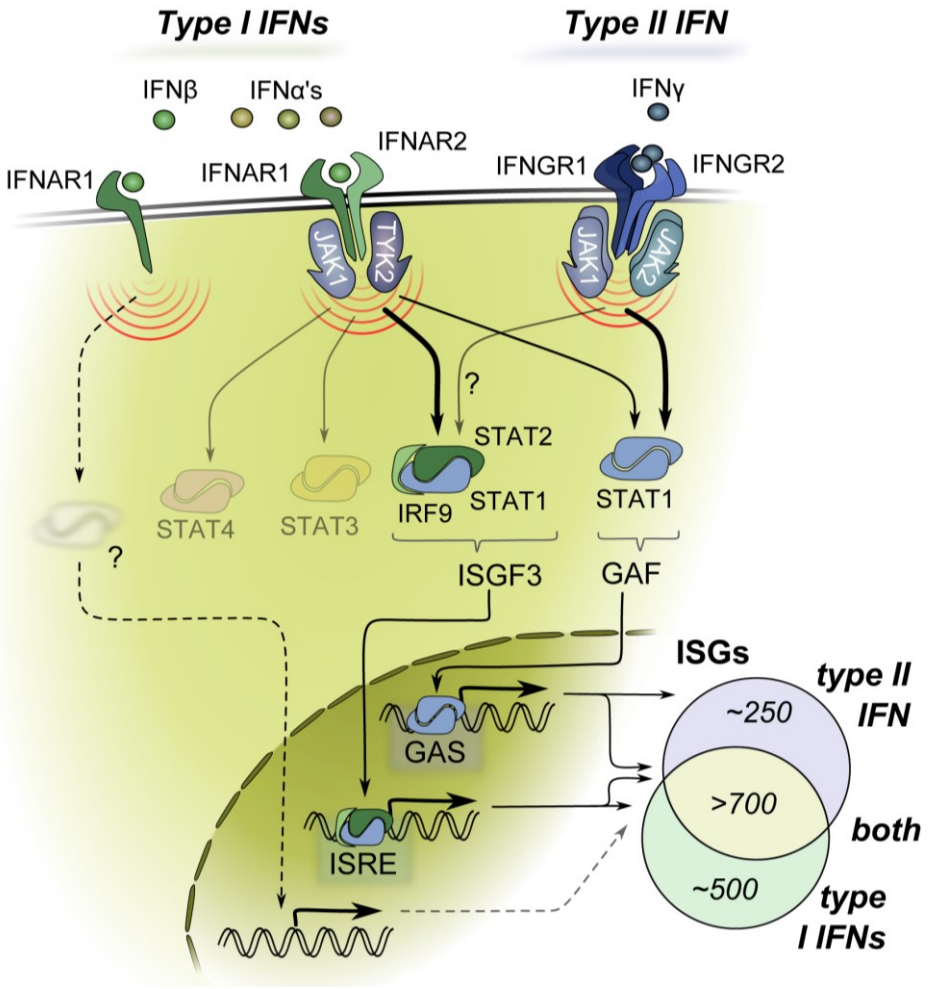

Figure 1.3 Overview of signaling cascades initiated by type I and/or II IFNs [74]. Numbers of ISGs induced by type I and II IFNs are according to the ISG database INTERFEROME and were published elsewhere [83].

In summary, a main consequence of IFN signaling, either by type I or type II IFNs, is the transcriptional induction of ISGs. However, while some ISGs are regulated by both, IFNα/β and IFNγ, others are selectively regulated by either IFNα/β or IFNγ [84].

1.2.1.3 Effector mechanisms induced by IFNs

More than half a century ago Isaacs and Lindenmann described a "new factor […] recognized by its ability to induce interference" of the growth of influenza virus in fragments of chicken chorio-allantoic membrane upon pre-treatment with heat-inactivated influenza virus [85]. This factor subsequently was termed interferon, and is today known as type I IFN. Since then, much progress has been made in elucidating the underlying mechanisms of this interfering action. Today it is well established that this relies on the stimulation of the expression of interferon stimulated genes (ISGs), a mechanism shared by type I and type II IFNs (Figure 1.3). IFNs are among the most potent modulators of gene expression and recent advancements in large scale analyses like microarray technologies led to the identification of almost 1500 genes to be positively regulated by type I and/or type II IFNs [82,83]. Interestingly, almost half of all the identified ISGs are regulated by both IFNs [83], possibly reflecting the shared and overlapping signaling pathways or alternatively, the presence of ISRE as well as GAS sites within the promoter region of many of those genes.

Traditionally type I IFNs have been associated with antiviral immunity, while type II IFN is thought to defend against non-viral pathogens. However, this differentiation might have been oversimplified [86]. Many recent large scale studies addressed the function of those ISGs and several were identified to act antiviral or being involved in pattern recognition processes [87–95]. However, the exact molecular mechanisms of most of the known ISGs remains largely unknown [82].

ISGs with antiviral function

Many type I IFN-induced ISGs have been found to contribute to anti-viral defense, including proteins of the oligoadenylate synthase (OAS) [96], IFN-induced protein with tetratricopeptide repeats (IFIT) and IFN- inducible transmembrane (IFITM) [97] families as well as virus inhibitory protein, endoplasmic reticulum-associated, IFN-inducible (viperin) [98] and ISG15 [99]. These ISGs were shown to confer host defense at various stages of viral infection and the intracellular replication cycle. While members of the OAS and IFIT families are involved in the recognition of viral nucleic acids [96,97] thereby controlling and directing subsequent steps, IFITMs are thought to interfere with viral entry and uncoating [82,97]. ISG15, an ubiquitin-like protein that can be transferred to pathogen and host proteins in an ubiquitinylation-

like process called ISGylation, can modify cellular host proteins as well as viral proteins. While ISGylation of the host protein HERC5 is thought to stabilize IRF3 and thereby augmenting the antiviral IFN signaling, direct ISGylation of viral proteins might interfere with viral assembly [82,99]. Viperin finally can interfere with host cell metabolism and signaling events, although the exact mechanisms remain elusive, but is also thought to inhibit viral assembly [82,98]. In the case of influenza virus this might be due to the disruption of ER-derived lipid rafts that transport viral envelope proteins to the plasma membrane [100].

Currently little experimental evidence exists, that these ISGs with established antiviral functions might also target intracellular bacteria or parasites. However, the fact that they are highly expressed also upon bacterial infection or stimulation with bacterial PAMPs like LPS led to the speculation that some of them might exert also antibacterial functions [97,98,101].

IFN inducible GTPases as antibacterial and antiparasitic acting ISGs

Besides ISGs with established antiviral functions, several ISGs have been found to be crucial for antibacterial and antiparasitic defense. Among those, several belong to a large superfamily of proteins known as IFN inducible GTPases. These GTPases can be further subdivided into four subfamilies namely guanylate binding proteins (GBPs), immunity-related GTPases (IRGs), myxoma (MX) resistance proteins and very large inducible GTPases (GVINs) [102]. All of which are inducible by type I IFNs, while GBPs, immunity-related GTPases and GVINs are also induced by type II IFN [102]. Several immunity-related GTPases and GBPs have well established roles in cell-autonomous defense against intracellular bacteria and parasites, including *Salmonella enterica* serovar Typhimurium (*S.* Typhimurium), *Listeria monocytogenes* and *Toxoplasma gondii*. In contrast MX proteins are known to be involved in antiviral defense, including HCV and influenza viruse [102], whereas GVINs are poorly characterized.

Immunity-related GTPases where the first IFN-inducible GTPases found to be important for defense against intracellular bacteria and parasites [103,104]. They comprise a group of proteins with approximately 47 kDa in size and are therefore also known as p47-GTPases [104,105]. Most members were found to localize to pathogen containing vacuoles ranging from bacterial phagosomes and chlamydial

inclusion bodies to protozoan parasitophorous vacuoles [102]. Partially contrasting this view, a recent report showed that IRGM1 and IRGM3 reside on "self" organelles including lipid droplets within the host cell rather than on pathogen-containing vacuoles that harbored *Chlamydia trachomatis* or *T. gondii*. While IRGM1/3 decorated lipid droplets were guarded from accumulation of other immunity-related GTPases and GBPs, IRGM1/3-stripped lipid droplets became highly affine for further immunity-related GTPase /GBP-association. IRGM1/3 are thus thought to help to discriminate "self" organelles from pathogen-containing "non-self" vacuoles that are then targeted by further immunity-related GTPases and GPBs to exert the effector function [106].

The group of immunity-related GTPases can be further subdivided into GKS- and GMS-containing immunity-related GTPases, based on their canonical (lysine-containing) and non-canonical (methionine-containing) G1 motifs within the conserved catalytic GTPase domain [107–109]. The GMS subclass in mice includes IRGM1-3, which seem to act as intrinsic regulators, that control further effector molecules including other immunity-related GTPases [82]. In contrast the GKS subclass proteins are thought to act as effector-immunity-related GTPases and may operate in a membranolytic way on pathogen-containing vacuoles, as shown for IRGA6 and IRGB10 [82]. Among the immunity-related GTPases, IRGM1 is thought to be a master regulator, a view that is supported by reports showing increased susceptibility of mice lacking IRGM1 to a broad range of pathogens, including *Mycobacterium tuberculosis*, *M. avium*, *S.* Typhimurium, *L. monocytogenes*, *C. trachomatis*, *T. gondii* and *Trypanosoma cruzi* [102].

GBPs are highly conserved throughout the vertebrate lineage and belong to the most strongly IFNγ-induced proteins [102,109]. All members of this subfamiliy are approximately 65 kDa in size and are therefore also known as p65-GTPases [108,109]. Although initially thought to be important for antiviral defense [104], many of them were shown to target to pathogen-containing vacuoles (e.g. *C. trachomatis*, *M. bovis*, and *T. gondii*) as well as directly to cytosolic pathogens (e.g. *L. monocytogenes*, *Shigella flexneri*, *S.* Typhimurium and, *Francisella tularensis* subspecies *novicida*) that have escaped their vacuole [82,110,111]. Recent reports have now demonstrated the importance of GBPs in antibacterial defense and shed some light on how GBPs mediate host resistance [112–116]. A family-wide siRNA-screen

identified GBP1, GBP6, GBP7 and GBP10 to promote cell-autonomous resistance against *M. bovis* BCG and *L. monocytogenes* in IFNγ-activated macrophages. Further functional characterization showed that GBPs might coordinate a potent oxidative program by targeting members of the NOX protein family to the vacuole which contribute to pathogen killing by production of reactive oxygen species (ROS) (see chapter "Cytotoxic gases – highly efficient but unspecific", p.16) Additionally, GBPs were shown to promote the delivery of antimicrobial peptides to autophagolysosomes, which killed mycobacteria when the *Mycobacterium*-containing vacuole fuses with these autophagolysosomes [112]. Another report demonstrated, that GBP5 is involved in assembly of the NLRP3 inflammasome, specifically in response to bacteria [114]. Also the AIM2 inflammasome was found to be GBP-dependently activated. This seemed to involve direct targeting of cytosolic *F. novicida* leading to release of bacterial DNA which then can activate AIM2 [110,111]. Furthermore, it was shown that GBPs are involved in activation of the non-canonical caspase-11 inflammasome [115,116]. This process most likely relies on GBP-mediated lysis of pathogen-containing vacuoles and thereby releasing the pathogens into the cytosol where LPS can then be directly detected by caspase-11 leading to pyroptotic cell death [116,117].

IRG1 – a long known ISG with newly described functions

Immunoresponsive gene 1 (IRG1) was first identified 20 years ago as a gene strongly induced shortly upon LPS stimulation in RAW264.7 macrophages [118]. However, except one report showing IRG1 to be highly induced by several proinflammatory stimuli like TNFα, IL-1β as well as type I and II IFNs and reporting its mitochondrial localization [119], the role of IRG1 in immune defense and its mechanism of action remained largely elusive. First evidence for a protective function of IRG1 came from studies in neuronal cells, indicating a reduced susceptibility to positive-stranded RNA viruses when IRG1 was overexpressed [120]. This was followed by another report identifying IRG1 as an enzyme that links cellular metabolism to immune defense. The enzyme was shown to decarboxylate the TCA cycle intermediate cis-aconitate into itaconic acid [121]. Itaconic acid was known for a long time to interfere with microbial metabolism by inhibiting isocitrate lyase-activity [122], an enzyme important for the glyoxylate shunt which is used by bacteria, but not animals, when growing on acetate and fatty acids as carbon

source [123]. Additionally it was shown, that *M. tuberculosis* persistence in macrophages and mice relies on isocitrate lyase-activity [124] and that *Yersinia pestis*, *P. aeruginosa* as well as other intracellular bacteria possess an operon encoding for three enzymes that are responsible for itaconic acid degradation and known to be important for pathogenicity [125]. Taken together, IRG1 seems to inhibit intracellular bacteria via itaconic acid-mediated inhibition of bacterial metabolism. Finally two groups independently found a role of IRG1 in ROS production [126,127]. The first study described a more systemically role of IRG1-dependent ROS production in LPS tolerance [126]. The second study found that IRG1 is necessary for fatty acid β-oxidation-driven mitochondrial ROS production and IRG1 depletion resulted in reduced mROS production and subsequently in defective bactericidal activity against *S.* Typhimurium [127].

Cytotoxic gases – highly efficient but unspecific

Cytotoxic gases, which include reactive oxygen and nitrogen species (ROS and RNS, respectively) are among the most ancient forms of cell-autonomous defense. They act by targeting a diverse range of pathogen- and host-derived macromolecules in a rather unspecific manner, including nucleic acids, lipids and proteins and therefore have to be tightly regulated [82].

A well-studied example of IFN-driven RNS production is the NO-synthesis via the inducible NO-synthase (iNOS). iNOS has long been known to be regulated by IFNγ [128] as well as IFNα/β [129]. NO, which is produced from L-arginine and molecular oxygen is thought to exert antimicrobial activity by direct effects on DNA including induction of mutations and inhibition of repair and synthesis, inhibition of protein synthesis, modification of proteins by S-nitrosylation, ADP-ribosylation or tyrosine nitration, inactivation of enzymes or by peroxidation of membrane lipids [130]. A relevant role for iNOS in host defense was shown for intracellular parasites like *Leishmania major* and *T. gondii* as well as intracellular bacteria including *M. tuberculosis*, *S.* Typhimurium and *L. monocytogenes*, however iNOS seems to be dispensable for defense against *L. pneumophila* infection [131]. In accordance with the well-established role in the defense against many intracellular pathogens, iNOS was shown to localize to phagosomes of internalized latex beads when macrophages were pretreated with IFNγ [132].

ROS, the second group of cytotoxic gases, are produced by different cytokine-inducible oxidoreductases, namely NADPH oxidases (NOXs), which directly catalyze the production of O_2^- and dual oxidases (DUOXs) which produce H_2O_2 [82], respectively. Recently, subunits of the NADPH oxidase have been shown to interact with the IFN-inducible GBP7 (see chapter "IFN inducible GTPases as antibacterial and antiparasitic acting ISGs", p. 13), which might act as a bridging protein to target these subunits to phagosomal membranes for NADPH oxidase assembly [112]. Additionally another ISG, IRG1, has been implicated to be involved in ROS production [126,127] and thereby contributing to antibacterial host defense [127] (see also chapter "IRG1 – a long known ISG with newly described functions", p. 15).

Cell death

IFNs can directly and indirectly regulate and modulate different forms of cell death. A IFNAR-dependent cell death has been described for many intracellular bacteria like *F. tularensis*, *S.* Typhimurium, *M. tuberculosis* and *L. monocytogenes,* which seems to be rather detrimental to the host [133]. Additionally it was shown that also viral infection-induced type I IFNs can increase apoptosis of granulocytes which leads to a defect in clearance of bacterial super-infections by Gram-positive or Gram-negative pathogens [134]. Besides apoptosis, also RIP3 kinase-dependent programmed necrosis (necroptosis) was linked to IFNAR-signaling upon stimulation with LPS, polyI:C or infection with *S.* Typhimurium [135,136]. Additionally treatment with recombinant IFNβ and IFNγ was shown to induce RIP1/RIP3-dependent necroptosis under certain conditions, e.g. when the adaptor protein Fas-associated death domain (FADD) was missing [137].

Besides these rather direct mechanisms, IFNs can contribute to host cell death also indirectly. By partially regulating the expression of inflammasome components like NLRP3, AIM2 and CASP1[137] IFNs might prime cells for subsequent inflammasome activation. Moreover, several reports demonstrate an IFN-dependent induction of AIM2-mediated cell death [110,111,138,139]. IFN-driven expression of guanylate binding proteins, which directly target intracellular *F. novicida* led to the release of bacterial DNA, the activator of AIM2 [110,111]. Additionally, non-canonical caspase-11 inflammasome-induced pyroptosis was recently linked to IFN signaling [140,141], a process that most likely involves the transcriptional regulation of caspase-11 [140] as well as the well-known

IFN-stimulated GBPs (see also chapter "IFN inducible GTPases as antibacterial and antiparasitic acting ISGs", p. 13) [115,116].

Taken together, the large number of genes regulated by IFNs leads to a highly diverse array of defense mechanisms directed by IFNs and executed by their ISGs. While the loss of single ISGs only occasionally results in severe immune defects, most likely due to compensatory mechanisms via other ISGs, the lack of the entire IFN signaling often has dramatically consequences for the host. This severe phenotype as well as the high redundancy of IFN-driven effector mechanisms highlights the particular importance of IFNs and their ISGs for the cell-autonomous antimicrobial defense.

1.2.2 The adaptive immune system

Antigen presenting cells (APCs), namely DCs and macrophages, collect invading pathogens in the periphery to present their antigens in the context of MHC molecules. They migrate into lymph nodes and the spleen where T and B lymphocytes, the main players of the adaptive immune system, reside [142]. Both cell types possess highly specific antigen receptors, according to the cell type known as B cell receptor (BCR) and T cell receptor (TCR), respectively [143]. These receptors are randomly generated out of a virtually unlimited pool and therefore can potentially recognize virtually every antigen [33]. The activated lymphocytes are then able to differentiate into several types of effector cells depending on the type of antigen (and thereby class of pathogen) they recognize [143]. However, since the antigens detected by the BCR and TCR typically lack any information about the type of pathogen they are derived from, lymphocyte differentiation relies on further instruction signals derived from the APC [35,38]. One well-known example are the MHC class I and II molecules. While antigens derived from the host cell cytosol, e.g. viral particles, are presented in the context of MHC-I and lead to the activation of $CD8^+$ cytotoxic T cells, antigens from phagocytosed extracellular pathogens are presented in the context of MHC-II to activate $CD4^+$ T helper cells. These $CD4^+$ T cells then further differentiate into Th1, Th2 and Th17 cells depending on their transcription factor expression which is again controlled by cytokines from the APC [38,143]. However, the instructional signaling is not a one way street leading from innate to adaptive cells, but goes also *vice versa*. Th1 cells for example are well

known producers of IFNγ, a cytokine with well-established functions in macrophage activation. Furthermore, Th17 cells are strong producers of IL-17, a cytokine that directs non-hematopoietic cells, including epithelial cells, to secrete chemokines that lead to neutrophil recruitment. Finally T cell derived cytokines also direct B cells to produce certain subclasses of antibodies, like Th1-derived IFNγ and Th2-derived IL-4 leading to the production of IgG2 and IgE, respectively [142].

1.3 Immune defense against L. pneumophila *infection*

As an accidental pathogen typically residing and replicating within freshwater protozoans there has been no selection pressure on *L. pneumophila* to establish mechanisms to evade the mammalian immune system. Nevertheless *L. pneumophila* is perfectly adapted to an intracellular life style also within alveolar macrophages since they share many features with amoeba, *Legionella*'s natural host. Within these alveolar macrophages *L. pneumophila* is then well hidden and protected from a broad range of immune defense strategies.

1.3.1 Innate immunity to *L. pneumophila* infection

After infection, *L. pneumophila* is recognized by several transmembrane and cytosolic pattern recognition receptors that cooperatively mediate protective immune responses [144]. The transmembrane Toll-like receptors (TLRs) 2, -5, and -9 detect bacterial cell wall components, flagellin and unmethylated CpG-rich DNA, respectively [145–149]. These TLRs stimulate the production of several NF-κB-dependent cytokines such as TNFα which contribute to resistance of mice towards *L. pneumophila* infection [150–153]. Several studies demonstrated that mice deficient in TLR2 and the other above mentioned TLRs alone or in different combinations have defects in the defense against *L. pneumophila* compared to wild-type mice [146,147,150,153–155]. The cytosolic NOD-like receptors (NLRs) NOD1 and NOD2 are activated by *Legionella* peptidoglycan that might get access to the cytosol through the T4SS, and mice deficient in both NLRs or in the shared signaling mediator RIP2 show impaired neutrophil recruitment and attenuated bacterial clearance during pneumonia [156,157].

Other cytosolic sensors of *L. pneumophila* in macrophages are the canonical NAIP5 and NLRP3 inflammasomes and the non-canonical caspase-11-dependent inflammasome. Different alleles of NAIP5 have long been known to determine whether a mouse is resistant or (moderately) susceptible to *Legionella* infection [158,159]. NAIP5 forms together with the NLR molecule NLRC4 the NAIP5 inflammasome, which can additionally contain the adapter molecule ASC and caspase-1 [160–164]. This multi-protein complex is activated by T4SS-mediated translocation of flagellin and mediates growth restriction of wild-type but not flagellin-deficient *L. pneumophila* in macrophages of most mouse strains (e.g. C57BL/6). This is dependent on the caspase-1-mediated cell death called pyroptosis and on enforcement of the phagolysosomal pathway leading to an enhanced fusion of LCVs with lysosomes [164–168]. Another canonical inflammasome that is activated by *L. pneumophila* and additionally controls IL-1β and IL-18 production consists of NLRP3, ASC and caspase-1, although its function in controlling infection *in vivo* might be less important [169,170]. Furthermore, *L. pneumophila* stimulates a cytosolic non-canonical caspase-11-dependent inflammasome depending on its T4SS [141,169,171]. The exact mode of action of this inflammasome and its molecular components are ill-defined. Upon *L. pneumophila* infection of macrophages, the caspase-11 inflammasome contributes to the NLRP3 inflammasome-mediated IL-1β production and cell death, and stimulates a NLRP3-independent cell death and IL-1α release [141,169,171]. Moreover, caspase-11 has been indicated to stimulate fusion of LCVs with lysosomes [172]. Thus, different inflammasomes are important mediators of the macrophage-intrinsic defense against *L. pneumophila*.

The innate immune response to *L. pneumophila* is further shaped by translational inhibition and biasing to favor production of some proinflammatory mediators [173,174]. This translational regulation is dependent on the T4SS and possibly on some effector proteins and/or on an effector protein-independent inhibition of the mTOR pathway [174].

The function of neutrophils in *Legionella* infection is incompletely understood. Recruitment of neutrophils to the lung during infection is dependent on TLR- and NOD1/2-dependent chemokine production [156], and on release of IL-1α as well as IL-1β by hematopoietic cells [175], activation of IL-1R and production of chemokines by non-hematopoietic cells [176]. *Legionella spp*. appear to be resistant to neutrophilic

killing [177,178], but antibody-mediated depletion of neutrophils impairs clearance of *L. pneumophila* from the lung at later time points [52]. This might be related to production of cytokines such as IL-18 by neutrophils which together with IL-12 activate NK cells to produce the host protective type II IFN (IFNγ) [53,151]. IFNγ activates macrophages to restrict *L. pneumophila* replication and mice lacking IFNγ or its receptor IFNGR are highly susceptible towards *L. pneumophila* infection [179–181]. Yet, the identity of the responsible antibacterial factors and their modes of action in *L. pneumophila* infection are still unknown (Figure 1.4).

Besides neutrophils and NK cells, pDCs have been demonstrated to make important contributions to the restriction of *L. pneumophila* infection in mice [182]. These cells were recruited during infection, and depletion of pDCs significantly reduced bacterial clearance from the lung. Interestingly, although pDCs are well known for their ability to produce type I IFNs upon viral infection, the protective effect of pDCs on *L. pneumophila* infection is independent of these cytokines [182].

1.3.1.1 Production of type I IFNs in *L. pneumophila* infection

In addition to the above mentioned pathways, *L. pneumophila* infection of macrophages is also detected by the recognition of bacterial nucleic acids in the host cell cytosol, and restricted by subsequently produced type I IFNs (Figure 1.4). It has previously been shown that host cells infected with *L. pneumophila* produce type I IFNs [183,184]. This response requires bacterial uptake and expression of the bacterial T4SS, but is independent of bacterial replication and the *IcmS*-dependently translocated bacterial effector proteins [183–185]. Although the sensor molecule is still unknown, several lines of evidence suggest that bacterial DNA is the molecule that is detected in the host cell cytosol and triggers type I IFN production. First, intracellular delivery of purified *Legionella* DNA into macrophages stimulates a similar type I IFN production as infection with viable bacteria [184,185]. Second, type I IFN responses to *L. pneumophila* are dependent on the T4SS, and the T4SS has been shown to conjugate DNA to recipient bacteria [186]. Third, digestion of *Legionella* extracts with DNAse (but not RNAse or proteinase) inhibited their ability to induce IFNβ expression [184,185]. Fourth, the expression of the T4SS effector molecule *SdhA* negatively correlates with both, *Legionella* DNA release into the host cell cytosol and type I IFN responses [187–189]. Fifth, *L. pneumophila*-induced

type I IFN production is significantly reduced in macrophages after gene-silencing of STING [185]. STING is an ER-anchored molecule that serves as a key adapter protein for most cytosolic DNA sensing pathways [190,191]. These cytosolic DNA sensor molecules include cyclic-AMP-GMP synthase (cGAS), DAI, IFI16, DDX41 and RNA polymerase III/RIG-I [66,192–196]. While DAI is not involved [197], and the function of RNA polymerase III/RIG-I is controversial [189,193] the role of the other DNA sensors in *L. pneumophila*-induced type I IFN responses needs to be examined.

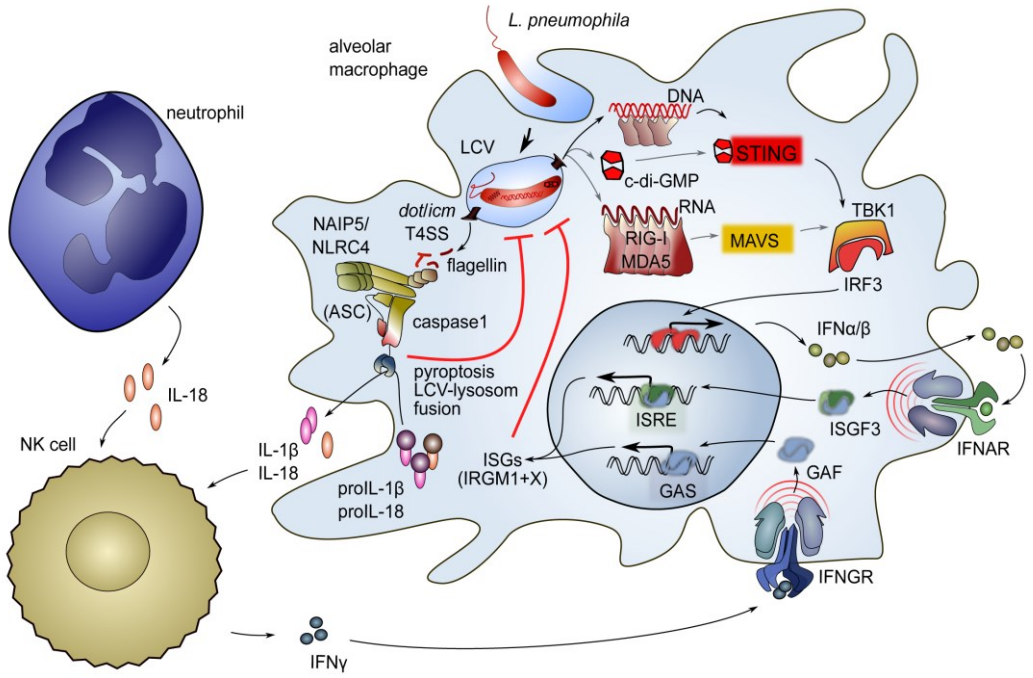

Figure 1.4 Overview of innate immune defense mechanisms against *L. pneumophila* with focus on type I and II IFNs, as well as the NAIP5/NLRC4-inflammasome. See text for detail.

In addition to DNA, detection of other bacterial molecules might contribute to stimulation of type I IFN responses during *L. pneumophila* infection. For example, *Legionella* second messenger molecules such as the cyclic dinucleotide c-di-GMP might also be involved in triggering STING-dependent innate immune responses, as STING also serves as receptor for c-di-GMP and c-di-AMP [198,199]. Indeed, a recent study found that the amount of IFNβ expression in macrophages positively correlated with c-di-GMP levels in *L. pneumophila* [200]. Moreover, one study indicated that recognition of *Legionella* RNA by the cytosolic RNA receptors RIG-I and MDA5 stimulated type I IFN response in macrophages [189]. Downstream of the sensor and adapter molecules, the kinase TBK1 and the transcription factor IRF3 are required for stimulating type I IFN responses to *L. pneumophila* [183,184].

1.3.1.2 Function of type I IFNs in *L. pneumophila* infection

The first evidence for a host-protective function of type I IFNs in *L. pneumophila* infections came from a study showing that IFNβ treatment inhibited growth of *L. pneumophila* in permissive murine A/J macrophages. Furthermore, addition of inhibitory anti-IFNα/β antibodies allowed bacterial growth in otherwise restrictive cells [201]. Subsequently, it was shown that inhibition of IRF3 expression by RNAi, and thus suppression of type I IFN production, resulted in enhanced *L. pneumophila* replication in human cells. The enhanced bacterial replication in IRF3-depleted cells could be reversed by treatment of the cells with exogenous IFNβ [183]. Similarly, mouse macrophages deficient in IRF3 or IFNAR allowed bacterial replication, whereas wild-type macrophages from C57BL/6 mice inhibited wild-type *L. pneumophila* replication [185,202,203]. These studies together show that endogenously produced type I IFNs act in an autocrine/paracrine fashion to activate a macrophage-intrinsic antibacterial defense pathway that restricts *L. pneumophila*. Importantly, recombinant IFNβ inhibited the growth of flagellin-deficient *Legionella* in wild-type macrophages, indicating that the type I IFN-mediated antibacterial defense acts independently of the flagellin-detecting NAIP5 inflammasome [185]. Whereas activity of both pathways (NAIP5, type I IFN) efficiently suppresses bacterial replication, functional defects in either pathway allow for substantial growth of *L. pneumophila* in macrophages.

The mechanism of the type I IFN-mediated cell-autonomous resistance pathway is still incompletely understood but appears to act after LCV establishment, as it does not interfere with the trafficking of the LCV [185]. Recent results further indicate that the type I IFN-mediated resistance pathway affects bacterial numbers in replication vacuoles by activating bacterial killing [185]. This pathway most likely involves the IFN-stimulated GTPase IRGM1 and other genes that are type I IFN-dependently up-regulated in *L. pneumophila*-infected cells [185].

During intranasal infection of mice with *L. pneumophila* Δ*flaA*, type I and II IFNs appear to play a partly redundant role. Whereas mice deficient for the IFNGR have impaired bacterial clearance from the lung compared to wild-type mice, mice lacking type I IFN signaling show no defect [185]. Importantly, however, mice lacking receptors for both type I and II IFNs have a strongly enhanced bacterial load after

infection as compared to mice lacking IFNGR only [185]. Moreover, type I and II IFNs contribute to expression of IFN-stimulated genes in the lung during infection. Whereas some genes are dependent on either type I or II IFNs, others such as IRGM1 are regulated by both types of IFNs [185]. Although further investigations are required, it appears reasonable to assume that both types of IFNs stimulate defense against *L. pneumophila* through expression of antibacterial acting proteins that possibly locate to the LCV. Considering the partly redundant effects of the type I and II IFNs on *L. pneumophila* infection *in vivo*, these antibacterial acting proteins are possibly induced by both types of IFNs although IFNγ may have a stronger inducing activity.

1.3.2 Adaptive immunity to *L. pneumophila*

First evidence for a relevant role of adaptive immune mechanisms in defense against *L. pneumophila* came from studies with T cell depleted mice [204]. Here it was observed that in untreated wild-type mice, pulmonary clearance of *L. pneumophila* occurred not before T cell recruitment into the lungs, and depletion of $CD4^+$ and $CD8^+$ T cells impaired bacterial clearance and increased mortality [204]. Another study showed that mice were protected from a lethal dose of *L. pneumophila* when they, prior to infection, received DCs overexpressing the T cell chemoattractant CX3CL1 (Fractalkine) and pre-incubated with heat-killed *L. pneumophila*. This was completely abolished when $CD4^+$ and $CD8^+$ T cells as well as B cells were depleted [205]. One important role of $CD4^+$ T cells might be the production of IFNγ. IFNγ levels increase dramatically upon infection [204] and bone marrow-derived DCs and macrophages were able to stimulate IFNγ production in $CD4^+$ T cells *in vitro* [206,207]. However, a main source of IFNγ in *L. pneumophila* infection might be NK cells [53].

Besides T cell mediated mechanisms also B cell derived antibody responses seem to be important, since *L. pneumophila*-induced antibody production and increased clearance of antibody-opsonized *L. pneumophila* were reported [208,209]. Furthermore, it was demonstrated that antibody-opsonized *L. pneumophila* are phagocytosed via a Fcγ receptor-dependent pathway leading to lysosomal degradation of the bacteria, a mechanism that subverts *L. pneumophila*'s evasion of the phagolysosomal fusion [210].

1.4 Aim of this study

Upon infection, many intracellular pathogens establish characteristic membrane-bound compartments within macrophages, where they resist lysosomal degradation [12,211]. Such specialized vacuoles provide a growth niche with access to cellular nutrients while protecting the bacteria from humoral immune responses. As a result of co-evolution, however, host cells have developed sophisticated strategies to target the vacuoles or the bacteria inside in order to control infections [82,212]. IFNs are among the most potent stimulators of those cell-autonomous resistance mechanisms. Yet, the molecular mechanisms of the IFN-induced, macrophage-intrinsic antibacterial defense pathways remain incompletely understood.

The aim of the present study was the systematic examination of the IFN-dependent antibacterial innate immune response to *L. pneumophila* infection by a combination of transcriptome and subcellular quantitative proteome analyses using *in vivo*, *ex vivo* and *in vitro* infection models.

2 RESULTS

2.1 *Type I and II IFNs are key regulators of early gene expression in* L. pneumophila *infection in vivo*

In order to identify master regulators of the innate immune response to intracellular bacteria, gene expression in the lungs of *L. pneumophila*-infected and sham-treated C57BL/6 wild-type (WT) mice was compared 2 days post infection (d p.i.). 1526 genes were found to be induced upon infection. To find the upstream regulators capable of inducing these genes, an upstream regulator analysis using Ingenuity Pathway Analysis (IPA) was performed (Figure 2.1a). This analysis predicts that type I and II IFNs and their related transcription factors such as STAT1 play a predominant role in controlling early gene transcription in response to *L. pneumophila* infection (Figure 2.1b). This *in silico* prediction was confirmed by transcriptome analysis of *L. pneumophila*-infected *Ifnar*$^{-/-}$, *Ifngr*$^{-/-}$ and *Ifnar*/*Ifngr*$^{-/-}$ mice, all of which showed a severely impaired transcriptional response compared to WT animals (Figure 2.1c).

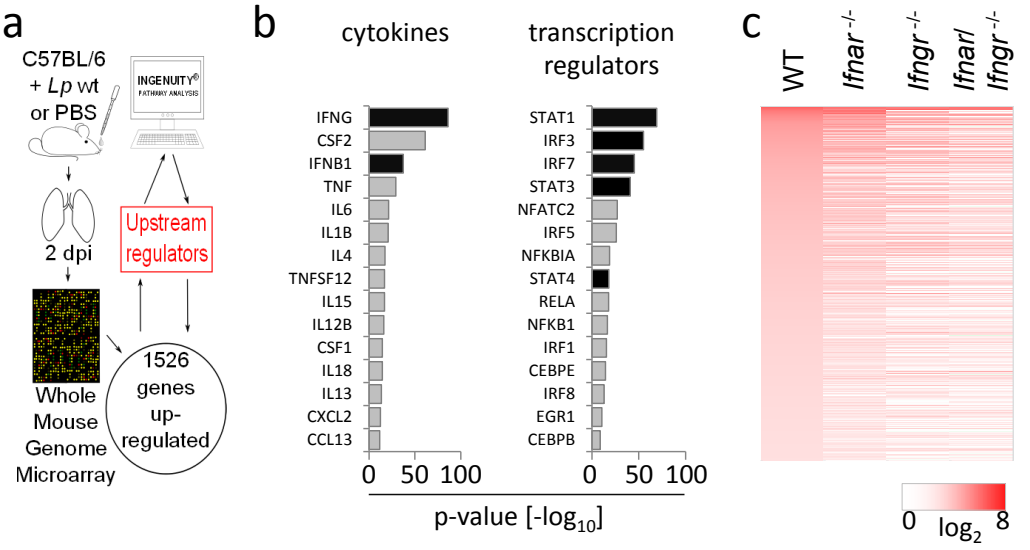

Figure 2.1 Type I and II IFNs are key regulators of the early gene expression during *L. pneumophila* infection *in vivo*. (a) Overview of the workflow for upstream regulator analysis depicted in (b). (b) WT mice were intranasally infected with 1×10^6 *L. pneumophila* wt or treated with PBS. Mice were sacrificed on day 2 p.i., total RNA was isolated from whole lungs and mRNA microarray analysis was performed. Genes found to be significantly up-regulated (> 2-fold change, $p < 0.05$) in *L. pneumophila* infected WT mice compared to PBS controls were analyzed for their predicted upstream regulators using Ingenuity Pathway Analysis (IPA). Black bars highlight molecules with established functions in type I and/or type II IFN signaling. (c) WT, *Ifnar*$^{-/-}$, *Ifngr*$^{-/-}$ and *Ifnar/Ifngr*$^{-/-}$ mice were intranasally infected with 1×10^6 *L. pneumophila* wt or treated with PBS. Mice were sacrificed on day 2 p.i., total RNA was isolated from whole lungs and mRNA microarray analysis was performed. Heatmap displays the 1526 genes significantly up-regulated in *L. pneumophila*-infected compared to PBS-treated WT mice. (5 mice per group, pooled for RNA isolation; ratio of infected versus PBS-treated mice for respective strain is depicted).

2.2 *Type I and II IFNs mediate antibacterial immunity during* L. pneumophila *infection in the lung*

To investigate the relevance of the type I and II IFN pathways individually and in combination for their role in antibacterial defense against *L. pneumophila*, bacterial clearance following *L. pneumophila* infection of WT, *Ifnar*$^{-/-}$, *Ifngr*$^{-/-}$ and *Ifnar*/*Ifngr*$^{-/-}$ mice was analyzed. Whereas WT, *Ifnar*$^{-/-}$ and *Ifngr*$^{-/-}$ mice were able to clear or strongly reduce bacterial burdens by day 6 p.i., bacterial loads remained high in *Ifnar*/*Ifngr*$^{-/-}$ mice (Figure 2.2a). This persistently high pulmonary bacterial load in *Ifnar*/*Ifngr*$^{-/-}$ mice was accompanied by high neutrophil counts in the blood and lung (Figure 2.2b, c).

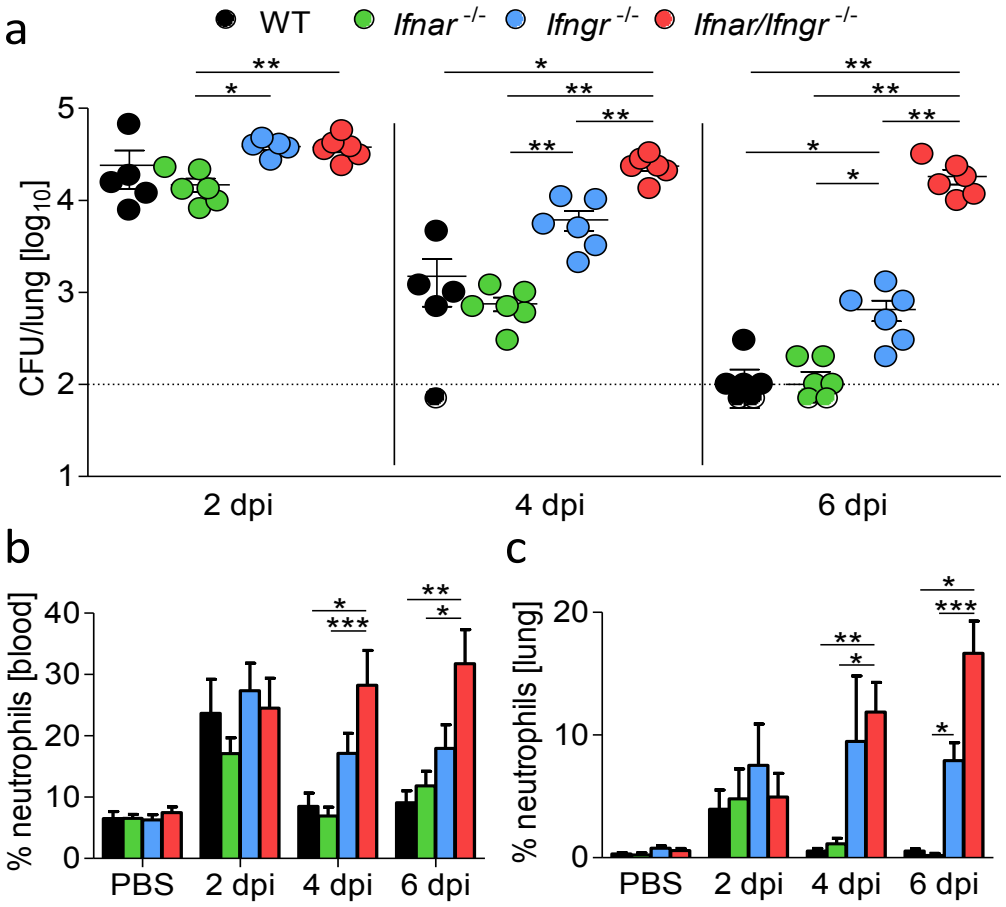

Figure 2.2 Type I and II IFNs mediate host-protective immune response during *L. pneumophila* infection *in vivo*. WT, *Ifnar*$^{-/-}$, *Ifngr*$^{-/-}$ and *Ifnar/Ifngr*$^{-/-}$ mice were intranasally infected with 1×10^6 *L. pneumophila* wt or treated with PBS. Mice were sacrificed on day 2, 4 or 6 p.i. and bacterial loads in lungs were determined (dotted line indicates lower detection limit) (a). Neutrophils in the blood (b, percent of total leukocytes) and in the lung (c, percent of total lung cells) were determined by flow cytometry (b) and manual differentiation of May-Grünwald-Giemsa-stained cytospin preparations from lung homogenates (c), respectively. Data represent mean + s.e.m. of 5-6 mice per group. * $p<0.05$, ** $p<0.01$, *** $p<0.001$ (Kruskal-Wallis analysis of variance followed by two-tailed Mann-Whitney U test with Bonferroni correction for multiple comparisons (a) or Dunn's multiple comparison (b,c)).

The continuing neutrophil influx led to highly inflamed lung tissue in those animals after infection with either *L. pneumophila* wt or Δ*flaA* (Figure 2.3a). Defective innate host defense and exacerbated pneumonia were further evidenced by a continued weight loss in *Ifnar*/*Ifngr*$^{-/-}$ mice until day 8 p.i. with *L. pneumophila* wt or Δ*flaA* (when most likely an effective adaptive immune response is initiated) (Figure 2.3b, c). All other mice (WT, *Ifnar*$^{-/-}$, *Ifngr*$^{-/-}$) exhibited early bodyweight loss, probably reflecting the acute inflammatory response, but rapidly recovered their bodyweight after infection. Together, these data indicate that type I and type II IFNs are critical regulators of the early gene expression and the antibacterial innate immune response during *L. pneumophila* infection.

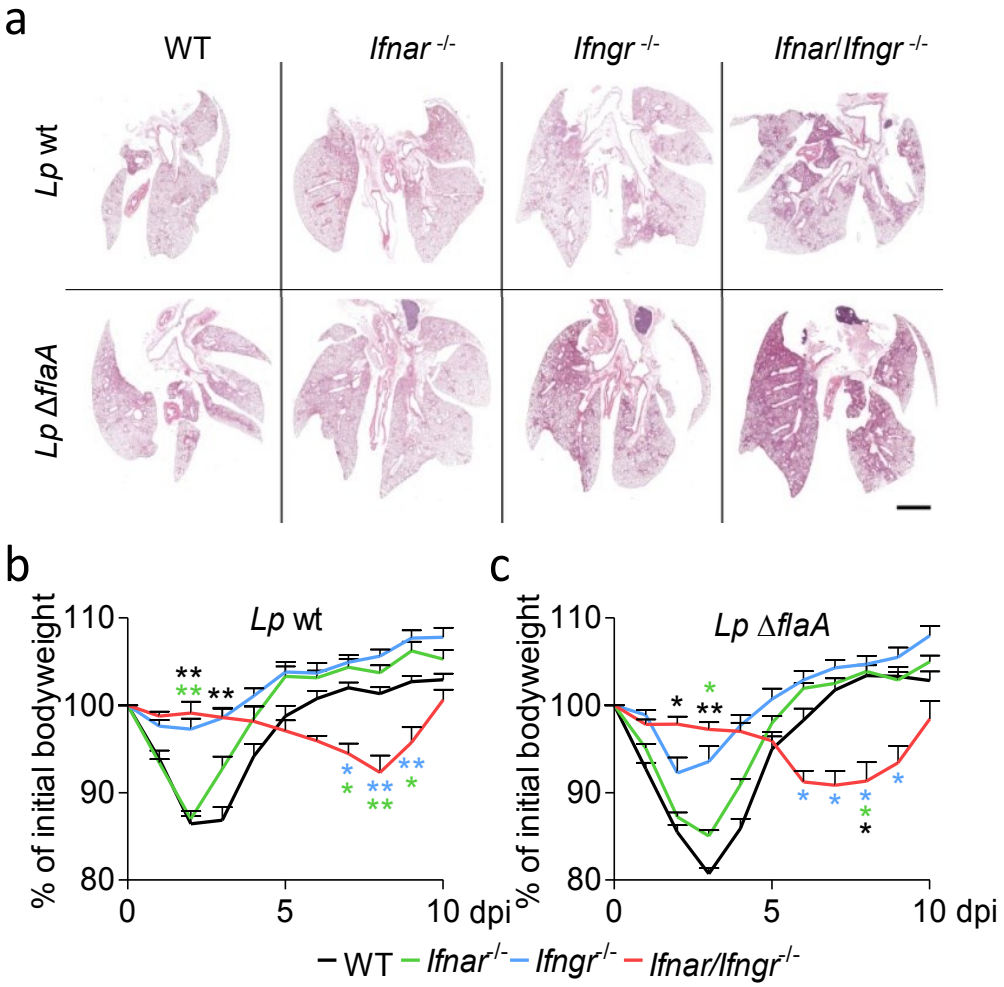

Figure 2.3 Lack of type I and II IFN signaling results in highly inflamed lung tissue and delayed but prolonged bodyweight loss during *L. pneumophila* infection *in vivo*. WT, *Ifnar*$^{-/-}$, *Ifngr*$^{-/-}$ and *Ifnar/Ifngr*$^{-/-}$ mice were intranasally infected with 1 × 10^6 (a) or 1 × 10^7 (b, c) *L. pneumophila* wt or Δ*flaA*. (a) Mice were sacrificed 6 d p.i. and histopathology of lungs was analyzed by hematoxylin and eosin staining (representative images of 4 mice per group, scale bar indicates 2 mm). (b, c) Bodyweight of infected mice was determined over time. Data represent mean + s.e.m. of 10 mice per group. * $p<0.05$, ** $p<0.01$, *** $p<0.001$ (two-way ANOVA followed by Bonferroni posttest).

2.3 *An alveolar macrophage-intrinsic antibacterial defense pathway is activated by IFNs to restrict* L. pneumophila *infection*

Alveolar macrophages, but not dendritic cells (DCs), are thought to be the primary cell type supporting *L. pneumophila* infection *in vivo* [213–215]. To test whether the protective role of IFNs during *L. pneumophila* infection was mediated at the level of an alveolar macrophage-intrinsic defense pathway, a mouse model in which IFN signaling was selectively abrogated in alveolar macrophages and DCs, which both express CD11c was examined (Figure 2.4).

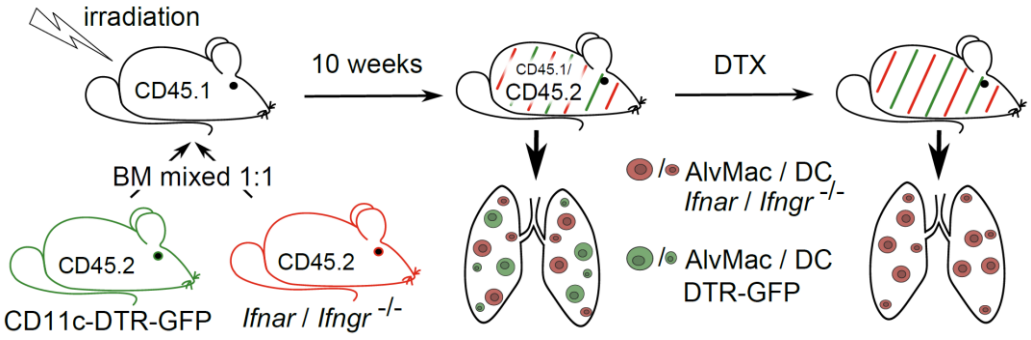

Figure 2.4 Overview of the generation of mixed bone marrow chimeric mice and the subsequent diphtheria toxin (DTX) mediated depletion of CD11c$^+$ DTR-GFP expressing cells.

To this end CD45.1$^+$ mice were lethally irradiated and reconstituted with a 1:1 mixture of CD45.2$^+$ bone-marrow cells from *Ifnar*/*Ifngr*$^{-/-}$ and CD11c-DTR-GFP mice (expressing the diphtheria toxin receptor (DTR) under the control of the CD11c promoter). Repopulation was assessed to be > 90% after 10 weeks (Figure 2.5a). Treatment with diphtheria toxin (DTX) depleted CD11c$^+$ GFP$^+$ DTR-expressing cells in the lung (Figure 2.5b), generating mice in which all CD11c$^-$ cell types express the type I and II IFN receptors, whereas only CD11c$^+$ cells (alveolar macrophages and DCs) were unresponsive to IFNs. First, only bone-marrow-chimeric mice which showed highly efficient DTX-mediated depletion of CD11c$^+$ GFP$^+$ DTR-expressing cells (with < 10% remaining, Figure 2.5c) were examined. Strikingly, chimeric mice lacking the IFN receptors in CD11c$^+$ cells were unable to clear *L. pneumophila* wt infection (Figure 2.5d), phenocopying mice lacking IFN signaling in all cell types (Figure 2.2a), whereas bacterial burdens were reduced in the control animals. Second, when analyzing all mice repopulated with *Ifnar*/*Ifngr* $^{-/-}$ and CD11c-DTR-GFP cells including those showing a weak depletion

of CD11c$^+$ GFP$^+$ cells (Figure 2.5c), a significant negative correlation between remaining CD11c$^+$ GFP$^+$ cells (expressing IFN receptors) and pulmonary bacterial load was observed (Figure 2.5e). Given that dendritic cells do not support *L. pneumophila* growth [213,214], these data strongly suggest that IFNs directly activate *Legionella*-containing alveolar macrophages to restrict intracellular infection.

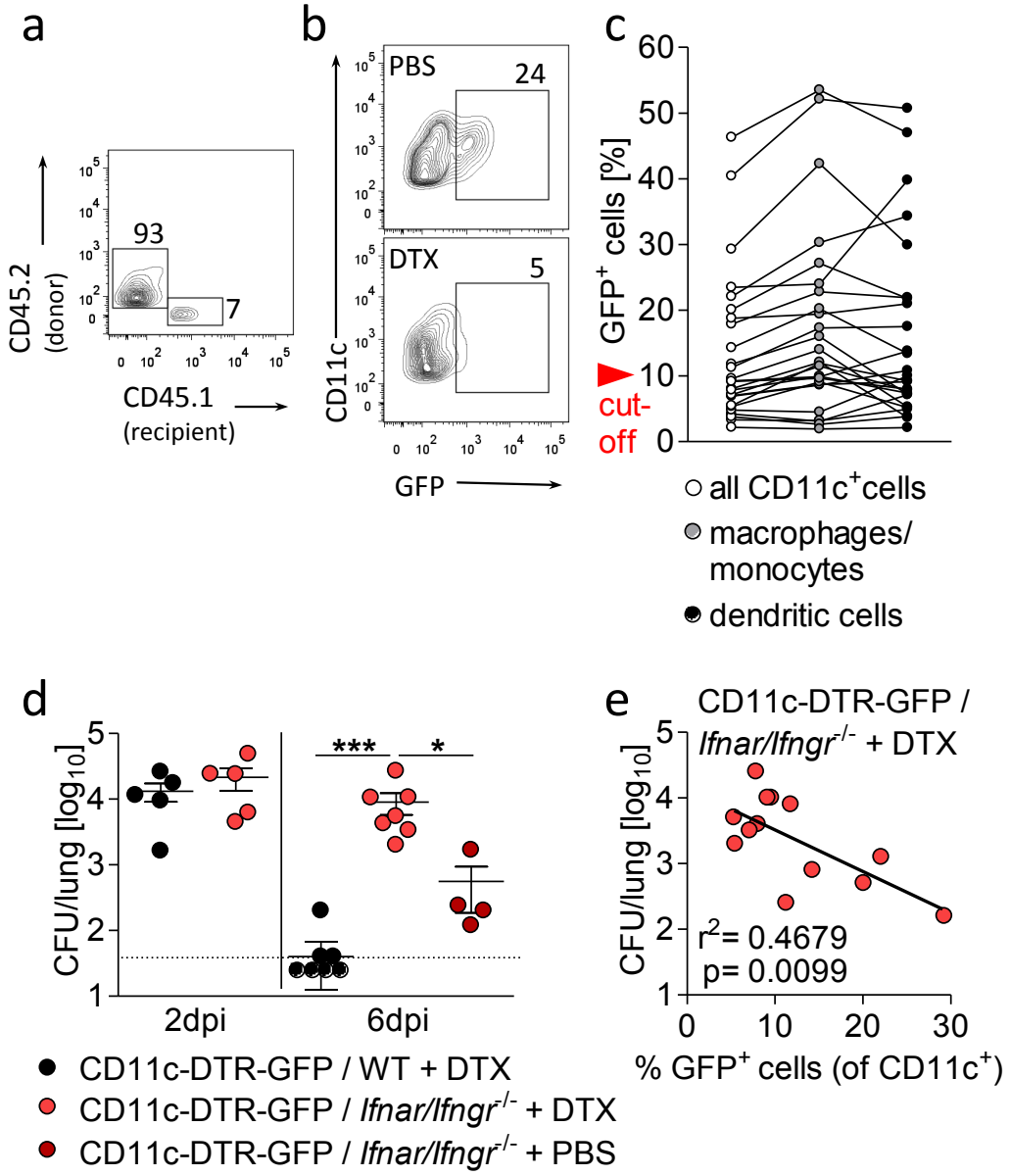

Figure 2.5 Type I and II IFNs restrict *L. pneumophila* infection through a cell-intrinsic mechanism within CD11c$^+$ cells in the lung. CD45.1 recipient mice were lethally irradiated and repopulated with a 1:1 mixture of bone-marrow cells from CD45.2 transgenic CD11c-DTR-GFP and *Ifnar*/*Ifngr*$^{-/-}$ or WT donor mice. (a) Repopulation with CD45.2 donor cells within CD45.1 recipient mice was assessed by flow cytometry of whole lung cells (representative dot plot). (b, c) diphtheria toxin (DTX) mediated depletion of CD11c$^+$ GFP$^+$ DTR-expressing cells was assessed by flow cytometry of whole lung cells (representative dot plots). (c) Total CD11c$^+$ (CD45$^+$ CD11c$^+$) cells were further differentiated in macrophages/monocytes (CD45$^+$ CD11c$^+$ SiglecF$^+$/CD64$^+$) and dendritic cells (CD45$^+$ CD11c$^+$ CD64$^-$ SiglecF$^-$ MHC-II^{hi}). Only mice with < 10% GFP$^+$ (of all CD11c$^+$ cells) were considered for analysis depicted in (d). (d) Bacterial load of mixed bone marrow-

chimeric mice was determined after infection with *L. pneumophila* wt (4-7 mice per group, dotted line indicates lower detection limit). (e) Frequency of remaining $CD11c^+$ GFP^+ cells was correlated to bacterial load in the lungs of CD11c-DTR-GFP / *Ifnar*/*Ifngr* $^{-/-}$ + DTX chimeric mice including all DTX-treated mice (13 mice). * $p<0.05$, ** $p<0.01$, *** $p<0.001$, Kruskal-Wallis analysis of variance, Dunn's multiple comparison (d), Pearson correlation (e).

To further analyze the IFN-driven antibacterial mechanism, primary alveolar macrophages from WT, *Ifnar*$^{-/-}$, *Ifngr*$^{-/-}$ and *Ifnar/Ifngr*$^{-/-}$ mice were isolated and purity confirmed by flow cytometry analysis (Figure 2.6a).

In line with the conclusion that the IFN-dependent effect observed *in vivo* relies on alveolar macrophages, *L. pneumophila* Δ*flaA*, which is able to replicate in B6 WT alveolar macrophages due to evasion of the NAIP5/NLRC4-mediated restriction [164,165,167,168], is partly or completely, respectively, inhibited by IFNβ or IFNγ treatment (Figure 2.6b). Conversely, *Ifnar*$^{-/-}$ and *Ifnar*/*Ifngr*$^{-/-}$ alveolar macrophages supported replication of otherwise growth-restricted *L. pneumophila* wt (Figure 2.6c). These data indicate that endogenously produced type I IFNs control bacterial growth, whereas type II IFN is not relevant in this *ex vivo* model since alveolar macrophages hardly produce IFNγ (data not shown). Collectively, these data strongly suggest that *L. pneumophila* infection is controlled by an IFN-mediated alveolar macrophage-intrinsic mechanism.

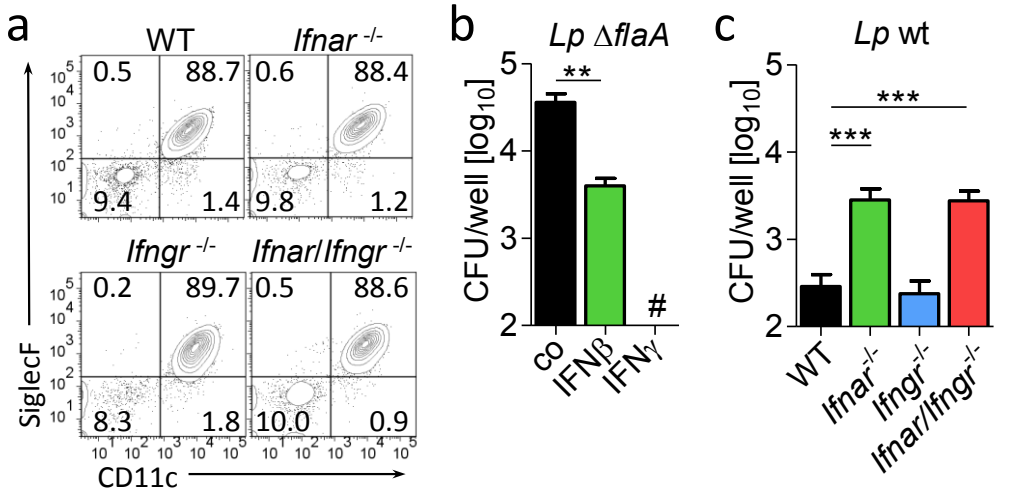

Figure 2.6 Primary alveolar macrophages restrict *L. pneumophila* replication upon activation by IFNs. Alveolar macrophages of WT, *Ifnar*$^{-/-}$, *Ifngr*$^{-/-}$ and *Ifnar/Ifngr*$^{-/-}$ mice were isolated and checked for purity by flow cytometry (a); numbers adjacent to outlined areas indicate percent cells. Cells were left untreated (c) or were treated with 50 U/ml IFNβ or IFNγ (b) 16-18 h prior to and during infection with *L. pneumophila* Δ*flaA* (b) or wt (c). Bacterial growth was determined by CFU counting after 72 h. Data represent 3 independent experiments done in triplicates. * $p<0.05$, ** $p<0.01$, *** $p<0.001$ (two-tailed Mann-Whitney U test). # No bacteria were detected

2.4 *The IFN-mediated intracellular bacterial killing within macrophages is largely independent of cell death and inducible NO synthase*

To determine how macrophages restrict *L. pneumophila* upon activation by IFNs, bone marrow-derived macrophages (BMMs) were used, an easily available and frequently used cell model to study *L. pneumophila* infection [164,165,167,168,185,202]. As shown in alveolar macrophages (Figure 2.6c), treatment of BMMs with IFNβ or IFNγ restricted the growth of *L. pneumophila* Δ*flaA* (Figure 2.7a, b), which is in line with previous reports [185,202].

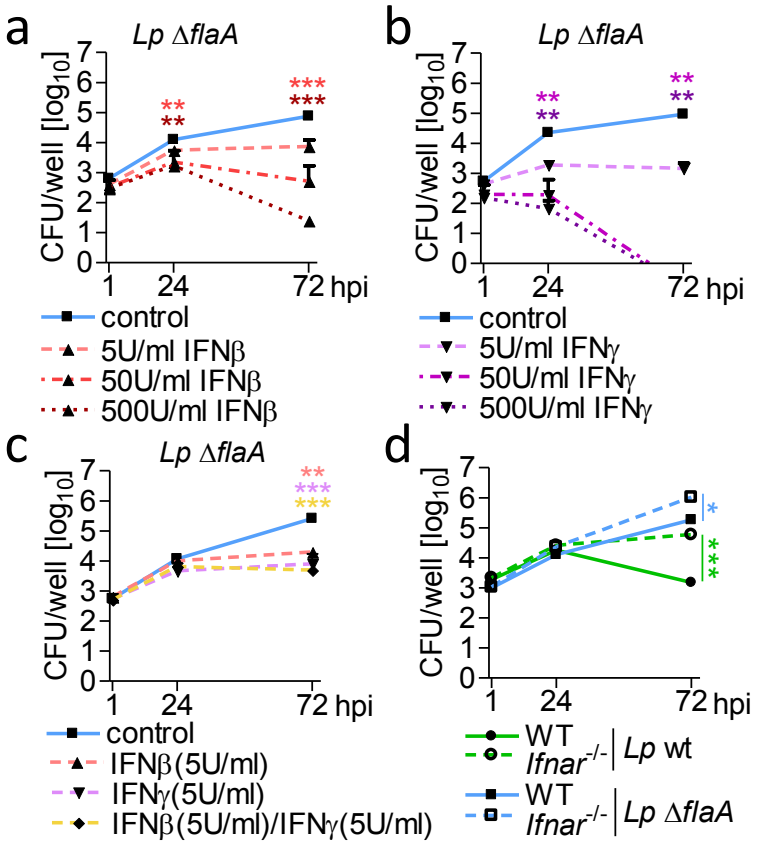

Figure 2.7 Type I and II IFNs restrict *L. pneumophila* in bone marrow-derived macrophages. (a-c) Intracellular growth of *L. pneumophila* Δ*flaA* in WT BMMs left untreated or treated with IFNβ, IFNγ or both 16-18 h prior to and during infection. (d) Intracellular growth of *L. pneumophila* wt and Δ*flaA* in WT and *Ifnar*$^{-/-}$ BMMs. Data represent mean + s.e.m. of 2 (b), 4 (c) or 5 (a, d) experiments done in triplicates. * $p<0.05$, ** $p<0.01$, *** $p<0.001$, no indication if not significant (two-tailed Mann-Whitey U test), significance was tested against untreated control (a-c) or between wild-type and knock-out cells for each condition (d).

Importantly, treatment of BMMs with suboptimal doses of both cytokines alone or in combination resulted in comparable growth inhibition (Figure 2.7c), suggesting that type I and II IFNs might activate a similar intracellular restriction mechanism. Moreover, lack of responsiveness to auto-/paracrine IFNβ in *Ifnar*$^{-/-}$ BMMs resulted in replication of otherwise growth-restricted *L. pneumophila* wt, and further enhanced the growth of *L. pneumophila* Δ*flaA* (Figure 2.7d).

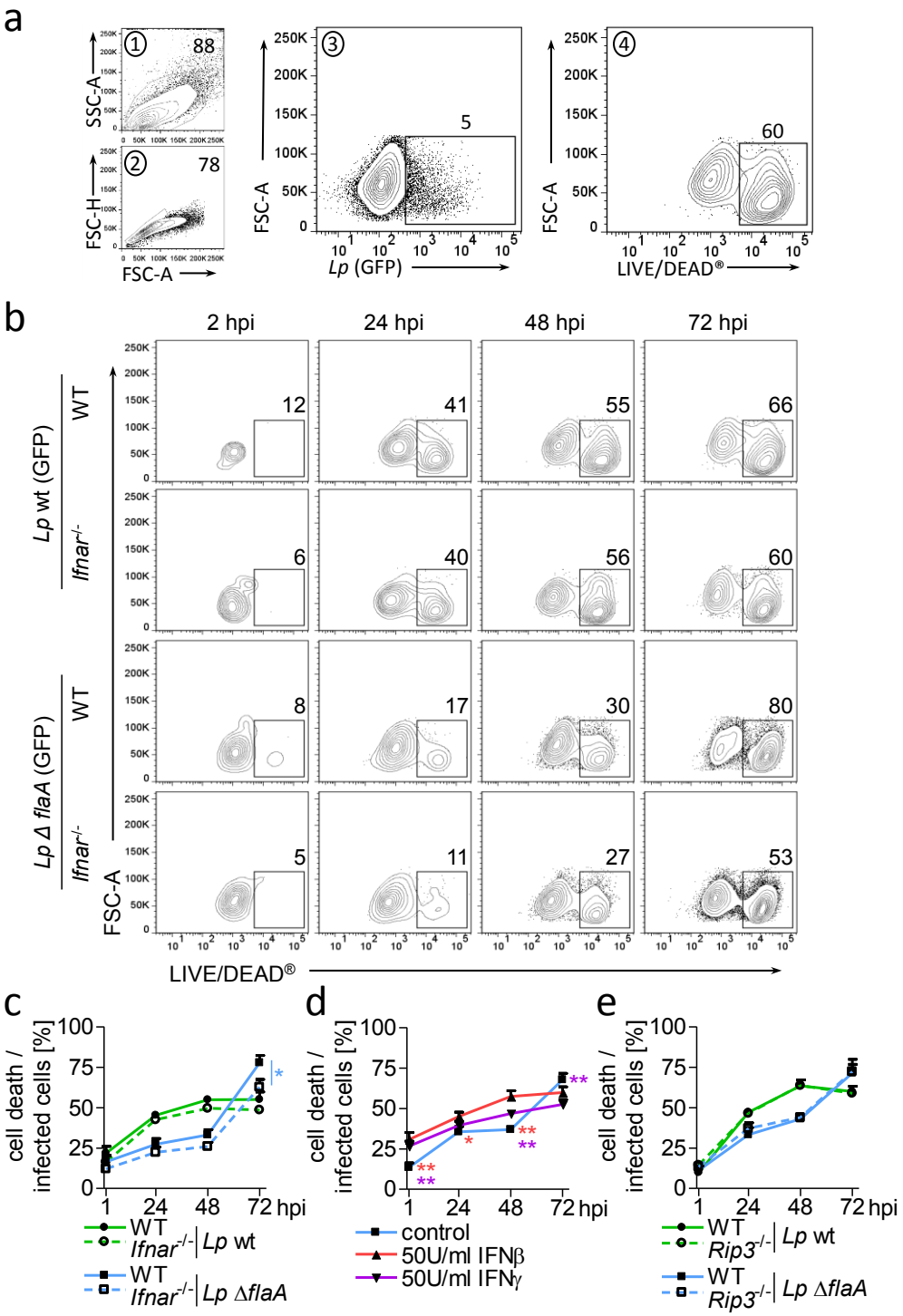

Figure 2.8 Type I and II IFNs restrict *L. pneumophila* in macrophages largely independent of cell death. Cell death of infected (GFP$^+$) cells was analyzed by flow cytometry; the gating strategy is depicted (a; encircled numbers indicate gating order). Numbers adjacent to outlined areas indicate percent cells. (b, c) Cell death in bacteria-harboring (GFP$^+$) WT and *Ifnar*$^{-/-}$ BMMs upon infection with *L. pneumophila* wt or Δ*flaA* expressing eGFP analyzed by LIVE/DEAD staining and flow cytometry. Representative blots (b) and summarized results (c) of 4 experiments done in tricplicates are shown. (d, e) Cell death in bacteria-harboring (GFP$^+$) WT IFN-treated BMMs (d), and Rip3$^{-/-}$ (e) BMMs infected with *L. pneumophila* wt or Δ*flaA* expressing eGFP was determined by flow cytometry. Data represent mean + s.e.m. of 2 (e) or 4 (c, d) experiments done in triplicates. * $p<0.05$, ** $p<0.01$, *** $p<0.001$, no indication if not significant (two-tailed Mann-Whitey U test), significance was tested against untreated control (d) or between wild-type and knock-out cells for each condition (c, e).

In order to assess whether IFNs restrict *L. pneumophila* growth by inducing cell death, e.g. via caspase-11-dependent pyroptosis or RIP3-dependent necroptosis [135,171], cell viability of BMMs infected with *L. pneumophila* was measured. To determine viability exclusively in cells that are infected and thus harbor bacteria, a flow cytometry based approach using GFP-expressing *L. pneumophila* was established (Figure 2.8a). Cell death in infected cells was minimally affected by IFN treatment (Figure 2.8d), or by the lack of IFNAR (Figure 2.8b, c) or RIP3 (Figure 2.8e). As expected, however, infection with *L. pneumophila* wt enhanced cell death compared to Δ*flaA* as a consequence of NAIP5/NLRC4/caspase-1-dependent pyroptosis [164,167,168] (Figure 2.8c, e).

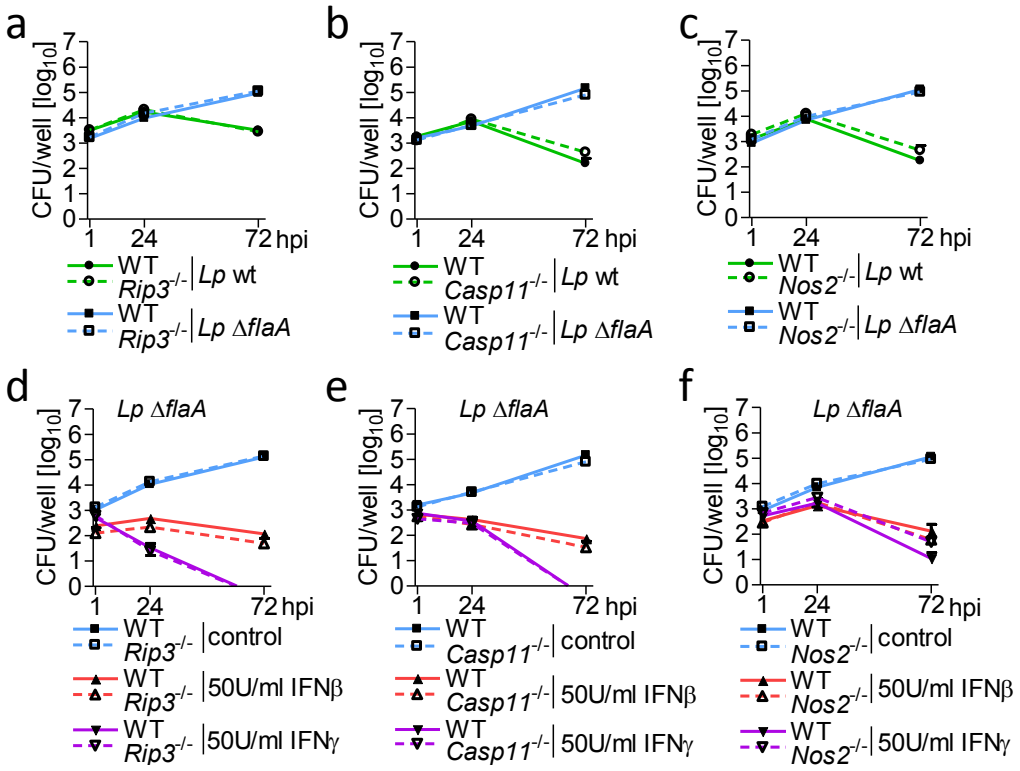

Figure 2.9 Type I and II IFNs restrict *L. pneumophila* in macrophages independently of RIP3, caspase-11 and iNOS. Intracellular growth of *L. pneumophila* wt and ΔflaA in WT, *Rip3*$^{-/-}$, *Casp11*$^{-/-}$ and *Nos2*$^{-/-}$ BMMs left untreated or treated with IFNβ, IFNγ or both 16-18 h prior to and during infection. Data represent mean + s.e.m. of 2 (a, b, d, e) or 3 (c, f) experiments done in triplicates. * $p<0.05$, ** $p<0.01$, *** $p<0.001$, no indication if not significant (two-tailed Mann-Whitey U test), significance was tested against wild-type and knock-out cells for each condition.

Furthermore, RIP3 and caspase-11 deficiency did not influence bacterial growth or its inhibition by IFNs at 24 and 72 h p.i. (Figure 2.9a, b, d, e). Another important restriction mechanism against intracellular bacteria is the production of NO via inducible NO synthase (iNOS) [130,131]. However, *L. pneumophila* wt and Δ*flaA*

replication and IFN-mediated bacterial clearance were comparable in WT and iNOS-deficient (*Nos2*$^{-/-}$) macrophages (Figure 2.9c, f). Thus, neither cell death nor production of reactive nitrogen species by iNOS appears to be critical for the IFN-mediated control of *L. pneumophila* infection.

2.5 *Subcellular quantitative proteomics reveal that type I and II IFNs markedly modify the vacuolar protein composition*

Based on previously published data [185] and the results shown above, it was hypothesized that IFNs target antibacterial effector proteins to the LCV to restrict the bacterial replication inside. In order to identify putative IFN-regulated effectors in an unbiased manner, the LCV proteome of untreated and IFN-treated macrophages was examined (Figure 2.10).

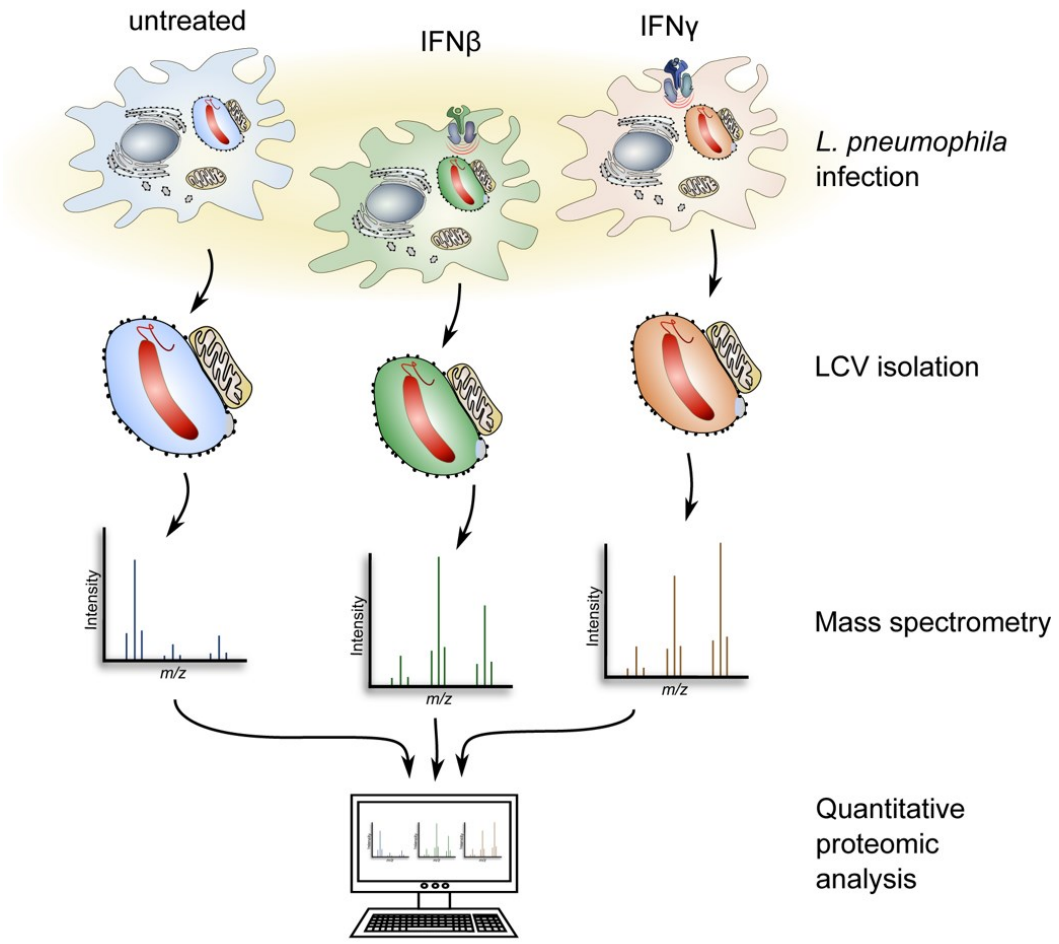

Figure 2.10 LCVs from untreated and IFN-treated BMMs are isolated and their protein composition analyzed by quantitative label-free proteomics in order to identify putative IFN-regulated effector molecules.

To this end, untreated and IFNβ- or IFNγ-treated BMMs were infected with *L. pneumophila* Δ*flaA* (to prevent NAIP5-mediated restriction), LCVs were enriched by immuno-affinity separation and density gradient centrifugation [216,217] (Figure 2.11a, b), and analyzed by label-free quantitative mass spectrometry.

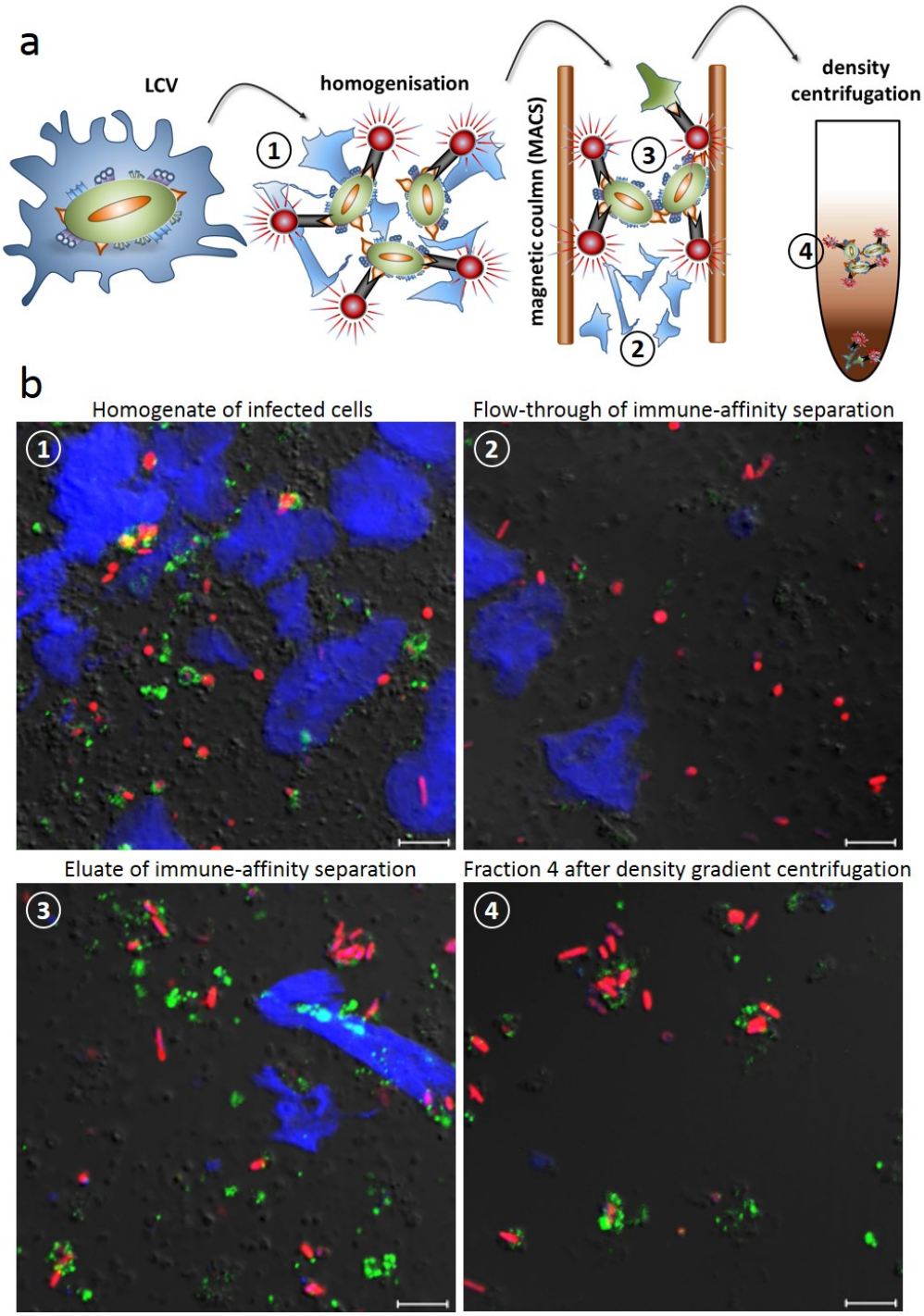

Figure 2.11 Schematic overview (a) and immunofluorescence images (b) of single steps of the immuno-affinity separation and subsequent density gradient centrifugation to isolate LCVs. Encircled numbers from (a) correspond to respective images in (b). (b) LCVs harboring red fluorescent *L. pneumophila* Δ*flaA* (red) were visualized by staining for SidC (green), a *L. pneumophila* effector protein that localizes to the surface of LCVs. Contaminating DNA and cell

debris were visualized by DAPI staining (blue) and differential interference contrast microscopy (grey), respectively. LCVs from infected BMMs were enriched in the eluate of immune-affinity separation and were further purified in fraction 4 after density gradient centrifugation (scale bar indicates 5 µm).

2854 proteins were identified in 6 of 6 samples from LCVs of untreated macrophages at a false-discovery rate (FDR) < 1%, 2307 derived from the host and 547 from the bacterium (Figure 2.12a). Computed gene ontology (GO) enrichment analysis of all identified host proteins for cellular components revealed the highest significance values for the GO terms *'membrane-bounded organelle'* ($p = 1 \times 10^{-305}$) and *'intracellular membrane-bounded organelle'* ($p = 3.55 \times 10^{-300}$). As expected [12,22], further evaluation revealed highest significance values for the *'mitochondrion'* ($p = 2.38 \times 10^{-296}$), *'endoplasmic reticulum'* ($p = 7.08 \times 10^{-100}$) and *'vacuole'* ($p = 9.67 \times 10^{-62}$) as predicted child terms of *'intracellular membrane-bounded organelle'* (Figure 2.12b).

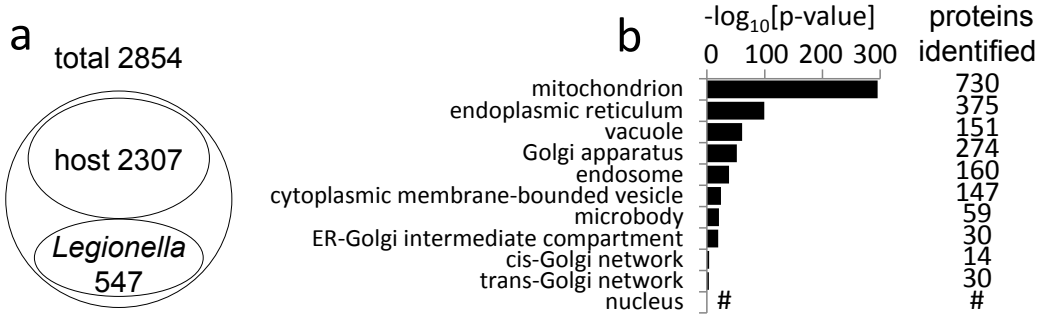

Figure 2.12 Proteomic analysis of LCVs from untreated BMMs infected with *L. pneumophila* Δ*flaA*. (a) 2854 proteins were detected in all six replicates of which 2307 were identified as host- and 547 as *L. pneumophila*-derived. (b) GO enrichment analysis for overrepresented cellular components of the host proteins was done and overrepresented child terms of GO:0043231 '*intracellular membrane-bounded organelle*' were extracted. Depicted are *p*-values for the indicated GO terms as well as the number of identified proteins annotated with each term; # no *p*-value for GO term '*nucleus*' was computed.

Additional GO enrichment analyses of biological processes indicated an enrichment of proteins involved in metabolic (e.g. *'glucose catabolic process'*, *'tricarboxylic acid cycle'* and *'fatty acid metabolic process'*), and transport and localization processes (e.g. *'ER to Golgi vesicle-mediated transport'* and *'actin cytoskeleton organization'*) (Figure 2.13).

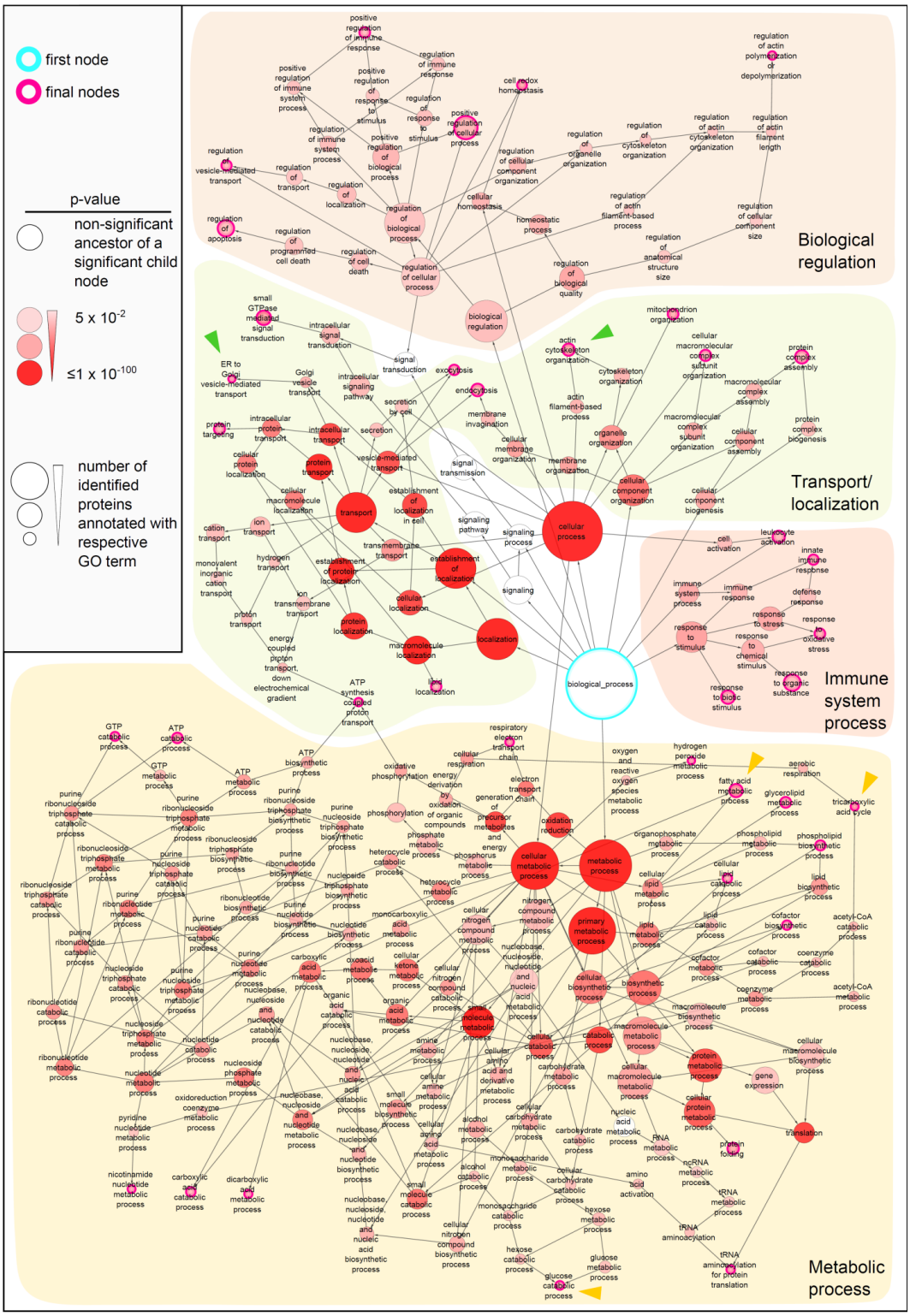

Figure 2.13 Proteins involved in metabolic processes and transport and localization are strongly enriched at LCVs. GO enrichment analysis of the 2,307 host proteins identified in untreated LCV samples for biological processes using BiNGO (Cytoscape). Hierarchical structure, read from inside (first node, blue encircled) to outside (final nodes, pink encircled). Subnetworks of highly enriched biological functions are highlighted (metabolic process, transport/localization, biological regulation, immune system process) and GO terms mentioned in the text are indicated by green and yellow triangles. Significance cut-off value for visualization was set to 10^{-10}, ancestor terms with $p > 10^{-10}$ are depicted if final child term had p-value $< 10^{-10}$.

Next, LCV proteins from IFNβ- or IFNγ-treated BMMs were compared to vacuolar proteins from untreated cells as well as to each other. Treatment with either IFN did not change the abundance of LCV marker proteins like ARF1, RAB1 and SEC22b, or ER marker proteins such as calreticulin and calnexin, nor did it lead to an enrichment of endosomal or lysosomal proteins like RAB5, RAB7, vacuolar ATPases and LAMP1 (Table 2-1). These data are in line with previously published data [185] and indicate that IFNs do not affect the trafficking of the LCV or its general composition of ER-derived material.

Table 2-1 Fold change in abundance of selected host proteins upon IFN-treatment identified by mass spectrometry on purified LCVs.

	IFNβ/untreated	IFNγ/untreated
LCV marker		
ARF1	1,7	1,7
RAB1a	1,3	1,1
RAB1b	1,0	1,1
SEC22b	1,1	1,0
ER marker		
Calreticulin	1,0	1,1
Calnexin	1,2	1,2
endosome marker		
RAB5a	1,8	1,8
RAB5b	1,5	1,7
RAB5c	1,6	1,7
RAB7a	1,2	1,2
RAB7b	1,2	1,1
endosome/lysosome		
vATPase subunit A	1,0	1,1
vATPase subunit C1	0,9	1,0
vATPase subunit G1	1,0	1,2
lysosome marker		
LAMP1	0,7	0,7
Cathepsin B	0,4	0,4
Myeloperoxidase	0,6	0,7

However, IFNβ or IFNγ treatment led to a significant ($p < 0.05$) vacuolar enrichment (> 2-fold) of 260 or 321 proteins, respectively, and to a decreased (< 0.5-fold) vacuolar abundance of 60 or 67 proteins (Figure 2.14a-f). The direct comparison between LCV proteomes from IFNβ- or IFNγ-treated cells revealed rather minor differences with many proteins being similarly regulated and only few, although distinct, proteins being differentially affected (Figure 2.15a-c). For example, RSAD2, GBP2 and IFIT1 were the three proteins with the strongest enrichment at the LCV upon both, IFNβ and IFNγ treatment (Figure 2.14d, f). Proteins that differed significantly between IFNβ- and IFNγ-treated samples included proteins involved in MHC class II-dependent antigen presentation (e.g. H2-AB1, H2-AA). Those MHC class II-associated proteins were preferentially regulated by type II IFN (Figure 2.15b, c, Figure 2.16).

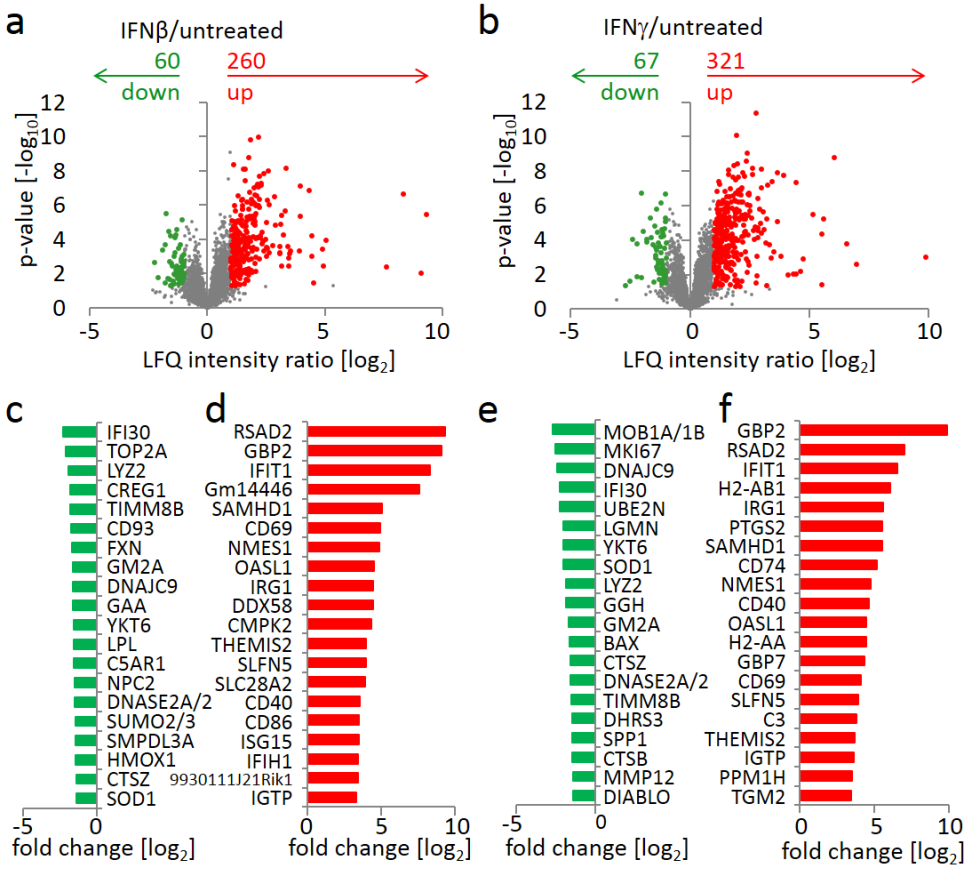

Figure 2.14 Type I and II IFNs alter the protein composition of LCVs. Quantitative proteomic analysis of LCVs from BMMs left untreated or treated with 50 U/ml IFNβ or IFNγ 16-18 h prior to infection with *L. pneumophila ΔflaA*. (a, b) Volcano plots show proteins with a significant higher (red) or lower (green) abundance at LCVs from IFNβ- (a) or IFNγ- (b) treated BMMs compared to untreated cells (LFQ = label free quantity; LFQ intensity ratio = fold change). (c-f) List of proteins with highest change upon IFNβ (c, d) or IFNγ (e, f) treatment compared to untreated samples. Proteomic analysis was done from 6 (untreated), 5 (IFNγ) and 4 (IFNβ) individual LCV isolations.

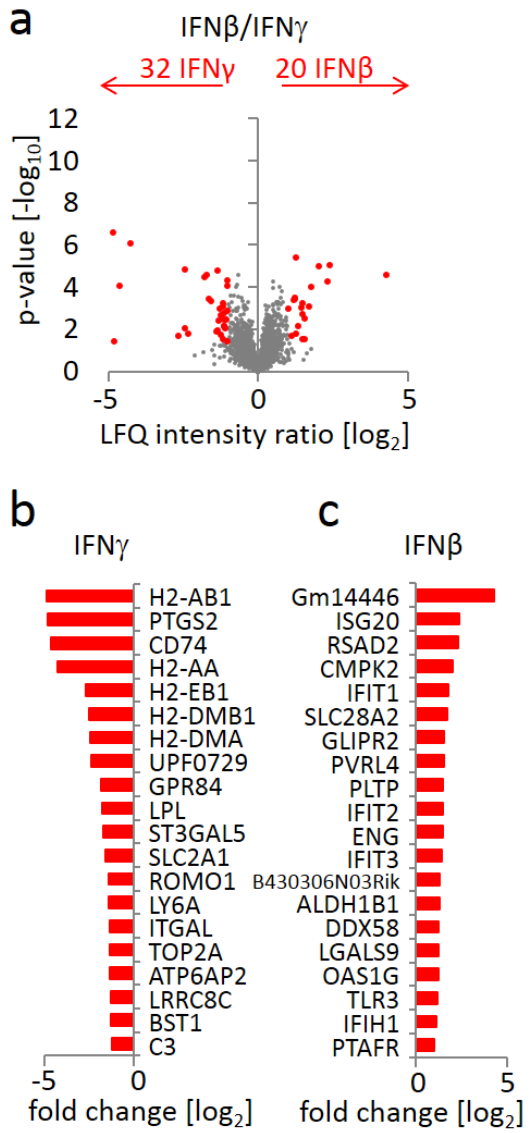

Figure 2.15 LCV proteomes from IFNβ- or IFNγ-treated cells reveal few but distinct differences in protein abundance. Quantitative proteomic analysis of LCVs from BMMs left untreated or treated with 50 U/ml IFNβ or IFNγ 16-18 h prior to infection with *L. pneumophila* Δ*flaA*. (a) Volcano plot shows proteins with a significantly different abundance at LCVs from IFNβ- and IFNγ- treated BMMs compared against each other (LFQ = label free quantity; LFQ intensity ratio = fold change). (b, c) List of proteins with higher abundance in IFNγ- (b) or IFNβ- (c) treated samples. Proteomic analysis was done from 5 (IFNγ) and 4 (IFNβ) individual LCV isolations.

Next, all proteins found to be enriched IFN-dependently at the LCV were analyzed using the database STRING (http://string-db.org), which integrates known and predicted protein interactions from different sources. This analysis generated a dense network of protein interactions, with many proteins being involved in immune response processes (Figure 2.16). These proteins included molecules contributing to DNA/RNA detection (e.g. TMEM173 [also known as STING], TLR3), ubiquitinylation/ISGylation (e.g. ISG15, TRIM25), antimicrobial defense (e.g. IRGM1, IRGM2, GBP2, GBP7, NRAMP1, IRG1), antigen processing/presentation, and the proteasome complex. Finally, the list of IFN-dependently LCV-enriched proteins was compared with the INTERFEROME database of IFN-regulated genes [218] as well as own transcriptome data. Importantly, this analysis revealed distinct subsets of IFN-regulated proteins (Figure 2.16). Whereas several LCV-enriched proteins are also transcriptionally induced by IFNs and thus represent *bona fide* ISGs, others such as Psmc1-6 or Psmd1-3 are not directly transcriptionally regulated but appear spatially affected by IFNs. Taken together, these data demonstrate that IFNs markedly modify the protein composition of LCVs, and that some of the proteins targeted to the vacuole might be spatially, rather than directly transcriptionally, regulated by IFNs.

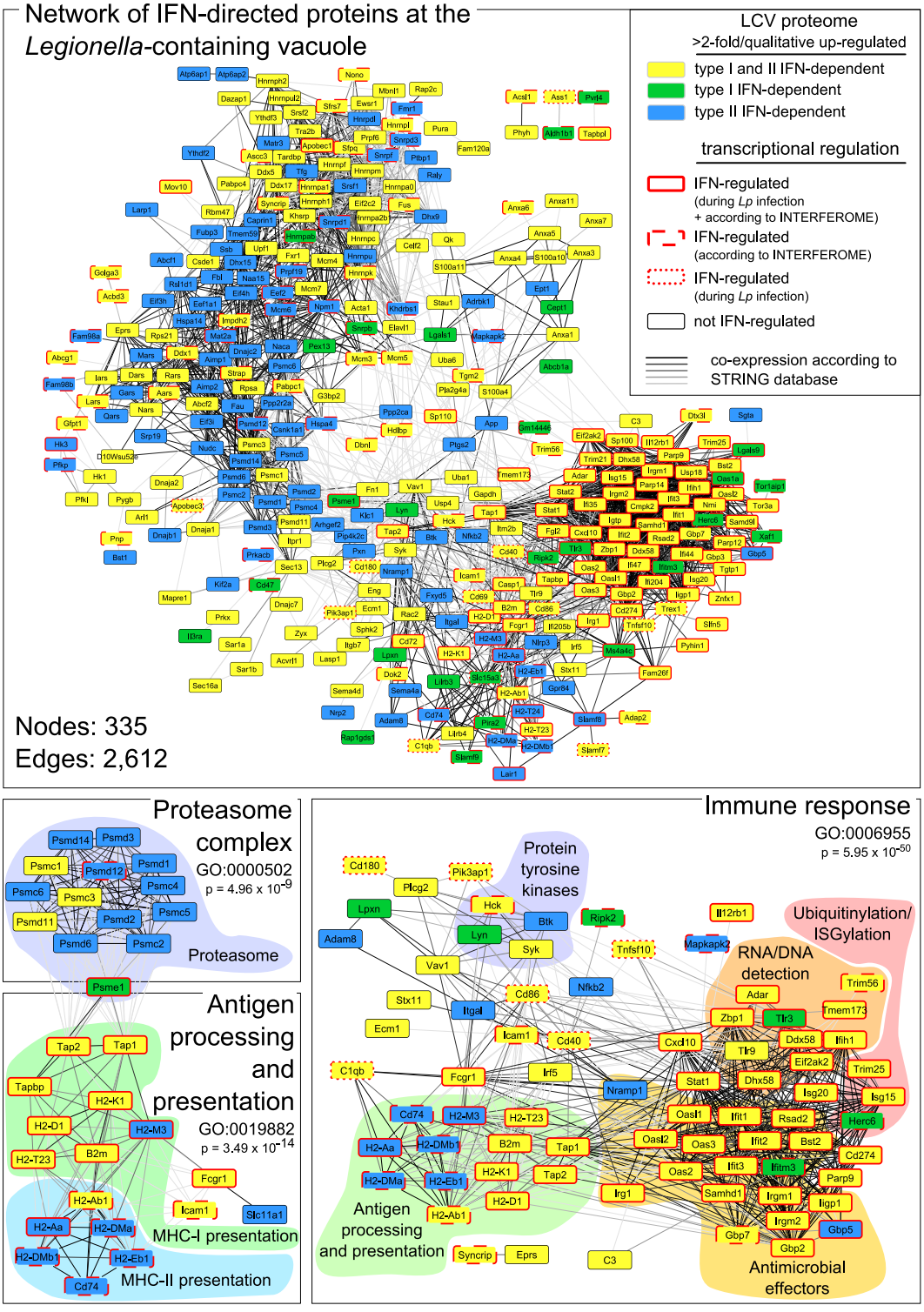

Figure 2.16 Integrated network analysis of IFN-regulated proteins of the LCVs. Proteins with higher abundance at LCVs from IFNβ- and/or IFNγ-treated compared to untreated cells were analyzed with the STRING database. The proteome data were further compared with the whole genome microarray data (compare Figure 2.1c; > 2-fold higher expressed in infected WT vs. *Ifnar*/*Ifngr*$^{-/-}$ mice) and the INTERFEROME database to indicate molecules which are also transcriptionally regulated by IFNs. A GO enrichment analysis was performed for extracting significant subnetworks of a complex network composed of 335 nodes and 2,612 edges. Shown are subnetworks positively affected by IFNβ and/or IFNγ activation such as *'immune response'*, *'antigen processing and presentation'* and the *'proteasome complex'*.

2.6 *IRG1 restricts* L. pneumophila *replication within the vacuole*

Next, it was assessed whether the proteins identified by quantitative proteomics as enriched at the LCV upon IFN treatment were involved in restricting bacterial growth. Considering the partly redundant functions of type I and II IFNs in restricting *L. pneumophila* infection (Figure 2.2a, Figure 2.7c), analyses particular focused on proteins that were most strongly targeted to the LCV by both types of IFNs. BMMs were first transfected with a pool of two siRNAs for each of the candidate molecules as well as IFNAR1 as a control, and efficient gene silencing was verified (Figure 2.17a). It was found that silencing the expression of IRG1 enhanced replication of *L. pneumophila* wt to a similar extent as silencing of IFNAR1 and thereby the entire type I IFN signaling (Figure 2.17b). Silencing THEMIS2, GBP3 and GBP7 also augmented the bacterial growth of *L. pneumophila* to some extend compared to control siRNA, while the other tested candidates had no effect.

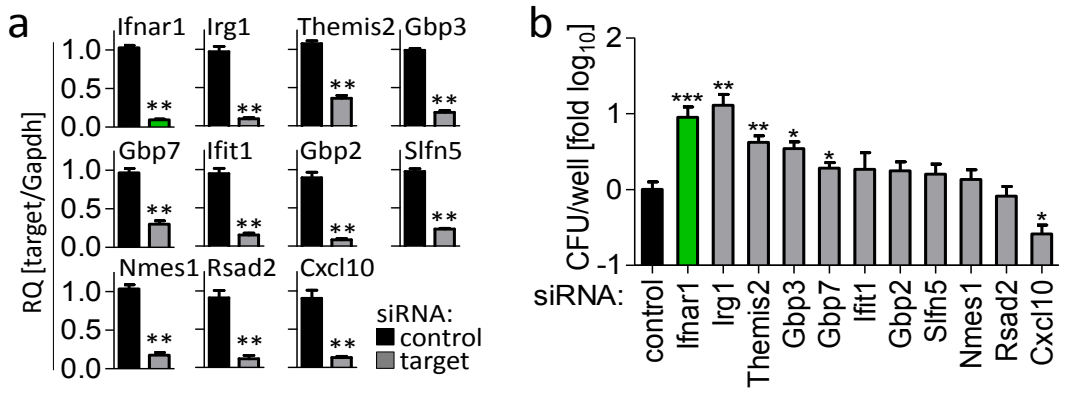

Figure 2.17 siRNA based screen of candidate proteins targeted IFN-dependently to the LCV identifies IRG1 as crucial IFN-driven effector molecule. BMMs were transfected with control siRNA or a pool of two specific siRNAs per gene 24 h prior to infection. Knock-down efficiency was assessed by qRT-PCR 24 h p.i. (a) and numbers of bacteria were determined by CFU counting 72 h p.i. (b). Data are mean + s.e.m. of 2 (a) or 4 (b) independent experiments done in triplicates. * $p<0.05$, ** $p<0.01$, *** $p<0.001$, no indication if not significant (two-tailed Mann-Whitney U test).

In order to confirm the location of IRG1 at the LCV microscopic analyses of cells overexpressing IRG1 were conducted. A previously reported mitochondria-like distribution of IRG1 [119] could be confirmed (data not shown, Figure 2.18a, d), and a close association with the LCV was demonstrated (Figure 2.18a, b).

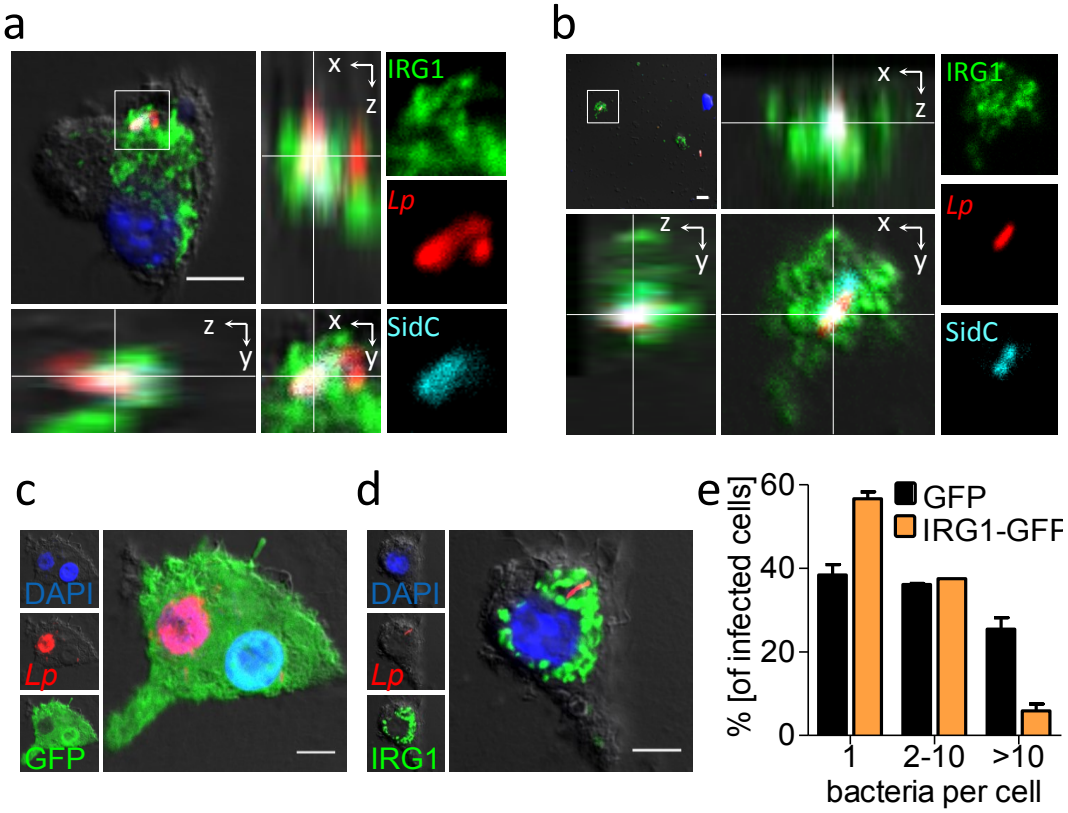

Figure 2.18 IRG1 associates with LCVs, and restricts replication of *L. pneumophila* within macrophages. *Ifnar*$^{-/-}$ BMMs overexpressing IRG1-GFP (a, b, d) or GFP only (c) were infected with DsRed-expressing *L. pneumophila* wt (red). (a, b) 2 h p.i. cells were fixed (a) or homogenized and fixed (b) and LCVs and nuclei were visualized by SidC (LCV-located *L.pneumophila*-protein; cyan) and DAPI (blue) staining, respectively. Details from upper left are shown as z-stack and as single channels for depicted x-y-plane. (c-e) Cells were fixed 24 h p.i. and intracellular bacteria were counted (e). Scale bars indicate 5 µm. (e) 150-250 GFP- / IRG1-GFP-expressing cells were counted, data represent mean + s.e.m. of 2 independent experiments.

Importantly, overexpression of IRG1 in *Ifnar*$^{-/-}$ cells, which express only little amounts of endogenous IRG1 upon *L. pneumophila* infection (data not shown), markedly decreased intracellular growth of *L. pneumophila* wt as compared to control-transfected *Ifnar*$^{-/-}$ cells. This was indicated by a lower percentage of IRG1-expressing macrophages harboring >10 bacteria and a higher percentage of cells harboring only one bacterium inside (Figure 2.18c-e). These data demonstrate that IRG1 is regulated by IFNs, localizes to the LCV, and restricts intracellular replication of *L. pneumophila* within macrophages.

2.7 *IRG1 restricts* L. pneumophila *through production of the antibacterial metabolite itaconic acid*

IRG1 is a newly characterized mitochondrial protein which has recently been implicated in the production of mitochondrial ROS (mROS) as well as the metabolite itaconic acid, and in antibacterial defense in macrophages [121,127]. To assess whether mROS is IRG1- and IFNAR-dependently produced in *L. pneumophila* infected cells, BMMs were infected with GFP-expressing *L. pneumophila* to measure mROS production by flow cytometry. It was found that mROS is produced in infected cells by a largely IRG1- and IFNAR-independent mechanism (data not shown), thus arguing against a major role of mROS in IRG1-mediated restriction of *L. pneumophila*.

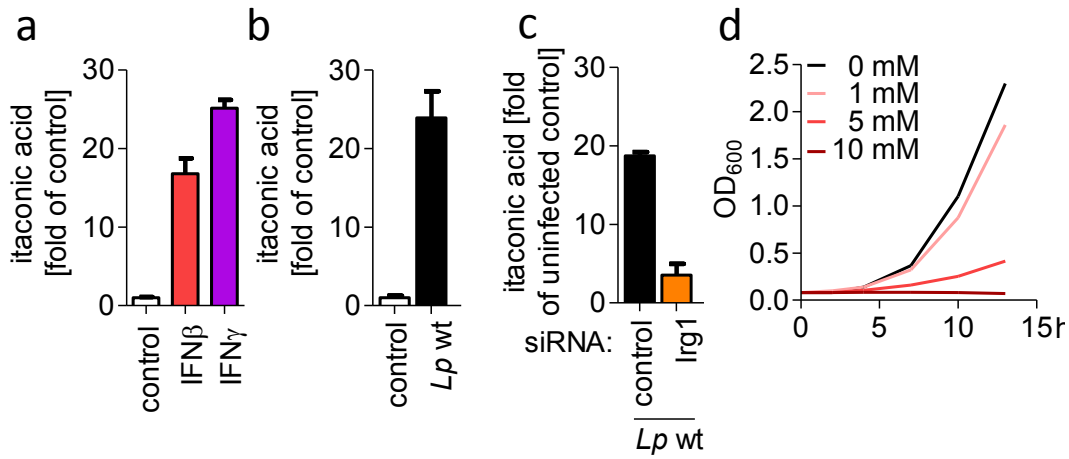

Figure 2.19 IRG1 restricts *L. pneumophila* through production of the antibacterial metabolite itaconic acid. (a-c) Intracellular levels of itaconic acid were measured by GC/MS in WT BMMs 18 h post stimulation with 50U/ml IFNβ or IFNγ (a) or 24 h post infection with *L. pneumophila* wt (m.o.i. 10) in cells left untreated (b) or transfected with control siRNA or IRG1-siRNA (c). (d) Indicated concentrations of itaconic acid were added to *L. pneumophila* in liquid culture and OD_{600} was determined over time to assess bacterial growth.

Next, the production of itaconic acid was examined. Treatment of macrophages with type I and II IFNs as well as infection with *L. pneumophila* strongly stimulated the production of itaconic acid (Figure 2.19a, b), whereas gene-silencing of IRG1 largely reduced the production of this metabolite (Figure 2.19c). Importantly, itaconic acid dose-dependently inhibited *L. pneumophila* growth in liquid culture (Figure 2.19d) at a physiological concentration [121]. Thus it seems that IRG1 restricts *L. pneumophila* through catalyzing the production of the antibacterial metabolite itaconic acid.

2.8 *IRG1 restricts* L. pneumophila *in alveolar macrophages and IFN-dependently produces itaconic acid in vivo*

In order to assess the role of IRG1 in antibacterial defense in primary cells alveolar macrophages from WT mice were isolated. Importantly, knock-down of IRG1 expression by specific siRNAs significantly increased bacterial replication (Figure 2.20a, b). It was further found that IRG1 was IFN-dependently expressed *in vivo* in mouse lungs upon *L. pneumophila* infection (Figure 2.20c) resulting in an IFN-dependent itaconic acid production (Figure 2.20d).

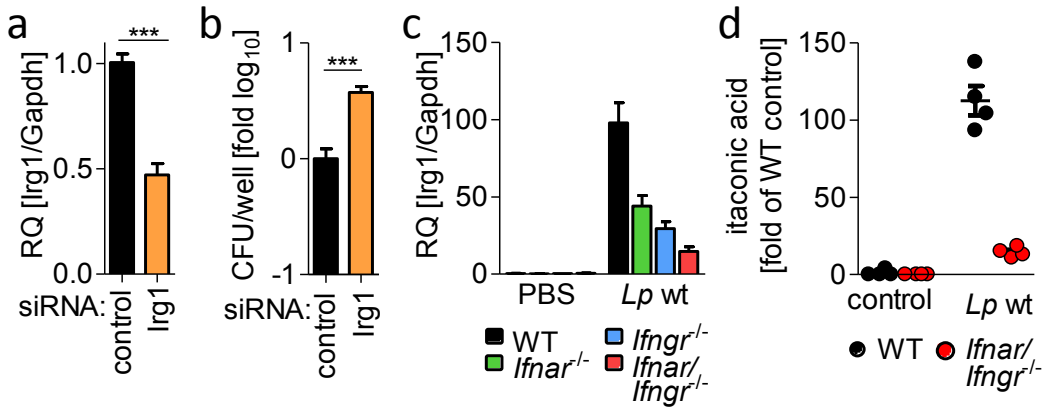

Figure 2.20 IRG1 restricts replication of *L. pneumophila* within primary alveolar macrophages and is regulated by IFNs *in vivo*. (a, b) Alveolar macrophages were transfected with control siRNA or a pool of two IRG1-specific siRNAs 24 h prior to infection. Knock-down was assessed by qRT-PCR 24 h p.i. (a) and CFUs were counted 72 h p.i. (b). (c, d) WT, *Ifnar*$^{-/-}$, *Ifngr*$^{-/-}$ and *Ifnar*/*Ifngr*$^{-/-}$ mice were infected with *L. pneumophila* wt, treated with PBS or left untreated. 2 d p.i.. *Irg1* expression (c) and itaconic acid production (d) were determined by qRT-PCR and GC/MS, respectively. (a, b) Data are mean + s.e.m. of 3 independent experiments done in quadruplicates. * $p<0.05$, ** $p<0.01$, *** $p<0.001$, (two-tailed Mann-Whitney U test). (c, d) Data represent mean + s.e.m. of 5 (c) and 4 (d) mice per group.

Together with the initial findings that *Ifnar*/*Ifngr*$^{-/-}$ mice are severely impaired in controlling *L. pneumophila* infection (Figure 2.2a) and that IFN signaling is of particular importance in CD11c^{+} cells (Figure 2.5d), these data suggest that *L. pneumophila* replication in alveolar macrophages *in vivo* is restricted by IFN-regulated IRG1 producing itaconic acid.

3 DISCUSSION

3.1 Summary

Several different PRRs, including TLR2, -5 and -9, NOD1 and -2, NAIP5/NLRC4 as well as yet-to-be identified cytosolic nucleic acid sensors are well known to contribute to the early detection of *L. pneumophila*. Recognition via these receptors initiates a complex network of signaling cascades, including NF-κB- and IRF3/7-dependent pathways. This finally leads to dramatic transcriptional changes within infected cells, and via the induction of a wide variety of cytokines also within uninfected neighboring cells and whole tissues and organs in general. The relative importance of individual cytokines and signaling pathways for these global transcriptional changes are, however, largely unknown. Furthermore, while the relevance of single signaling pathways and cytokines for the outcome of *L. pneumophila* infection are at least to some extent reported, the exact molecular effector mechanisms underlying the final restriction of the pathogen are less clear.

The present study uncovers that type I and II IFNs together are the master regulators of the early pulmonary transcriptional response to *L. pneumophila* infection. While the lack of one system could partially be compensated by the other system, the lack of both signaling pathways results in tremendous defects in gene expression and leads subsequently to the loss of the capability to control the infection. This type I and II IFN-driven host-protective effect is shown here to rely on $CD11c^+$ cells, which are most likely alveolar macrophages. Activation of macrophages by IFNs leads to substantial changes of the protein composition of the *Legionella*-containing vacuole (LCV), the place where *L. pneumophila* replicates. The reported changes are to a great extent overlapping between both types of IFNs, demonstrating the partial redundancy of both systems. These protein composition changes involve proteins which are also transcriptionally regulated by IFNs and are therefore *bona fide* ISGs. Surprisingly, also proteins that are not IFN-dependently influenced in their mRNA expression are, however, IFN-dependently targeted to the LCV. This spatially regulation of proteins is a hitherto unrecognized mechanism of action mediated by IFNs. Among proteins that are IFN-dependently targeted to the LCV, IRG1 was identifies as a crucial antibacterial effector molecule. Since IRG1 was previously reported to localize to mitochondria, which are long known to closely associate with the LCV, IRG1 could be induced by IFNs and localize to the LCVs together with mitochondria. IRG1 exerts its antimicrobial force via the

production of itaconic acid, a metabolite found here to efficiently block *L. pneumophila* growth at concentrations previously measured in activated murine macrophages.

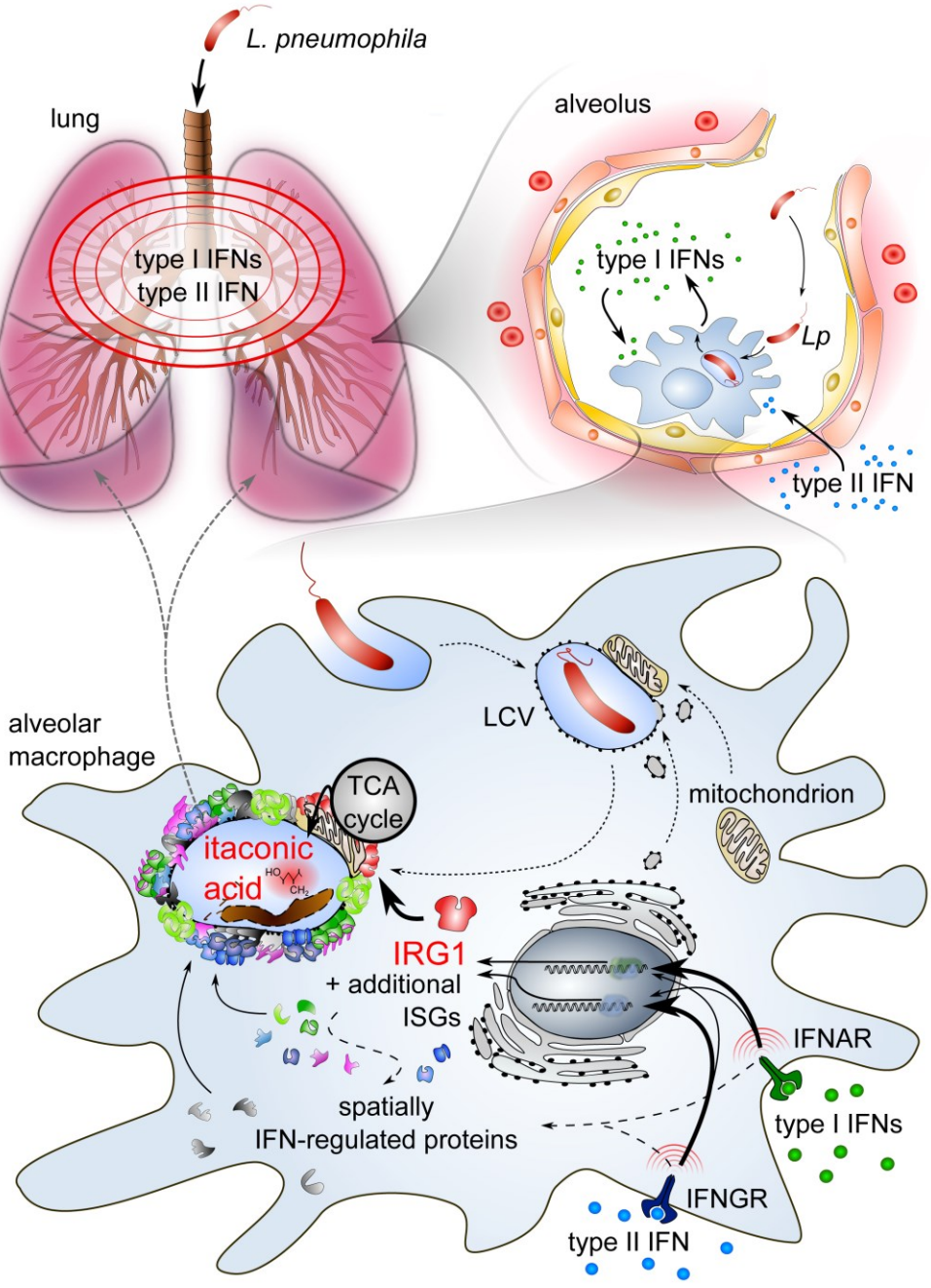

Figure 3.1 Overview of the IFN-mediated host protection against *L. pneumophila* via IRG1-derived antibacterial itaconic acid. See text for details.

In conclusion, the present study demonstrates the high relevance of a macrophage-intrinsic IFN-driven cell autonomous defense mechanism against *L. pneumophila in vivo*. Furthermore, it provides for the first time comprehensive insight into the transcriptional and spatial regulations induced by type I and II IFNs that lead to

critical modifications in the proteome of bacterial vacuoles, and it identifies a novel IFN-controlled defense pathway against *L. pneumophila* infection which relies on the IRG1-dependent production of the antimicrobial metabolite itaconic acid.

3.2 *IFNs – master regulators of the alveolar macrophage intrinsic defense* in vivo

Several different innate immune mechanisms have been shown to contribute to the defense against *L. pneumophila in vivo*, including TLR-dependent TNFα production [150–153,155], NOD1/2-dependent neutrophil recruitment [156], NLRC4/caspase-1 dependent pyroptosis [162] and the production of IL-1α by hematopoietic cells [175]. Furthermore, an important role for the type II IFN IFNγ in *L. pneumophila* defense [179–181], as well as a strong induction of type I IFNs in *L. pneumophila* infected cells have been reported [183–185]. Finally it was shown, that the infection of human monocyte-derived macrophages and primary human lung tissue with *L. pneumophila* led to dramatic transcriptional changes [219,220], whereas the key regulators and the individual importance of different signaling pathways for these changes remained unknown. Here it was found that the tremendous transcriptional changes observed upon *L. pneumophila* infection *in vivo* (Figure 2.1a, c) are in large part regulated by the concerted action of type I and II IFNs (Figure 2.1b, c). Besides the remarkable importance of type I and II IFNs, cytokines like TNF, IL-1β and IL-18 as well as the transcription regulator NF-kB were predicted *in silico* to be involved in regulation of pulmonary gene expression, which is in line with previous studies, reporting a contribution for these factors in defense against *L. pneumophila* [151,157,173,175].

The striking inability of mice lacking both IFN receptors to control *L. pneumophila* infection compared to WT and single knock-out mice (Figure 2.2a, Figure 2.3a) is in line with previous findings [185], and underlines the importance of both IFNs for the antibacterial defense. It also demonstrates the potential to compensate the lack of only one of both receptors by signaling via the other receptor. This is most likely explained by the induction of many ISGs by both types of IFNs, and, accordingly, due to partially overlapping and redundant patterns of gene expression induced by type I and II IFNs [83].

While innate immune mechanisms and especially IFNs are crucial to control the early defense against *L. pneumophila*, they might be dispensable during the later phase of infection (Figure 2.3b, c). The late but distinct onset of recovery of mice deficient in both IFN receptors at 7 to 8 d p.i. might be explained by the initiation of an efficient adaptive immune response at this stage of infection. It was reported, that IgA antibody titers in the BAL fluid of intranasally *L. pneumophila* infected mice started to rise at day 7 p.i. and increased during the following days [209]. A second report showed that antibody-opsonized and therefore FcγR-dependently phagocytosed *L. pneumophila* are unable to evade the phagosolysosomal fusion and killing [210]. It is thus tempting to speculate that an efficient antibody production combined with an altered phagocytosis might contribute to bacterial clearance at later stages of infection. Further studies addressing these questions might compare bacterial clearance in IFNAR- and IFNGR-deficient mice left untreated or treated with antibodies to block the FcγR or to deplete antibody-producing B cells.

Alveolar macrophages are the primary target and host cells of *L. pneumophila* in men and experimentally infected mice. But which cell type is responsible for an efficient control and final elimination of *L. pneumophila* in an IFN-dependent and also -independent way? Neutrophils were found here to be recruited into the lung of *L. pneumophila* infected mice and their numbers increase especially in *Ifnar*/*Ifngr* $^{-/-}$ mice over time, correlating with consistently high pulmonary bacterial load in these animals (Figure 2.2c). This clearly shows that the lack of IFN signaling does not interfere with neutrophil recruitment and that neutrophils in these mice are apparently insufficient to control the infection. This might be due to the previously described resistance of *Legionella* spp. to neutrophil-mediated killing [53,178]. On the other hand, neutrophils were reported to be required for efficient clearance of *L. pneumophila* from the lung [52,53]. Neutrophils therefore seem to be involved in defense against *L. pneumophila* rather indirectly via immunomodulatory effects through their secreted cytokines [52,53] than through a direct antibacterial mechanism.

The data shown here demonstrate that IFNs activate macrophages to restrict *L. pneumophila* infection (Figure 2.6a-c, Figure 2.7a-d). Furthermore, IFN signaling in CD11c^{+} cells is indispensable for control of *L. pneumophila* infection *in vivo* (Figure 2.5d, e). Since DCs do not support *L. pneumophila* replication [182,213,214], the findings presented here indicate that IFNs mediate their

host protection by activating a cell-intrinsic antibacterial mechanism in alveolar macrophages. This idea is further supported by the finding that IFNs also activate primary alveolar macrophages *ex vivo* to restrict *L. pneumophila* replication (Figure 2.6a-c).

While type II IFN is well-known for its activation of antibacterial immunity to most intravacuolar bacteria, type I IFNs have been shown to either enhance or inhibit those responses [86]. The present study shows that type I IFNs are protective during *L. pneumophila* infection, which is in line with previous reports [185,201]. One could speculate that the differential roles of type I IFNs in various bacterial infections might be explained by differences in the relative contribution of IFN-dependent defense systems versus other intracellular or extracellular immune mechanisms.

3.3 It's neither cell death nor iNOS - then what?

IFNs can execute their antimicrobial functions via several different mechanisms, including the induction of cell death and the production of RNS [82]. Yet, both of these mechanisms have been shown here to have no major impact on IFN-mediated host defense against *L. pneumophila* (Figure 2.8a-e, Figure 2.9a-f).

IFN-driven cell death has been shown to occur during infections with several intracellular pathogens, however, this had rather detrimental consequences for the host [133]. In *S.* Typhimurium infection the IFNAR-dependent necroptosis was shown to rely on the activation of RIP3 kinase [135,136]. But, while macrophages infected with *L. pneumophila* underwent flagellin-dependent and –independent cell death as previously reported [164,167,168], the *L. pneumophila*-induced cell death in macrophages was neither influenced by treatment with recombinant IFNβ or IFNγ nor by the lack of IFNAR (Figure 2.8b-d). Furthermore, since the lack of RIP3 kinase did not affect cell death or intracellular replication of *L. pneumophila*, a relevant role of necroptosis in IFN-mediated defense can be excluded (Figure 2.8e, Figure 2.9a, d). The recently identified non-canonical caspase-11 inflammasome can be regulated by type I IFNs, can mediate cell death, and its stimulation by *L. pneumophila* has been reported [140,141,169,171]. Therefore, the involvement of caspase-11 in IFN-dependent cell-autonomous immunity against *L. pneumophila* in macrophages was tested. The data shown here demonstrate that caspase-11 is not

required for IFN-mediated defense against *L. pneumophila* (Figure 2.9b, e). Taken together, cell death seems to play no major role in IFN-dependent cell-autonomous resistance against *L. pneumophila* in macrophages. This is in line with the host-protective role of both IFNs during *L. pneumophila* infection and the rather detrimental consequences of IFNAR-driven cell death in other intracellular bacterial infection models [133].

RNS and particularly NO production by iNOS are known to be triggered by type I and II IFNs [128,129]. Furthermore NO production has been reported to correlate with clearance of *L. pneumophila* in macrophages from mice and guinea pigs [221]. However, the role of iNOS-mediated NO production for the control of *L. pneumophila* infection *in vivo* is controversial [131,179,222]. The data presented here show that iNOS is dispensable for host-defense against *L. pneumophila* in both unstimulated and IFN-stimulated macrophages (Figure 2.9c, f). Moreover, although an IFNAR-dependent expression of iNOS upon *L. pneumophila* infection was observed (data not shown) and iNOS has been found to be largely enriched on latex-bead phagosomes of IFNγ-activated macrophages [132], iNOS was undetectable on LCVs from either untreated or IFN-treated macrophages (data not shown). One could therefore speculate that *L. pneumophila* has evolved strategies to inhibit targeting of iNOS to the LCV to escape from NO-mediated killing, a strategy already described for *M. tuberculosis* [223,224]. This idea might further be supported by the previous finding, that an avirulent strain of *L. pneumophila* led to the production of significantly more NO in murine macrophages than the virulent parental strain from which the avirulent strain was derived by multiple passages [221].

Classical and long known IFN-driven defense mechanisms like cell death and RNS production were found to play no major role in IFN-mediated antibacterial defense against *L. pneumophila*. In contrast, it has recently been shown that the immunity-related GTPases IRGM1 and IRGM3 are involved in the IFN-dependent host-defense against *L. pneumophila* [115,185]. Additionally, other reports showed that IRGM1 as well as other members of the large family of IFN inducible GTPases are targeted to pathogen-containing vacuoles and confer host-resistance against bacteria and parasites [109,112,225–228]. Last but not least a recent report demonstrated the tremendous changes of the proteome composition of latex-bead phagosomes in macrophages upon IFNγ stimulation [132]. These studies, together with the discussed

findings that IFNs stimulate an alveolar macrophage intrinsic defense mechanism against *L. pneumophila* stimulated the idea to apply a new approach here to further characterize the IFN-mediated antibacterial mechanism against *L. pneumophila*. By quantitative comparison of the proteome composition of untreated and IFN-treated macrophages, new IFN-driven effector molecules were identified (Figure 2.10, Figure 2.14d, f, Figure 2.17b).

3.4 Legionella's protected niche – not destroyed by IFNs, but heavily targeted

After phagocytosis by macrophages, *L. pneumophila* employs a large arsenal of bacterial effector molecules to remodel its phagosome by recruitment of ER-derived, ribosome-decorated vesicles and mitochondria to establish the LCV [12,13,22,23,26,229]. Proteomic analyses of these LCVs from untreated macrophages shown here identify a high number of host proteins to be inside, on the surface of or in contact with the LCV (Figure 2.12a*). In silico* analyses of the cellular localization of these host proteins reveal a large subset of mitochondrial proteins as well as ER- and GOLGI-derived proteins (Figure 2.12b). This is in line with the current knowledge about the LCV biology and confirms recently published LCV proteome data from a murine macrophage cell line, showing mitochondrial proteins being the largest group of proteins at the LCV, followed by ER-derived proteins [217]. Given the recruitment and possibly even fusion of entire mitochondria with the LCV compared to the recruitment of only ER-derived vesicles [22], it is not surprising, that mitochondrial proteins are almost 2-fold more enriched at the LCV than ER proteins (Figure 2.12b). Looking at the biological processes in which these proteins are known to be involved and thereby looking at their functions, it becomes clear that a distinct proportion of these proteins is involved in metabolic processes (Figure 2.13) which is in line with a previous study [217] and nicely reflects the association of mitochondria and ribosomes, organelles with high metabolic activity, with the LCV. Furthermore, the appearance of many proteins known to be involved in transport and localization processes (Figure 2.13) mirrors the high degree of ongoing remodeling of the initial phagosome driven by the pathogen to establish its protected niche, the LCV. The occurrence of a certain amount of proteins known to be involved in immune system processes, demonstrates that even in unstimulated

cells, a defense response against the invading pathogen is initiated rapidly (Figure 2.13). Together these data confirm the close association of the LCV with mitochondria and the ER and identify the LCV as place of high metabolic activity.

Comparing the LCVs from untreated and IFN-treated macrophages, it becomes clear that fundamental characteristics of the LCV structure are not influenced, as indicated by equal abundance of well-established LCV and ER marker proteins (Table 2-1). Importantly, neither endosomal nor lysosomal marker proteins increase at the LCV upon IFN-stimulation, clearly demonstrating that IFNs do not force phagolysosomal fusion. This finding is in accordance with published data showing no enhanced LAMP-1 (lysosomal marker) or reduced calnexin (ER marker) staining of LCVs from IFNβ treated versus untreated cells [185]. On the other hand, activation of macrophages with type I and II IFNs leads to the vacuolar targeting of hundreds of proteins, while only few proteins show reduced vacuolar abundance upon IFN stimulation (Figure 2.14a, b). Notably, the direct comparison between both types of IFNs reveals only minor differences in the vacuolar proteome changes stimulated by each IFN individually (Figure 2.15a). This further supports the idea that type I and II IFNs stimulate similar or largely overlapping effector mechanisms against *L. pneumophila*. Computed network and GO-enrichment analyses reveal that many proteins targeted to the LCV upon IFN stimulation are involved in diverse aspects of immune response mechanisms (Figure 2.16). This subgroup of proteins includes several proteins known to be involved in nucleic acid detection (e.g. STING [Tmem173], TLR9, TLR3, RIG-I [Ddx58], MDA5 [Ifih1], LGP2 [Dhx58]), a process well known to be a vital part of innate defense against *L. pneumophila* [183–185,189]. Furthermore, SLC15A3 was found to enrich at the LCV upon IFNβ stimulation (Figure 2.16). SLC15A3 was recently found to localize to endosomes and mediate the egress of bacteria-derived products which can then be sensed on the cytosolic side of the phagosomal membrane [230]. IFNs might thus enhance the expression and vacuolar localization of proteins involved in pattern recognition and enhance transport of bacteria derived molecules into the cytosol to improve bacterial detection.

Another study analyzed the role of NLRP3-driven caspase-1 activation in phagosome acidification. It was reported that active caspase-1 enriches on bacteria-containing phagosomes and locally controls the pH by modulating the NADPH

oxidase NOX2 [231]. Likewise, caspase-1 was found here to be localized at the LCV and this is enhanced by both IFNs (Figure 2.16). Furthermore, NLRP3 is enriched at the LCV upon IFNγ treatment (Figure 2.16). Finally also NOX2 is abundant at the LCV (data not shown). Since additionally to NLRP3 also NAIP5/NLRC4 stimulation, which is highly relevant in *L. pneumophila* infection, activates caspase-1 a caspase-1-mediated control of the pH within the LCV should be addressed in further studies.

Among immune response-related proteins, proteins with reported antimicrobial effector functions form the largest subgroup. This includes proteins with known antiviral functions like RSAD2 (also known as viperin) [98] and SAMHD1 [232,233] as well as proteins acting antibacterial or antiparasitic like IRGM1 [185,228,234], GBP2 [111,226], GBP7 [112], NRAMP1 [235] and IRG1 [121,127]. Given the already described IFN-dependent expression and phagosomal/vacuolar localization of some of these proteins (e.g. IRGM1, GBP2, GBP7) [105,225], it might be not surprising to find them on LCVs from IFN-activated macrophages. One could argue that this reflects the IFN-driven expression of these proteins followed by an unspecific targeting to all kinds of phagosomes, including the LCV. A finding strongly arguing against this simplistic view is that other ISGs known to localize to bacteria-/parasite-containing vacuoles and found also on latex-bead phagosomes from IFNγ activated macrophages, like GBP1 and iNOS [112,132,223,225], were undetectable at LCVs from IFN-treated and untreated cells. This might be explained by a pathogen-mediated inhibition of vacuolar targeting of these proteins, as described for iNOS on *M. tuberculosis*-containing phagosomes [223,224]. Alternatively the phagosomal targeting of those proteins might be tightly controlled by the host cell and might differ depending on the phagocytosed content. Additionally, some proteins identified on the LCV, including RSAD2 and IRG1 have not been previously found on bacteria-containing vacuoles or latex-bead phagosomes upon IFNγ treatment [119,132]. Instead, they were described to localize to cellular organelles such as the ER or mitochondria [98,119]. While this could further support the idea of a content-dependent phagosomal targeting, it might also reflect differences in the phagosome architecture. The proteome of latex bead phagosomes contains only 3 - 4% mitochondrial proteins [236], in contrast mitochondrial proteins account for almost one third of the LCV proteins (Figure 2.12a, b). Thus, especially

mitochondrial and ER-located ISGs enrich at the LCV, which is known to associate with mitochondria and to fuse with ER-derived vesicles [22].

3.5 Spatial protein regulation – a new mode of action of IFNs

Interestingly, the comparison of IFN-directed vacuolar proteins with the INTERFEROME database of known ISGs as well as own transcriptome data uncovers a large subset of proteins showing an IFN-dependent vacuolar targeting without any apparent IFN-dependent transcriptionally regulation (Figure 2.16). This suggests that IFNs are able to control the spatial distribution of a subset of proteins, a previously unrecognized mode of action of IFNs. Interesting examples of this spatial protein regulation include, but are not limited to, proteins from the proteasome complex (Figure 2.16). Although they are not known to be IFN-dependent transcriptionally regulated, they were found here to accumulate at the LCV upon stimulation with IFNβ and/or IFNγ.

Another group of proteins, which is quite interesting in this context, are proteins involved in MHC-I/II dependent antigen processing and presentation. Several of which localize to the LCV in an IFN-driven fashion. Many of those proteins are known ISGs (Figure 2.16) and were also reported to enrich on latex bead phagosomes in IFNγ-activated macrophages [132]. The data presented here show for the first time that proteins involved in MHC class I and II antigen presentation are also targeted to bacterial vacuoles by IFNs. However, while IFNγ treatment leads to the accumulation of MHC-I- and -II-related molecules, IFNβ treatment targets primarily MHC class I antigen presentation-related molecules to the LCV. This is in line with the important functions of both, type I IFNs and MHC-I, in antiviral immunity. However, according to the INTERFEROME database both types of IFNs can potentially regulate most of these molecules transcriptionally, although levels of induction might differ. Nevertheless, the differential abundance of MHC-I and -II proteins at the LCV might further point towards a transcriptionally independent spatial regulation by IFNs, which would in this case be a negative regulation.

Potential mechanisms of such a positive or negative spatial protein regulation might involve the induction, activation or maybe even suppression of signaling molecules that control recruitment and localization of certain proteins by IFNs. Interestingly,

a previous study reported that IFNγ treatment influences both, the abundance as well as the phosphorylation status of several phagosomal proteins [132], the latter of which might affect their signaling properties and cellular localization. In line with this idea, several proteins involved in protein phosphorylation and dephosphorylation such as the protein-tyrosine kinases SYK, BTK, HCK and LYN as well as the protein phosphatases PPM1H, PPP2CA and PPP2R2A are enriched on LCVs upon IFN treatment (Figure 2.16). Furthermore, IFNs increase the abundance of molecules involved in phosphatidylinositol signaling such as PIP4K2C and PI3KAP1. Phosphatidylinositol phosphates (PIPs) are long known regulators of membrane trafficking and provide binding sites for a wide variety of proteins on membranes [237]. Modifying these PIPs can therefore lead to distinct changes in the membrane protein composition. This newly identified and hitherto unreported spatial regulation of proteins by IFNs represents an interesting new mechanism of action of IFNs and should be addressed in more detail in further studies.

3.6 IRG1 is a key effector molecule against L. pneumophila

After exploring the IFN-driven changes in protein abundance at the LCV in general, single IFN-dependent LCV-targeted proteins were analyzed for their individual role in host defense against *L. pneumophila* (Figure 2.17). This includes proteins showing the strongest quantitative increase in vacuolar abundance driven by both IFNs (Figure 2.14d, f). Additionally, proteins highly enriched at the LCVs upon IFN treatment but undetectable on LCVs from unstimulated cells (e.g. GBP3, GBP5) were selected. While several of these candidate-proteins showed no impact on intracellular bacterial growth, the knock-down of some proteins led to a significant increase in *L. pneumophila* replication, suggesting a role in antibacterial defense.

Most importantly, IRG1 was found to most strongly inhibit *L. pneumophila* in macrophages. Knock-down of IRG1 affected the bacterial growth to a similar extent as inhibition of IFNAR1 expression (Figure 2.17, Figure 2.20a, b). While this strong phenotype of IRG1 knock-down could mean that the entire type I IFN-mediated antibacterial defense relies on IRG1, it is more likely that it reflects possible

differences in the efficiency of the siRNA-mediated knock-down. While knock-down efficiency for IRG1 and IFNAR1 were comparable on mRNA level, differences might occur on protein level. IRG1 is expressed at very low levels at steady state, but strongly induced upon infection. siRNA transfection prior to infection might thus efficiently prevent translation of infection-induced mRNA into the IRG1-protein. In contrast, IFNAR1 is expressed constitutively at high levels and although mRNA levels appear to be low upon siRNA treatment, the IFNAR1 protein might still be present to some extend due to the protein turnover time. An alternative explanation might include the previously reported findings indicating that IRG1 is induced also by other stimuli including several proinflammatory cytokines like IFNγ, TNF and IL-1β as well as different bacteria and LPS [118,119,126,238]. IRG1 might therefore still be expressed to some extend when IFNAR1 is knocked down, which was observed here in IFNAR-deficient mice (Figure 2.20c).

The data presented here are the first to show that IRG1 localizes to bacterial vacuoles in activated macrophages. Interestingly, IRG1 was not detected on latex-bead phagosomes from IFNγ-treated macrophages [132], although it is induced by IFNγ as reported previously [119] and indicated by own data. One out of several differences between latex bead phagosomes and LCVs is that only the latter are known to co-localize with mitochondria [22,26]. The proteome data of untreated LCVs confirm this previous observation and reveal a high content of mitochondrial proteins associated with the LCV (Figure 2.12), possibly derived from entire mitochondria that attached to and therefore co-purified with the LCVs. IRG1 is considered to be a mitochondrial protein [119]. The mitochondria-localized protein IRG1 might hence indirectly be targeted to the LCV together with mitochondria. IRG1 was shown recently to mediate defense against *S.* Typhimurium potentially by two different mechanisms [121,127] and mechanisms relevant for IRG1-mediated defense against *L. pneumophila* are discussed below.

Besides IRG1 also knock-down of the IFN-inducible GTPases GBP3 and GBP7 was found here to result in a less pronounced but significant increase in *L. pneumophila* replication (Figure 2.17). Together with GBP1, GBP2 and GBP5 these proteins are encoded on chromosome 3 of the mouse genome. It was recently demonstrated that mice lacking this region of chromosome 3 encoding for GBP1,

GBP2, GBP3, GBP5 and GBP7 were defective in the IFNγ-mediated host defense against *T. gondii*, [113]. However, while re-expressing GBP7 partially restored the IFNγ-driven protection against *T. gondii*, re-expression of GBP3 showed no effect [113]. Furthermore, another study found an important role of GBP7 in IFNγ-mediated defense against *L. monocytogenes* and *M. bovis* BCG, probably by regulation of oxidative killing and delivery of antimicrobial peptides, while knock-down of GBP3 had no effect [112]. Hence, the data presented here add to the knowledge about GBP7´s function in antimicrobial innate immunity and are the first to suggest a role of GBP3 in host defense against intracellular pathogens.

THEMIS2 is a further protein whose inhibition by siRNA leads to increase in *L. pneumophila* replication (Figure 2.17). THEMIS2 was identified as a scaffold protein involved in regulation of TLR signaling and cytokine production, and shown to be up-regulated by LPS and IFNγ [239]. It has, however, not yet been implicated in antibacterial defense. Taking the described role in regulation of TLR signaling and cytokine production into account, the potential effect of THEMIS2 on antibacterial defense might be rather indirect.

Several of the IFN-dependently LCV targeted proteins were found here in a siRNA-based screen to potentially contribute to the IFN mediated defense against *L. pneumophila*. However, siRNA based approaches might lead to unspecific off-target effects and thus to false positive results. Further studies should therefore address the validation of the findings reported here, by applying different siRNAs individually, making use of possibly already existing knock-out cells or by applying the rapidly emerging technique of CRISPR/CAS9 mediated gene silencing [240].

3.7 The key effector is a mitochondrial protein - are mitochondria at the LCV then blessing or curse for the pathogen?

Mitochondria have long been known to co-localize or even attach to LCVs as well as other microbe-containing vacuoles [22,241–244]. In *T. gondii* infection, a pathogen-mediated recruitment of mitochondria to the parasitophorous vacuole has been described and pathogen-derived effector proteins involved in this process were identified [242,244]. For *Legionella*, the mechanism underlying mitochondrial recruitment and attachment, and most importantly, their biological function at the

LCV remain, however, largely unknown. Although a *Legionella*-derived chaperonin was proposed to induce mitochondria recruitment, this has only been shown for latex-beads and all attempts to generate a *L. pneumophila* strain with a deletion of the encoding gene failed [245]. To date at least two *L. pneumophila*-derived proteins were identified to be targeted to mitochondria. The first protein was reported to be involved in sphingoine-1 phosphate metabolism, but its role in *Legionella* pathogenesis remains elusive [246]. Another study found that *L. pneumophila* secretes a mitochondrial carrier protein (LncP) through its T4SS which assembles within the mitochondrial inner membrane and transports ATP unidirectional across membranes [247]. Thus, *L. pneumophila* might actively recruit the mitochondria as a source of energy or nutritional metabolites.

Alternatively, mitochondria might be actively targeted to the LCVs by the host cell, as indicated by a recent report [248]. This report showed that mitochondria localize to phagosomes that contain bacteria or TLR agonists via a TLR-, TRAF6-, and ECSIT-dependent mechanism. This study further indicated that mitochondrial ROS production was crucial for defense against *Salmonella* infection [248]. Furthermore, mitochondria also contain several molecules involved in pattern recognition such as MAVS [249,250] together with further molecules involved in downstream signaling (e.g. TOM70, TRIM14) [251,252] as well as STING [253]. Additionally, release of mitochondrial DNA upon infection induced stress was found to trigger type I IFN responses via the cGAS-STING-IRF3 axis [254], a process which is tightly counter-regulated by apoptotic caspases in dying cells to protect from overwhelming inflammatory responses [255,256]. Thus, mitochondria might act as platforms for diverse innate immune functions to defend against intravacuolar and other pathogens, and similar mechanisms were described already in plants [257].

Many bacterial toxins are known to target to mitochondria and modulate their functions. However, whether this targeting aims to inhibit defense mechanisms or to provide the pathogen with mitochondria-derived nutrients is in most cases less clear [258]. Two studies shedding some light on these questions identified bacterial proteins from *L. monocytogenes* and *V. cholera* that modify the dynamics of mitochondria in order to interfere with mitochondria-mediated immune mechanisms against these pathogens [259,260]. Remarkably, it was recently reported

that bacterial targeting of mitochondria is surveyed by the host and leads to the initiation of innate immune responses in *Caenorhabditis elegans* [261]. Thus, mitochondria appear to be central organelles in the host-pathogen interaction and antimicrobial defense.

In *L. pneumophila* infection, it is not yet clear whether mitochondria are actively recruited to the LCV by the pathogen itself or targeted to the vacuole by the host. In an unstimulated infected cell, mitochondria might possess some benefit during the early phase of infection, when many of the immunity-related mitochondrial proteins are not expressed or only at low levels. Up-regulation of those proteins in an ongoing infection might lead to rather detrimental effects of the mitochondria for *L. pneumophila* at later time points and mitochondria were found to disappear from the LCVs 4-8 h post infection [22]. One could speculate that this is driven by *L. pneumophila* in order to evade immune effector mechanisms carried out by mitochondrial proteins that are up-regulated during the infection process, however there is so far no experimental evidence for this hypothesis. In contrast, in a pre-stimulated cell, e.g. by paracrine acting IFNs, mitochondrial proteins that target the pathogen, e.g. IRG1, are expressed already at high levels and the early recruitment of mitochondria to the LCV leads to restriction of the infection. In case of a TLR-mediated recruitment of mitochondria to the LCV and other pathogen-containing vacuoles the concomitant IFN-dependent up-regulation of antimicrobial molecules within this organelle might therefore represent a combined two-step strategy of the immune system to counteract intravacuolar pathogens.

3.8 It's all about metabolism – bacteria are restricted by a host derived metabolite

The mitochondrial protein IRG1 was identified here as highly enriched at the LCV in response to IFN stimulation, and importantly, as being a major restriction factor for *L. pneumophila*. IRG1 has recently been shown to exhibit antibacterial activity against the intracellular pathogen *S.* Typhimurium and two different mechanisms were proposed [121,127]. Two reports indicated an involvement of IRG1 in ROS production, with one of them finding an IRG1-mediated regulation of β-oxidation-dependent mitochondrial ROS production important for bacterial killing [126,127]. However, a contribution of IRG1 to mROS production during *L. pneumophila*

infection was not found here (data not shown). In contrast, another study identified IRG1 as an enzyme catalyzing the decarboxylation of the tricarboxylic acid (TCA) cycle metabolite *cis*-aconitate to itaconic acid [121,262], which is long known to inhibit bacterial growth under certain conditions [122]. Itaconic acid was initially described and for a long time thought to be a metabolite produced only by fungi [263]. Only recently it has been identified also within mammalian macrophages, where it was produced upon stimulation with LPS and might also be secreted [262,264,265]. Moreover, metabolic profiling of *M. tuberculosis*-infected mice also found itaconic acid to be produced *in vivo* [266]. A central role of IRG1 and its product itaconic acid in activated macrophages has been further evidenced recently. Integrating parallel metabolomic and transcriptomic data from polarized macrophages the authors found IRG1 and itaconic acid to be among the most strongly up-regulated genes and metabolites, respectively, in M1 macrophages. Furthermore, the entire TCA cycle in M1 polarized macrophages appeared to be redirected in order to provide substrates for itaconic acid synthesis by IRG1 [267]. In line with these previous findings, itaconic acid is produced by macrophages upon stimulation with IFNβ or IFNγ, as well as during *L. pneumophila* infection in an IRG1-dependent manner *in vitro* (Figure 2.19a-c). Strikingly, pulmonary IRG1 expression as well as pulmonary itaconic acid level are both strongly enhanced upon *L. pneumophila* infection *in vivo* and both highly depend on IFN signaling (Figure 2.20c, d).

As mentioned above, itaconic acid is known to inhibit different bacterial species including *Pseudomonas indigofera*, *S. enterica*, *M. tuberculosis* and *Yersinia pestis* when growing on minimal media with either acetate or fatty acids as limiting carbon source [121–123]. This was found to be due to the inhibition of the isocitrate lyase (ICL), an enzyme of the glyoxylate shunt which is essential for the survival of bacteria when growing on fatty acids or acetate [121,123,262]. Itaconic acid also efficiently inhibits the growth of *L. pneumophila* (Figure 2.19d). Interestingly, this appears not to require a restriction of carbon sources since bacteria were grown on a rich medium containing yeast extract and thereby providing a wide range of different carbon sources. Moreover, it is thought that the glyoxylate shunt, which is blocked by itaconic acid in other bacteria is absent in *L. pneumophila* [268]. So how does itaconic acid then inhibit *L. pneumophila* growth? *L. pneumophila* is well known to rely on amino acids as energy and carbon source when growing within host

cells [269–271]. Itaconic acid was reported to inhibit another enzyme within bacteria, the propionyl-CoA carboxylase (PCC) [262,272]. This enzyme is of high importance for the degradation of propionyl-CoA during the catabolism of the amino acids threonine, valine, isoleucine and methionine and is present from bacteria to humans [273]. According to available genetic information, this enzyme is also present in *L. pneumophila* [274] and might therefore also be blocked by itaconic acid. Another way to degrade propionyl-CoA is the methylcitrate cycle. Catabolism of propionyl-CoA via this pathway is of high importance especially in bacteria, fungi and apicomlexa to protect from toxic concentrations of propionate [275–277]. Moreover, for *L. pneumophila* and *M. tuberculosis* it was found that a defect in this pathway led to decreased intracellular replication and in the case of *L. pneumophila* also to faster bacterial killing [276,278]. An inhibitory effect of itaconic acid on the methylcitrate cycle by inhibiting the methylisocitrat lyase (MCL) activity of ICL or direct inhibition of the MCL, an enzyme involved in the methylcitrate cycle, has been discussed [121,262], although experimental evidence is still missing. The degradation of propionyl-CoA as an intermediate of amino acid catabolism seems to be of particular importance and inhibition might lead to rapid intoxication by propionate. Taken together, itaconic acid might act antibacterial on *L. pneumophila* by blocking propionyl-CoA catabolism via inhibiting the PCC or the MCL. Furthermore, itaconic acid might inhibit also other yet-to-be-identified mechanisms in *L. pneumophila*.

Besides direct growth inhibition of *L. pneumophila* and other bacteria an even broader application of itaconic acid might arise from a recent study demonstrating that ICL, which is blocked by itaconic acid, mediates broad tolerance against different antibiotics in *M. tuberculosis* [279]. Thus, a combined antibiotic-itaconic acid-treatment might increase the antibacterial efficiency against multi-drug resistant pathogens. Finally, the particular importance of itaconic acid as an antimicrobial metabolite was recently further highlighted by a study demonstrating that many bacteria and especially pathogens possess three genes for degradation of itaconic acid [125,262]. These genes had been known before to be crucial for the intracellular survival of some pathogens within macrophages, without knowing their exact function [125]. Although homologs of these genes were also found for *Legionella longbeachea*, no information was given for *L. pneumophila*.

Furthermore it is not clear whether these genes are expressed in *L. longbeachae* and if this itaconic acid-degrading pathway is functional.

3.9 Conclusion and Outlook

Since its first identification in 1976 *L. pneumophila* has caused several large outbreaks of Legionnaires' disease with high mortality rates, and has been more and more recognized as an important cause of community-acquired pneumonia. To meet the requirements of an efficient and targeted treatment of *Legionella* infections, it is of high importance to decipher the underlying mechanisms of an effective immune response. Understanding the molecular basis will help to develop more specific and therefore more efficient treatment strategies. Several previous studies addressed and identified different innate immune mechanisms being involved in antibacterial defense against *L. pneumophila*. The relative contributions of these individual pathways as well as the molecular mechanisms finally leading to the killing of the pathogens are however incompletely understood.

The data presented here demonstrate that type I and II IFNs are critical regulators of the early gene expression and antibacterial immune response against *L. pneumophila*. This IFN-mediated immune defense relies on cell-intrinsic mechanisms within $CD11c^+$ cells, most likely alveolar macrophages. Quantitative proteomic studies of the protein composition of the LCV, the place were *L. pneumophila* replicates, identifies several hundred proteins to be targeted to the LCV by IFNs. Interestingly, a large subset of those proteins are not transcriptionally regulated by type I or type II IFNs, which indicates a previously unrecognized spatial protein regulation by IFNs that should be addressed in further studies. Among the IFN-dependently LCV-targeted proteins, IRG1 was identified as crucial antibacterial effector molecule. IRG1 mediates the production of the metabolite itaconic acid to restrict *L. pneumophila in* macrophages. In times of increasing numbers of antibiotic resistant pathogens, new treatment options for bacterial infections are urgently needed. Further studies should therefore address itaconic acid´s potential as a therapeutic agent to treat *L. pneumophila* infections as well infections with other bacteria.

4 MATERIAL AND METHODS

4.1 Bacteria

Bacteria stocks were kept at -80°C in in ACES-buffered yeast extract (AYE) broth (10 g/l ACES buffer, 10 g/l yeast, 0.4 g/l cysteine, 0.135 g/l ferric nitrate, pH 6.9) containing 50% glycerol. The *L. pneumophila* serogroup 1 strain JR32 [280], the *flaA* mutant (Δ*flaA*) [162,168] and the corresponding strains constitutively expressing enhanced GFP or the red fluorescent protein DsRed [281] were cultured on buffered charcoal yeast extract (BCYE) agar [282] 2 d for *in vitro* infections. Δ*flaA* mutants expressing eGFP or DsRed have been generated in this study by isolating the encoding plasmids from the respective wt strain [281] using a commercial available plasmid isolation kit and introducing the plasmids into the *L. pneumophila* JR32 Δ*flaA* mutant by electroporation [283]. To maintain plasmids, chloramphenicol (cam) was added at 5 µg/ml to BCYE plates or AYE broth, respectively. For LCV-isolation bacteria were grown for 3 d on BCYE plates, and liquid cultures were inoculated in AYE broth at an OD_{600} of 0.1 and grown for 21 h at 37°C (post-exponential growth phase). For *in vivo* infections, bacteria were grown overnight to an OD_{600} of 1 in AYE broth. For all infections bacterial numbers were calculated by assuming that an OD_{600} of 1 corresponds to 10^9 bacteria/ml.

4.2 Mice

All animal experiments were approved by institutional and governmental animal welfare committees. All mice used were on C57BL/6J background, 8 - 10 weeks old and female. *Ifnar*$^{-/-}$ [284], *Ifngr*$^{-/-}$ [285], *Ifnar*/*Ifngr*$^{-/-}$ [185] and WT control mice were provided by Dr. Uwe Klemm (Max Planck Institute for Infection Biology, Berlin, Germany). C57BL/6 CD45.1 mice and transgenic CD11c-DTR-GFP [286] mice were provided by Dr. Sammy Bedoui (The Department of Microbiology and Immunology, The University of Melbourne, Melbourne, Australia) and maintained at the University of Melbourne.

4.3 *Murine* L. pneumophila *infection model*

Mice were anesthetized by intraperitoneal (i.p.) injection of 80 mg/kg ketamine and 25 mg/kg xylazine and transnasally inoculated with 1×10^6 or 1×10^7 *L. pneumophila* JR32 wt or Δ*flaA* in 40 µl PBS per mouse. Control groups were

sham-infected with 40 µl PBS. At indicated time points mice were anesthetized (160 mg/kg ketamine, 75 mg/kg xylazine), heparinized (60 µl 12,500 I.E.) and sacrificed by final blood withdrawal. Blood was collected and leukocytes quantified by flow cytometry. After exsanguination the lung was flushed with sterile 0.9% NaCl via the pulmonary artery (except for lungs used for histological analysis) before lung was removed and used for further analyses. For survival analysis bodyweight and temperature were recorded every 12 h for 10 d.

4.3.1 RNA extraction, microarray analysis and upstream regulator analysis

Lungs were flushed via the pulmonary artery with sterile 0.9% NaCl and homogenized in Trizol (Life Technologies). Homogenized lungs were pooled (5 mice per group) and RNA extraction was carried out according to manufacturer's instructions. RNA amounts were estimated with a NanoDrop 1000 UV-Vis spectrophotometer (Kisker) and RNA integrity was confirmed using an Agilent 2100 Bioanalyzer with a RNA Nano 6000 microfluidics kit (Agilent Technologies). Microarray analysis and data extraction was carried out by Dr. Hans-Joachim Mollenkopf (Max Planck Institute for Infection Biology, Berlin, Germany). Microarrays were performed as dual-color hybridizations. In order to compensate dye-specific effects and to ensure statistically relevant data, color-swap dye-reversal hybridizations were performed [287]. RNA labeling was done with a two-color Quick Amp Labeling Kit according the supplier's recommendations (Agilent Technologies). In brief, mRNA was reverse transcribed and amplified using an oligo-dT-T7 promoter primer, and labeled with cyanine 3-CTP or cyanine 5-CTP. After precipitation, purification, and quantification, 1.25 µg of each labeled cRNA was fragmented and hybridized to whole mouse genome 4x44k multipack microarrays (Design ID 014868) according to the manufacturer's protocol (Agilent Technologies). Scanning of microarrays was performed with 5 µm resolution using a G2565CA high-resolution laser microarray scanner (Agilent Technologies) with XDR extended range. Microarray image data were analyzed and extracted with the Image Analysis/Feature Extraction software G2567AA v. A.10.10.1.1 (Agilent Technologies) using default settings and the protocol GE2_1010_Sep10. The extracted MAGE-ML files were subsequently analyzed with the Rosetta Resolver, Build 7.2.2 SP1.31 (Rosetta Biosoftware). Ratio profiles comprising single

hybridizations were combined in an error-weighted fashion to create ratio experiments. A 1.5-fold change expression cut-off for ratio experiments was applied together with anti-correlation of ratio profiles, rendering the microarray analysis highly significant ($p < 0.01$), robust, and reproducible. Genes identified to be significantly up-regulated upon *L. pneumophila* infection (> 2-fold increase, $p < 0.05$ in infected versus PBS-treated mice) were analyzed for their predicted upstream regulators using the Ingenuity Pathway Analysis (IPA) software (Ingenuity System). Only upstream regulators with an activation z-score > 2 (predicted activators) were considered and further categorized in respective groups.

4.3.2 Determination of bacterial counts

Lungs were homogenized using a cell-strainer (100 µm, BD Bioscience). For determination of bacterial counts, the homogenates were lysed with 0.2% Triton X-100 for 10 min and serial dilutions were plated on BCYE agar plates.

4.3.3 Pulmonary leukocyte and blood leukocyte quantification

Pulmonary leukocytes were differentiated manually by light microscopy of May-Grünwald-Giemsa-stained cytospin preparations from lung homogenate prior to lysis. Leukocytes in the blood were analyzed by flow cytometry according to their side-scatter/forward-scatter properties and CD45 and Gr-1 expression. Briefly, red blood cells were removed using RBC Lysis Buffer (BD Biosciences) according to the manufacturer's recommendations and cell suspension was labelled with anti-CD45 (BD Pharmingen) and anti-Gr-1 (BD Pharmingen). Cells were analyzed on a Becton Dickinson FACSCalibur flow cytometer using CELLQuest software (BD Biosciences).

4.3.4 Histology

Anesthetized mice were heparinized by intracardial injection through the intact diaphragm and sacrificed by exsanguination via direct incision of the caudal *Vena cava*. Then, lungs were removed after tracheal ligation to exclude alveolar collapse and fixed in 4% formalin (pH 7.0). Immersion formalin-fixed lungs were embedded in paraffin, cut and stained with hematoxylin and eosin. Paraffin embedding,

cutting, staining and image acquisition were carried out by Dr. Olivia Kershaw (Department of Veterinary Pathology, Free University Berlin, Berlin, Germany).

4.3.5 Generation of bone marrow chimeric mice

Chimeric mice were generated by Andrew S. Brown (The Department of Biochemistry and Molecular Biology, The University of Melbourne, Melbourne, Australia) as described recently [288]. Briefly, CD45.1 mice were lethally irradiated twice with 550 cGy and reconstituted with a 1:1 mix of 1.5×10^6 bone marrow cells from C57BL/6 WT or *Ifnar*/*Ifngr*$^{-/-}$ and transgenic CD11c-DTR-GFP mice (all CD45.2). Chimeric mice were allowed to reconstitute for at least 10 weeks. Only those mice that contained < 10% host cells were included in experiments. Depletion of CD11c$^+$ cells was achieved by injection of CD11c-DTR-GFP chimeric mice intraperitoneally three times with 100 ng diphtheria toxin (Sigma) on days -2, +1 and +4 prior to and during infection.

4.3.6 Evaluation of cell exchange rate and depletion efficiency in chimeric mice

Lungs were finely minced using scissors and enzymatically digested in 3 ml of RPMI-1640 media supplemented with 3% fetal calf serum, 0.1% DNAse and 0.1% collagenase type III. Tissue digestion was achieved by constant and gentle pipetting for 20 min at room temperature. Undigested tissue was filtered out and red blood cells were removed using RBC Lysis Buffer (BD Biosciences) according to the manufacturer's recommendations. The lung cell suspension was labelled with anti-panCD45 (eBioscience), anti-CD45.1 (BD Pharmingen), anti-CD45.2 (BD Pharmingen), anti-Ly6G (BD Pharmingen), anti-CD11c (eBioscience) anti-MHC-II (eBioscience), anti-SiglecF, (BD Pharmingen) and anti-CD64 (BD Pharmingen). Cells were analyzed on a Becton Dickinson LSRFortessa flow cytometer using FACSDIVA software (BD Biosciences).

4.4 Cell culture

4.4.1 Alveolar macrophage isolation

For alveolar macrophages (AMs) isolation mice were anesthetized (160 mg/kg ketamine, 75 mg/kg xylazine), and sacrificed by final blood withdrawal. Afterwards the lungs were lavaged 10-times with 500 µl ice cold PBS + 0.5 mM EDTA. BAL fluid was centrifuged at 200 g for 10 min, cells resuspended in RPMI 1640 + 10% FCS + 4.5 mM L-glutamine + 100 µg/ml Pen/Strep at a density of 4×10^5 cells/ml and seeded in desired well-format one day before the experiment. For purity check cells were stained with anti-CD45 (BD Pharmingen), anti-SiglecF (eBioscience) and anti-CD11c (eBioscience) and analyzed on a MACSQuant (Miltenyi Biotec) flow cytometer.

4.4.2 Generation of bone marrow-derived macrophages

Isolation and culturing of bone marrow-derived macrophages (BMMs) was performed as described previously [289]. Bone marrow was isolated from the femurs and tibiae. The bones were washed in 70% ethanol and then rinsed with RPMI 1640. Afterwards, the bones were disrupted with a pestle in a sterilized mortar in 20 ml RPMI 1640. Cell suspension was passed through a 70 µm cell strainer and centrifuged at 200 g for 10 min. Cells were resuspended in FCS + 10% DMSO and stored at -80°C in aliquots of 10^7 cells/ml in liquid nitrogen. For generation of bone marrow-derived macrophages (BMMs), bone marrow aliquots were thawed and transferred into BMM growth medium (RPMI 1640 + 20% FCS + 30% L929 fibroblast supernatant + 4.5 mM L-glutamine + 100 µg/ml Pen/Strep). Cells were washed with BMM growth medium, resuspended in 20 ml BMM growth medium and divided into two petri dishes. 10 ml growth medium were added to each dish after 4 d of cultivation. After 10 d, confluent cells were incubated in 7 ml ice cold PBS + 2 mM EDTA and detached by scraping. Cells were resuspended in BMM replating medium (RPMI 1640 + 10% FCS + 15% L929 fibroblast supernatant + 4.5 mM L-glutamine) at a density of 4×10^5 cells/ml and seeded in desired well-format one day before the experiment. For medium preparation, L929 fibroblast were cultured in RPMI 1640 + 10% FCS + 4.5 mM L-glutamine for 10 d and

supernatant was harvested, sterile-filtered (0.2 µm) and stored at -80°C. All cells were cultured at 37°C and 5% CO_2.

4.4.3 Cell transfection

BMMs and AMs were transfected with control non-silencing or a mix of two gene-specific siRNAs (Table 4-1) (Life Technologies) using HiPerfect, according to the manufacturer's protocol, using 19 ng siRNA in total and 1.5 µl HiPerfect reagent per 1×10^5 cells. Cells were infected 24 h post transfection and knock-down efficiency was assessed by qRT-PCR 24 h p.i. (48 h post transfection).

Table 4-1 Oligonucleotides used for RNAi.

target gene	siRNA ID	target gene	siRNA ID
Cxcl10	s201504	*Ifnar1*	s68086
Cxcl10	s68048	*Irg1*(#1)	s68386
Gbp2	s66501	*Irg1*(#2)	s68387
Gbp2	s66503	*Nmes1*	s119452
Gbp3	s79881	*Nmes1*	s119453
Gbp3	s79882	*Rsad2*	s81519
Gbp7	s106347	*Rsad2*	s81520
Gbp7	s106348	*Slfn5*	s116120
Ifit1	s68058	*Slfn5*	s116121
Ifit1	s68059	*Themis2*	s106616
Ifnar1	s68085	*Themis2*	s106617

For overexpression *Ifnar*$^{-/-}$ BMMs were transfected with 0.8 µg plasmid DNA encoding for EGFP (pEGFP-N1, Clontech) or full-length murine IRG1 (NM_008392) with a carboxy-terminal TurboGFP (pCMV6-AC-GFP, OriGene) or Myc-DDK (pCMV6-Entry, OriGene) tag using 2.4 µl ViaFect per 2×10^5 cells according to manufacturer's recommendations. Cells were incubated for 48 h post transfection to ensure efficient expression of the respective construct.

4.4.4 Cell stimulation and infection

BMMs and AMs were infected with *L. pneumophila* wt or Δ*flaA* at the indicated multiplicity of infection (m.o.i.), centrifuged at 200 g for 5 min and incubated for the indicated time intervals. Where indicated, cells were incubated either with IFNβ, IFNγ or both 16-18 h prior to and during infection.

4.4.5 *In vitro* intracellular replication assays

Intracellular *L. pneumophila* replication assays in BMMs and AMs were performed by infecting 1×10^5 or 4×10^4 cells per 48-well or 96-well, respectively at an m.o.i. of 0.1 or 1. The plates were centrifuged at 200 g for 5 min and subsequently incubated at 37°C for 30 min. Cells were washed twice with PBS and then incubated with RPMI containing 50 µg/ml gentamicin for 1 h at 37°C in order to kill extracellular bacteria. Subsequently, cells were washed twice with PBS and incubated in BMM replating medium for different time intervals. At indicated time points, cells were lysed by addition of 0.1% saponin and vigorous pipetting. 10 µl of serial dilutions from the lysed cells were plated on BCYE agar plates and incubated for 3 d at 37°C to determine bacterial CFUs.

4.4.6 Cell death measurement

For determination of cell death by flow cytometry BMMs were seeded in suspension cell 24-well plates and infected with eGFP expressing *L. pneumophila*, as described above. At indicated time points supernatants were collected and cells were detached by addition of ice cold PBS containing 2 mM EDTA and gentle pipetting. Respective supernatants and cells were subsequently pooled, centrifuged at 350 g 5 min and stained for cell death using 7-AAD or LIVE/DEAD fixable red dead cell stain according to manufacturer's recommendations. Proportions of dead ($7AAD^+$ or $LIVE/DEAD^+$) cells were determined in infected (GFP^+) and uninfected (GFP^-) cell populations using a FACSScan or MACSQuant flow cytometer. Data analysis was done using FlowJo software (Tree Star).

4.5 LCV isolation and subsequent analyses

4.5.1 LCV isolation

LCVs from BMMs were isolated as described previously for RAW264.7 cells and amoeba [216]. A total of 6×10^7 BMMs per condition were seeded in 4 T75 cell culture flasks one day before the experiment. Where indicated cells were stimulated with 50 U/ml of recombinant murine IFNβ or IFNγ 16-18 h prior to the infection. Cells were infected with DsRed-expressing *L. pneumophila* JR32 Δ*flaA* at an m.o.i. of 50, centrifuged at 300 g for 10 min and incubated for 2 h at 37°C. Cells were then washed with PBS, scraped in 3 ml homogenization buffer (20 mM Hepes, 250 mM sucrose, 0.5 mM EGTA, pH 7.2) per flask and cells from corresponding flasks were pooled. Using a ball homogenizer with an exclusion size of 8 µm cells were homogenized by passing them 9-times through the cell homogenizer. Homogenates were incubated with 2% FCS for 30 min at 4°C followed by incubation with a rabbit anti-SidC antibody (1:3000) for 1 h at 4°C. After centrifugation at 1600 g at 4°C for 15 min, cells were resuspended in homogenization buffer and incubated with a secondary MACS anti-rabbit antibody (1:25) coupled to magnetic beads (Miltenyi Biotec) for 30 min at 4°C. Subsequently LCVs were separated using MiniMACS cell separation columns (Miltenyi Biotec), washed 3-times with homogenization buffer on the columns and eluted in homogenization buffer. The eluate was then applied on a continuous Histodenz density gradient (11 ml, from 10% to 35%) and centrifuged at 3500 g at 4°C for 1 h. 1.5 ml fractions were taken from the bottom of the tube. Fractions were centrifuged at 13000 g at 4°C for 15 min and pellets washed once with PBS, frozen in liquid nitrogen and stored at -80°C until further analysis.

During the isolation process, samples were collected from the homogenized cells, the flow through of the MACS cell separation columns, the eluate and all fractions of the Histodenz gradient. All samples were centrifuged on coverslips, fixed with 4% PFA for 20 min at RT and stained for SidC using a rabbit anti-SidC antibody and a secondary Cy5-labled anti-rabbit antibody to check the isolation process and identify the LCV-containing fractions by confocal microscopy.

4.5.2 Proteomic analysis

Mass spectrometry analyses and protein identification and quantification were performed by Dr. Brian D. Dill and Dr. Matthias Trost (MRC Protein Phosphorylation Unit, University of Dundee, Dundee, UK).

Isolated LCV from 4 IFNβ, 5 IFNγ, and 6 untreated biological replicates were solubilized in 1% RapiGest (Waters) in 50 mM Tris pH 8.0, reduced with 10 mM tris(2-carboxyethyl)phosphine (TCEP) (Pierce), and heated at 70°C for 10 min. After cooling, proteins were alkylated in 10 mM iodoacetamide (Sigma-Aldrich), and alkylation was quenched in 20 mM DTT. Protein concentrations were measured by the EZQ assay (Life Technologies), and 8 µg of protein was digested by trypsin overnight at 30°C, after diluting the Rapigest concentration to 0.1%. Rapigest was removed from the sample by acidification to 2% trifluoroacetic acid (TFA) and incubation at 37°C for 1 h, followed by centrifugation at 14000 g for 30 min. Peptides were then desalted with Microspin C18 solid phase extraction columns (The Nest Group). After drying down, peptides were redissolved in 1% TFA.

For each sample, 2 µg of peptides were analyzed on an Orbitrap Velos Pro mass spectrometer coupled to an Ultimate 3000 UHPLC system with a 50 cm EasySpray analytical column (75 µm ID, 3 µm C18) in conjunction with a Pepmap trapping column (100 µm x 2 cm, 5 µm C18) (Thermo-Fisher Scientific). Acquisition settings were: lockmass of 445.120024, MS1 with 60000 resolution, top 20 CID MS/MS using Rapid Scan, monoisotopic precursor selection, unassigned charge states and z=1 rejected, dynamic exclusion of 60s with repeat count 1. 6 h linear gradients were performed from 3% solvent B to 35% solvent B (solvent A: 0.1% formic acid, solvent B: 80% acetonitrile 0.08% formic acid) with a 30 min washing and re-equilibration step [290].

Protein identification and quantification were performed using MaxQuant Version 1.4.1.2 [291] with the following parameters: stable modification carbamidomethyl (C); variable modifications of methionine oxidation, and protein N-terminal acetylation, and 2 missed cleavages. Searches were conducted using a Uniprot-Trembl *Mus musculus* database downloaded May 1, 2013, *L. pneumophila* strain Philadelphia 1 downloaded December 4, 2013, and common contaminants. Identifications were filtered at a 1% false-discovery rate (FDR) at the protein level, accepting a

minimum peptide length of 7. Quantification used only razor and unique peptides, and required a minimum ratio count of 2. "Re-quantify" and "match between runs" were enabled. Protein quantification was conducted using label-free quantitation (LFQ) intensities [292].

4.5.3 Gene ontology analysis

The 2307 host proteins identified in all six LCV samples from untreated macrophages were analyzed for overrepresented cellular components using g:Profiler (http://biit.cs.ut.ee/gprofiler/) [293,294] with default settings including g:SCS algorithm for multiple testing correction. All overrepresented child terms of the GO term *intracellular membrane-bounded organelle* (GO:0043231, $p = 3.55 \times 10^{-300}$) were extracted. To identify and visualize biological processes that are overrepresented at LCVs of untreated cells, the same list of proteins was analyzed with BiNGO [295] for Cytoscape [296] using default settings including hypergeometric testing and Benjamini & Hochberg FDR correction. Significance level cut-off was set to $< 10^{-10}$ (terms with p-values $> 10^{-10}$ are depicted if p-value of final child term was $< 10^{-10}$).

4.5.4 Integrated STRING network analysis

Proteins identified in IFN-treated (in 4 of 4 IFNβ or 5 of 5 IFNγ–treated samples) but not in untreated samples (≤ 1 of 6 samples; hereafter called "qualitative changers") and proteins with significant higher abundance in IFN-treated versus untreated samples ($\log_2$ LFQ intensity ratio ≥ 1, $p < 0.05$; hereafter called "quantitative changers") were combined and analyzed for protein-protein interaction networks using STRING database (http://string-db.org/). The identified network was extracted and loaded into Cytoscape [296] for visualization; only interactions with a minimum STRING combined score of 0.400, which represents the default medium confidence level in STRING, were kept. For identification of subnetworks of overrepresented biological functions, the combined protein list was analyzed by g:Profiler (http://biit.cs.ut.ee/gprofiler/) [293,294]. Protein lists of overrepresented GO terms were extracted and subnetworks were built using STRING and Cytoscape. To identify proteins within the networks that were also transcriptionally induced by IFNs upon *in vivo L. pneumophila* infection, the

combined list of qualitative and quantitative changing proteins was compared to genes with a > 2-fold change ($p < 0.05$) in *L. pneumophila* infected *Ifnar*/*Ifngr*$^{-/-}$ versus WT mice. To cross-reference gene names from transcriptome analysis and Uniprot identifier from proteome analysis, both lists were uploaded to STRING and respective output lists were compared against each other. For identification of known ISGs the protein list was also compared against the INTERFEROME database of ISGs [218].

4.6 Molecular biology methods

4.6.1 Total RNA isolation and cDNA synthesis

Total RNA was isolated from BMMs or lung homogenates using the PerfectPure RNA purification system or Trizol, respectively, according to the manufacturer's protocol. Subsequently, RNA was reverse-transcribed into cDNA using high capacity reverse transcription (HCRT) kit according to the manufacturer's suggestions.

4.6.2 Quantitative real time-PCR

cDNA obtained from HCRT was subjected to quantitative real time-PCR (qRT-PCR). qRT-PCR was performed using TaqMan assays (Table 4-2) or self-designed primer sets (Table 4-3), respectively, on an ABI 7300 instrument.

Table 4-2 TaqMan assays used for quantitative real-time PCR in this study.

target gene	Taqman assay ID
Gbp7	Mm00523797_m1
Ifit1	Mm00515153_m1
Ifnar1	Mm00439544_m1
Slfn5	Mm00806095_m1

Primer design was done using PrimerExpress 3.0 software (Applied Biosystems) and self-designed oligonucleotides were dissolved in ddH_2O yielding a concentration of 18 nmol/ml for forward and reverse primer and 5 nmol/ml for the 5'-FAM-3'-TAMRA-labeled probe. For each sample a 20 µl qRT-PCR-reaction

(10 µl TaqMan Gene Expression Master, 4 µl ddH_2O 1 µl of respective TaqMan assay or self-designed primer/probe mix and 5 µl cDNA) was transferred into a 96-well plate and qRT-PCR performed using the following conditions: 2 min at 50°C, 10 min at 95°C followed by 40 amplification cycles (15 sec at 95°C, 1 min at 60°C). Automatic baseline and automatic Ct were applied and raw data extracted. Data analysis was done using the $2^{-\Delta\Delta Ct}$ method [297]. The input was normalized to the average expression of *Gapdh* and relative expression (relative quantity, RQ) of the respective gene in untreated cells or PBS-treated mice were set as 1.

Table 4-3 Primer sets used for quantitative real-time PCR in this study.

target gene	forward primer sequence (5' - 3')	revers primer sequence (5' - 3')	probe sequence (5'-FAM, 3'-TAMRA)
Cxcl10	CATCCCTGCGAGCCTATCC	GGATTCAGACATCTCTGCTCATCA	CCCACGTGTTGAGATCATTGCCACG
Gapdh	TGTGTCCGTCGTGGATCTGA	CCTGCTTCACCACCTTCTTGA	CCGCCTGGAGAAACCTGCCAAGTATG
Gbp2	GTTGAGAAGGGTGACAACCAGAA	TGGTTCCTATGCTGTTGTAGATGAA	CTGGATCTTTGCTTTGGCAGTCCTCCTC
Gbp3	AAGTCCTACCTCATGAATCGTCTTG	ACCCTTGGTTTCGGATTGC	AACCATGGCTTCTCCTTGGGCTCC
Irg1	AGGCACAGAAGTGTTCCATAAAGTC	AGTGAACAGCAACACCATTAACAAA	AGACTTCAGGCTCCCACCGACATATGCT
Nmes1	TCAACCCCAAAAGCTTATAACCA	CCCTCCGGACTTTTTGCA	CAACCAGCAATGGAAGCCCGTTG
Rsad2	TGGTGCCTGAATCTAACCAGAA	TCCACGCCAACATCCAGAAT	CGCTTTCTGAACTGTACCGGTGGCC
Themis2	TGATCCTAAAACCCCAGTATATGCT	GACGGGATCTTGACGATGCT	CAAGCCATCATGCACATGCGCA

4.6.3 Immunoblotting

For western blot analysis, cells were washed with washing buffer and lysed by scraping on ice with 100 µl lysis buffer per 1×10^6 cells. Cytoplasmic fraction was separated from nuclei by centrifugation at 16,000 g for 10 min at 4°C. Protein concentration was determined using Bradford reagent according to the manufacturer's protocol. 5 µl of protein lysate were added to 1 ml of 20% Bradford reagent in H_2O, mixed and OD_{595} measured. Protein concentrations were calculated assuming that an OD_{595} of 1 corresponds to 15.765 µg protein per µl. Proteins were

denatured at 95°C for 5 min together with loading buffer in a ratio of 1:1 and 40 µg total protein separated on a 10% SDS-gel at 80-120 V for 1h. SDS-polyacrylamide gels were blotted onto Hybond nitrocellulose membranes at 100 V for 1 h using a wet blot system (BioRad). Membranes were blocked in Odyssey Blocking Buffer for at least 1 h at RT or overnight at 4°C and probed with antibodies against IRG1 (HPA040143, Sigma) and actin (sc-1616, Santa Cruz) followed by respective fluorophore-linked secondary antibodies (Rockland). Blots were analyzed using an Odyssey infrared imaging system (Li-Cor). All buffers and gels used for western blot analyses are listed in Table 4-4.

Table 4-4 Buffers and gels used for western blot analysis.

Buffer/Gel	Composition
Phosphoprotein washing buffer	5 ml Sodium orthovanadate 98% (200 mM) 50 ml Sodium pyrophosphate (150 mM) 50 ml Sodium fluoride 99% (1 M) ad 395 ml ddH_2O
Lysis buffer	810 µl Phosphoprotein washing buffer 100 µl Tris-HCl, pH 7,4 (500 mM) 50 µl NP40 (20%) 40 µl cOmplete protease inhibitor cocktail (25-fold)
Loading buffer	1 ml Tris-HCl, pH 6.8 (500 mM) 0.8 ml Glycerol 1.6 ml SDS (10% w/v) 0.4 ml Bromophenol blue (1% w/v) 0.4 ml β-Mercaptoethanol (1% v/v) 3.8 ml ddH2O
Electrophoresis buffer	3 g Tris-Base 14.4 g Glycin 1 g SDS ad 1000 ml ddH_2O
Blot buffer	3 g Tris-Base 14.4 g Glycin 200 ml Methanol ad 1000 ml ddH_2O
SDS Collection gel	2,5 ml Tris-HCl, pH 6,8 (500 mM) 100 µl SDS (10% w/v) 1,33 ml Bis-acrylamide (40%) 10 µl TEMED 50 µl Ammonium persulfate (10%) 6 ml ddH_2O

SDS Separation gel (10 %)	2,5 ml Tris-HCl, pH 8,8 (1,5 M) 100 µl SDS (10% w/v) 2,5 ml Bis-acrylamide (40%) 10 µl TEMED 50 µl Ammonium persulfate (10%) 4,85 ml ddH_2O

4.6.4 Immunofluorescence microscopy

BMMs were seeded on glass coverslips in 24-well plates and fixed at indicated time points post infection with 3% PFA for 20 min at RT. Alternatively, cells were seeded in 6-well plates, cell homogenates generated as described in chapter 4.5.1, homogenates centrifuged onto glass coverslips and fixed with 3% PFA for 20 min at RT. For intracellular staining, cells were permeabilized with 0.1% Triton X-100 in PBS for 15 min at RT, blocked with 5% FCS in PBS for 20 min at RT, stained with an affinity purified rabbit anti-SidC antibody for 2-3 h at RT or overnight at 4°C, followed by Alexa Fluor 488- or Alexa Fluor 633-conjugated secondary antibody (Molecular Probes) for 1 h at RT, and mounted on slides using PermaFluor containing DAPI. Samples were examined with a LSM 780 microscope ([objectives: Plan Apochromat 63×/1.40 oil DIC M27]. Z-stack was taken with a 63x objective over 5.44 µm in 680 nm plane distance. Images were processed using ZEN 2010 (Zeiss) and ImageJ software (http://imagej.nih.gov/ij/).

4.6.5 GC/MS analysis

10^6 BMMs per 6-well were left untreated, were incubated either with IFNβ or IFNγ for 16-18 h or were infected with *L. pneumophila* at an m.o.i. of 10 for 24 h. Where indicated cells were transfected with control non-silencing or a mix of two gene-specific siRNAs as described above 24 h prior to infection. After washing with PBS, metabolism was stopped adding 200 µl cooled 50% MeOH (-20°C) and cells were collected by scraping in the MeOH solution. Cells from 6 wells were pooled, 240 µl chloroform were added, samples centrifuged for 10 min at 10000 g and supernatant containing polar metabolites was dried under vacuum overnight. For *in vivo* experiments mice were infected with *L. pneumophila* wt or left untreated. 2 d p.i. lungs were flushed with sterile PBS, shock frozen in liquid nitrogen and stored at -80°C. Lung tissue was homogenized using a Precellys24 bead homogenizer in

chloroform (6 mL/g), methanol (6 mL/g), and distilled water (4 mL/g). Samples were centrifuged for 10 min at 10000 g and supernatant containing polar metabolites was dried under vacuum overnight. GC/MS analysis was performed by Dr. Stefan Kempa (Integrative Metabolomics and Proteomics, Berlin Institute of Medical Systems Biology/Max-Delbrueck Center for Molecular Medicine, Berlin, Germany) and samples were processed using protocols and machine settings described elsewhere [298]. Data were analyzed using ChromaTOF (Leco) and the custom software MetMax [299]. Data were normalized on mean of total area of all analyzed metabolites (*in vitro* samples) or on internal standard (cinnamic acid; *in vivo* samples) and average relative amount of itaconic acid in untreated cells or control mice was set as 1.

4.6.6 Itaconic acid growth inhibition and killing assay

For growth inhibition bacteria were grown in AYE broth containing indicated amounts of itaconic acid and OD_{600} was determined over time.

4.7 Statistical analyses

Experiments were performed in a non-randomized and unblinded fashion. Data were statistically analyzed using GraphPad Prism software. Two groups were compared with two-tailed Mann-Whitney U test or, for multiple-group comparisons with Kruskal-Wallis analysis of variance followed by Dunn's multiple comparison test or two-way ANOVA followed by Bonferroni posttest. Differences with $p < 0.05$ were considered statistically significant.

4.8 Reagents, kits, consumables and instruments

Table 4-5 Reagents

Reagent	Company
7-AAD	eBioscience
ACES	Sigma
Ammonium persulfate	Serva
Ampicillin	Ratiopharm
Ampuwa® (RNase-free H2O)	Fresenius Kabi

Bacto yeast extract	BD Biosciences
Bis-acrylamide	Serva
Bradford solution	BioRad
Bromphenol blue	Biotech Pharmacia
Chloramphenicol	Sigma
Chloroform	Merck
Collagenase type III	Worthington-Biochemical
cOmplete protease inhibitor cocktail tablets	Roche
Cyteine	Sigma
DAPI	Invitrogen
DMSO	Sigma
DNase	Sigma
EDTA	Roth
EGTA	Sigma
Ethanol	Merck
FCS	PAA
Ferric nitrate	Sigma
Gentamicin	Gibco
Glutamine	PAA
Glycerol	Roth
Glycine	Sigma
Heparine	Ratiopharm
HEPES	Biochrom
HiPerfect	Qiagen
Histodenz	Sigma
Hybond nitrocellulose membrane	Santa Cruz
Isopropanol	Sigma
Itaconic acid	Sigma
Kanamycin	Sigma
Ketamine (Ketavet)	Sigma
L-glutamine	PAA
LIVE/DEAD fixable red dead cell stain	Life Technologies
Methanol	Merck
mIFNβ	PBL interferon source
mIFNγ	PBL interferon source
NaCl (0.9%)	B. Braun
NP40	Sigma
Odyssey blocking buffer	Li-COR
Paraformaldehyde	Sigma

PBS	Gibco
Penicillin/streptomycin	PAA
PermaFluor	Beckmann Coulter
poly-L-lysine	Sigma
RBC lysis buffer	BD Bioscience
RBC lysis buffer 10X	BioLegend
RPMI 1640	Gibco
Saponin	Sigma-Aldrich
SDS	Serva
Sodium fluoride	Sigma
Sodium orthovanadate	Sigma
Sodium periodate	Sigma
Sodium pyrophosphate	Sigma
Sucrose	Sigma
TaqMan® Gene Expression Master Mix	Applied Biosystems
TEMED	R&D Systems
Tris-HCl	Sigma
Triton X-100	Sigma
TRIzol®	Invitrogen
Tween-20	Sigma-Aldrich
ViaFect	Promega
Xylazine (Rompun)	Bayer
Yeast extract	BD Biosciences
β-mercaptoethanol	Sigma

Table 4-6 Kits

Kit	Company
PerfectPure RNA cultured cell kit	5 PRIME
PerfectTaq™ plus DNA polymerase	5 PRIME
HCRT	Applied Biosystems
Plasmid purification	Qiagen
TaqMan gene expression assays	Applied Biosystems

Table 4-7 Instruments

Instrument	Company
7300 Real-Time PCR System	Applied Biosystems
Ball homogenizer	Isobiotec
BD FACSCalibur™	BD Biosciences
BD FACSCanto™	BD Biosciences

BD FACSScan™	BD Biosciences
BD LSRFortessa™	BD Biosciences
BioRad gelelectrophoresis	BioRad
Cytospin 3	Shandon
Heracell™ 240i CO_2 incubator	Thermo Scientific
Herasafe™ KS	Thermo Scientific
LSM 780 microscope	Zeiss
LSM 5 PASCAL microscope	Zeiss
MACS® manual separators	Miltenyi Biotec
MACSQuant	Miltenyi Biotec
Mastercycler	Gradient Eppendorf
Microcentrifuge 5417R	Eppendorf
NanoDrop 2000 T	hermo Scientific
Odyssey infrared imaging system	LI-COR Inc.
Photometer	Eppendorf
Rotanta 460 R	Hettich
Thermomixer	Eppendorf
Vortex mixer, VV 3	VWR
Western blot system	Transblot

Table 4-8 Consumables

Consumable	Company
0.2 µm filters	BD Biosciences
Cell culture flasks	BD Biosciences
Cell culture tubes	Falcon
Cell strainers (100 µm, 70 µm, 40 µm)	BD Biosciences
Cuvettes	Fisher Scientific
Petri dish	BD Biosciences
Serological pipets	Thermo Scientific

5 APPENDIX

ABBREVATIONS

(ds)RNA	(double stranded) ribonucleic acid
AIM2	absent in melanoma 2
AM	alveolar macrophage
AMP	adenosine mono-phosphate
APC	antigen presenting cell
ASC	apoptosis-associated speck-like protein containing a carboxy-terminal CARD
BAL	bronchoalveolar lavage
BCG	Bacille Calmette-Guérin
BCR	B cell receptor
BIR	baculovirus inhibitor of apoptosis repeat
BMM	bone marrow-derived macrophage
CARD	caspase activation and recruitment
CASP1	caspase-1
CFU	colony forming unit
cGAMP	cyclic-GMP-AMP
cGAS	cGAMP synthase
DAPI	4',6-diamidino-2-phenylindole
DC	dendritic cell
DIC	differential interference contrast
DNA	deoxyribonucleic acid
DTR	diphtheria toxin receptor
DTX	diphtheria toxin
DUOX	dual oxidase
ER	endoplasmic reticulum
FADD	Fas-associated death domain
FcγR	fragment crystallizable (Fc) gamma receptor
GAF	gamma-activated factor
GAS	IFNγ activated site
GBP	guanylate binding protein
GFP	green fluorescent protein
GMP	guanosine mono-phosphate
GO	gene ontology
GTP	guanosine tri-phosphate
GVIN	very large inducible GTPases
HCV	Hepatitis C virus
ICL	isocitrate lyase
IFIT	IFN-induced protein with tetratricopeptide repeats
IFITM	IFN- inducible transmembrane
IFN	interferon
IFNAR	interferon α/β receptor
IFNGR	interferon γ receptor
IL-	interleukin-
iNOS	inducible nitrogen oxide synthase
IRF	interferon regulatory factor
IRG	immunity-related GTPase
IRG1	immunoresponsive gene 1
ISG	interferone stimulated gene
ISGF3	IFN–stimulated gene factor 3
ISRE	IFN-stimulated response elements
JAK	Janus kinase
LAMP-1	lysosome-associated membrane glycoprotein 1
LCV	*Legionella*-containing vacuole
LFQ	label free quantity

LGP2	laboratory of genetics and physiology 2
LPS	lipopolysaccharide
LRR	leucine rich repeat
m.o.i.	multiplicity of infection
MAVS	mitochondrial antiviral signaling
MCL	methylisocitrat lyase
MDA5	melanoma differentiation antigen 5
MDP	muramyl dipeptide
MHC	major histocompatibility complex
mROS	mitochondrial ROS
MX	myxoma resistance protein
MyD88	myloid differentiation primary response gene 88
NADPH	nicotinamide adenine dinucleotide phosphate
NAIP	NLR family, apoptosis inhibitory protein
NF-kB	nuclear factor 'kappa-light-chain-enhancer' of activated B-cells
NK cell	natural killer cell
NLR	NOD-like receptor
NO	nitrogen oxide
NOD	Nucleotide-binding, oligomerization domain
NOX	NADPH oxidase
OAS	oligoadenylate synthase
p.i.	post infection
PAMP	pathogen associated molecular pattern
PBS	phosphate buffered saline
PCC	propionyl-CoA carboxylase
PRR	pattern recognition receptor
PYD	pyrin domain
qRT-PCR	quantitative real-time polymerase chain reaction
Rab	Ras-related in brain
RIG-I	retinoic acid-inducible gene I
RIP1/3	receptor-interacting protein 1/3
RLR	RIG-I-like receptor
RNS	reactive nitrogen species
ROS	reactive oxygen species
RQ	relative quantity
RT	room temperature
s.e.m.	standard error of the mean
SNARE	soluble N-ethylmaleimide-sensitive-factor attachment receptor
STAT	signal transducer and activator of transcription
STING	stimulator of interferon genes
T4SS	type IV secretion system
TCA	tricarboxylic acid
TCR	T cell receptor
TLR	Toll-like receptor
TNF	tumor necrosis factor
TRIF	TIR-domain-containing adapter-inducing interferon-β
TYK	tyrosine kinase
WT	wild-type (concerning mice)
wt	wild-type (concerning bacteria)

REFERENCES

1. Fraser, D. W. *et al.* Legionnaires' disease: description of an epidemic of pneumonia. *N. Engl. J. Med.* **297,** 1189–97 (1977).
2. Brenner, D. J., Steigerwalt, A. G. & McDade, J. E. Classification of the Legionnaires' disease bacterium: Legionella pneumophila, genus novum, species nova, of the family Legionellaceae, familia nova. *Ann. Intern. Med.* **90,** 656–8 (1979).
3. Newton, H. J., Ang, D. K. Y., van Driel, I. R. & Hartland, E. L. Molecular pathogenesis of infections caused by Legionella pneumophila. *Clin. Microbiol. Rev.* **23,** 274–98 (2010).
4. Phin, N. *et al.* Epidemiology and clinical management of Legionnaires' disease. *Lancet Infect. Dis.* **3099,** 1–11 (2014).
5. Von Baum, H. *et al.* Community-acquired Legionella pneumonia: new insights from the German competence network for community acquired pneumonia. *Clin. Infect. Dis.* **46,** 1356–64 (2008).
6. Brodhun, B. & Buchholz, U. [Epidemiology of Legionnaires' disease in Germany.]. *Bundesgesundheitsblatt. Gesundheitsforschung. Gesundheitsschutz* **54,** 680–687 (2011).
7. Von Baum, H. & Lück, C. [Community-acquired Legionella pneumonia : Data from the CAPNETZ study.]. *Bundesgesundheitsblatt. Gesundheitsforschung. Gesundheitsschutz* **54,** 688–692 (2011).
8. Ginevra, C. *et al.* Host-related risk factors and clinical features of community-acquired legionnaires disease due to the Paris and Lorraine endemic strains, 1998-2007, France. *Clin. Infect. Dis.* **49,** 184–91 (2009).
9. Ricketts, K. D. & Joseph, C. A. Legionnaires disease in Europe: 2005-2006. *Euro Surveill.* **12,** E7–8 (2007).
10. Beauté, J., Robesyn, E. & de Jong, B. Legionnaires' disease in Europe: all quiet on the eastern front? *Eur. Respir. J.* **42,** 1454–8 (2013).
11. Beauté, J., Zucs, P. & de Jong, B. Legionnaires disease in Europe, 2009-2010. *Euro Surveill.* **18,** 20417 (2013).
12. Isberg, R. R., O'Connor, T. J. & Heidtman, M. The Legionella pneumophila replication vacuole: making a cosy niche inside host cells. *Nat. Rev. Microbiol.* **7,** 13–24 (2009).
13. Hubber, A. & Roy, C. R. Modulation of host cell function by Legionella pneumophila type IV effectors. *Annu. Rev. Cell Dev. Biol.* **26,** 261–83 (2010).
14. Rogers, J., Dowsett, A. B., Dennis, P. J., Lee, J. V & Keevil, C. W. Influence of temperature and plumbing material selection on biofilm formation and growth of Legionella pneumophila in a model potable water system containing complex microbial flora. *Appl. Environ. Microbiol.* **60,** 1585–92 (1994).
15. Murga, R. *et al.* Role of biofilms in the survival of Legionella pneumophila in a model potable-water system. *Microbiology* **147,** 3121–6 (2001).
16. Shin, S. & Roy, C. R. Host cell processes that influence the intracellular survival of Legionella pneumophila. *Cell. Microbiol.* **10,** 1209–20 (2008).
17. Garin, J. *et al.* The phagosome proteome: insight into phagosome functions. *J. Cell Biol.* **152,** 165–80 (2001).
18. Simonsen, A. *et al.* EEA1 links PI(3)K function to Rab5 regulation of endosome fusion. *Nature* **394,** 494–8 (1998).
19. Zerial, M. & McBride, H. Rab proteins as membrane organizers. *Nat. Rev. Mol. Cell Biol.* **2,** 107–17 (2001).
20. Luzio, J. P. *et al.* Relationship between endosomes and lysosomes. *Biochem. Soc. Trans.* **29,** 476–80 (2001).

21. Zhu, W. *et al.* Comprehensive identification of protein substrates of the Dot/Icm type IV transporter of Legionella pneumophila. *PLoS One* **6,** e17638 (2011).

22. Horwitz, M. A., A, J., Hartford, G. L. & Fellowship, F. Formation of a novel phagosome by the Legionnaires' disease bacterium (Legionella pneumophila) in human monocytes. *Infection* **158,** (1983).

23. Coers, J., Monahan, C. & Roy, C. R. Modulation of phagosome biogenesis by Legionella pneumophila creates an organelle permissive for intracellular growth. *Nat. Cell Biol.* **1,** 451–3 (1999).

24. Derré, I. & Isberg, R. R. Legionella pneumophila replication vacuole formation involves rapid recruitment of proteins of the early secretory system. *Infect. Immun.* **72,** 3048–53 (2004).

25. Kagan, J. C., Stein, M.-P., Pypaert, M. & Roy, C. R. Legionella subvert the functions of Rab1 and Sec22b to create a replicative organelle. *J. Exp. Med.* **199,** 1201–11 (2004).

26. Tilney, L. G., Harb, O. S., Connelly, P. S., Robinson, C. G. & Roy, C. R. How the parasitic bacterium Legionella pneumophila modifies its phagosome and transforms it into rough ER: implications for conversion of plasma membrane to the ER membrane. *J. Cell Sci.* **114,** 4637–50 (2001).

27. Horwitz, M. A. The Legionnaires' disease bacterium (Legionella pneumophila) inhibits phagosome-lysosome fusion in human monocytes. *J. Exp. Med.* **158,** 2108–26 (1983).

28. Horwitz, M. A. & Maxfield, F. R. Legionella pneumophila inhibits acidification of its phagosome in human monocytes. *J. Cell Biol.* **99,** 1936–43 (1984).

29. Wieland, H., Goetz, F. & Neumeister, B. Phagosomal acidification is not a prerequisite for intracellular multiplication of Legionella pneumophila in human monocytes. *J. Infect. Dis.* **189,** 1610–4 (2004).

30. Horwitz, M. A. & Silverstein, S. C. Legionnaires' disease bacterium (Legionella pneumophila) multiples intracellularly in human monocytes. *J. Clin. Invest.* **66,** 441–50 (1980).

31. Ramakrishna, B. S. Role of the gut microbiota in human nutrition and metabolism. *J. Gastroenterol. Hepatol.* **28,** 9–17 (2013).

32. Janeway, C. A. Approaching the asymptote? Evolution and revolution in immunology. *Cold Spring Harb. Symp. Quant. Biol.* **54,** 1–13 (1989).

33. Schatz, D. G., Oettinger, M. A. & Schlissel, M. S. V(D)J recombination: molecular biology and regulation. *Annu. Rev. Immunol.* **10,** 359–83 (1992).

34. Fearon, D. T. & Locksley, R. M. The instructive role of innate immunity in the acquired immune response. *Science* **272,** 50–3 (1996).

35. Iwasaki, A. & Medzhitov, R. Regulation of adaptive immunity by the innate immune system. *Science* **327,** 291–5 (2010).

36. Kupz, A. *et al.* NLRC4 inflammasomes in dendritic cells regulate noncognate effector function by memory $CD8^+$ T cells. *Nat. Immunol.* **13,** 162–9 (2012).

37. Ayres, J. S. & Vance, R. E. Cellular teamwork in antibacterial innate immunity. *Nat. Immunol.* **13,** 115–117 (2012).

38. Iwasaki, A. & Medzhitov, R. Control of adaptive immunity by the innate immune system. *Nat. Immunol.* **16,** 343–353 (2015).

39. Hemmi, H. *et al.* A Toll-like receptor recognizes bacterial DNA. *Nature* **408,** 740–5 (2000).

40. Alexopoulou, L., Holt, A. C., Medzhitov, R. & Flavell, R. A. Recognition of double-stranded RNA and activation of NF-kappaB by Toll-like receptor 3. *Nature* **413,** 732–8 (2001).

41. Pichlmair, A. *et al.* RIG-I-Mediated Antiviral Responses to Single-Stranded RNA Bearing 5'-Phosphates. *Science* **314,** 997–1001 (2006).

42. Smith, S. & Jefferies, C. Role of DNA/RNA sensors and contribution to autoimmunity. *Cytokine Growth Factor Rev.* **25,** 745–757 (2014).

43. Medzhitov, R. & Janeway, C. Innate immune recognition: mechanisms and pathways. *Immunol. Rev.* **173,** 89–97 (2000).

44. Janeway, C. A. & Medzhitov, R. Innate immune recognition. *Annu. Rev. Immunol.* **20,** 197–216 (2002).

45. Opitz, B., van Laak, V., Eitel, J. & Suttorp, N. Innate immune recognition in infectious and noninfectious diseases of the lung. *Am. J. Respir. Crit. Care Med.* **181,** 1294–309 (2010).

46. Metschnikoff, E. Lecture on Phagocytosis and Immunity. *Br. Med. J.* **1,** 213–7 (1891).

47. MacMicking, J. D. Recognizing macrophage activation and host defense. *Cell Host Microbe* **5,** 405–7 (2009).

48. Arango Duque, G. & Descoteaux, A. Macrophage cytokines: involvement in immunity and infectious diseases. *Front. Immunol.* **5,** 491 (2014).

49. Flannagan, R. S., Cosío, G. & Grinstein, S. Antimicrobial mechanisms of phagocytes and bacterial evasion strategies. *Nat. Rev. Microbiol.* **7,** 355–66 (2009).

50. Segal, A. W. How neutrophils kill microbes. *Annu. Rev. Immunol.* **23,** 197–223 (2005).

51. Pedrosa, J. *et al.* Neutrophils Play a Protective Nonphagocytic Role in Systemic Mycobacterium tuberculosis Infection of Mice. *Infect. Immun.* **68,** 577–583 (2000).

52. Tateda, K. *et al.* Early recruitment of neutrophils determines subsequent T1/T2 host responses in a murine model of Legionella pneumophila pneumonia. *J. Immunol.* **166,** 3355–61 (2001).

53. Spörri, R., Joller, N., Hilbi, H. & Oxenius, A. A novel role for neutrophils as critical activators of NK cells. *J. Immunol.* **181,** 7121–30 (2008).

54. Scapini, P. & Cassatella, M. A. Social networking of human neutrophils within the immune system. *Blood* **124,** 710–9 (2014).

55. Shi, C. & Pamer, E. G. Monocyte recruitment during infection and inflammation. *Nat. Rev. Immunol.* **11,** 762–774 (2011).

56. Medzhitov, R., Preston-Hurlburt, P. & Janeway, C. A. A human homologue of the Drosophila Toll protein signals activation of adaptive immunity. *Nature* **388,** 394–7 (1997).

57. Kawai, T. & Akira, S. Toll-like Receptors and Their Crosstalk with Other Innate Receptors in Infection and Immunity. *Immunity* **34,** 637–50 (2011).

58. Elinav, E., Strowig, T., Henao-Mejia, J. & Flavell, R. a. Regulation of the Antimicrobial Response by NLR Proteins. *Immunity* **34,** 665–79 (2011).

59. Schroder, K. & Tschopp, J. The inflammasomes. *Cell* **140,** 821–32 (2010).

60. Strowig, T., Henao-Mejia, J., Elinav, E. & Flavell, R. Inflammasomes in health and disease. *Nature* **481,** 278–286 (2012).

61. Kofoed, E. M. & Vance, R. E. Innate immune recognition of bacterial ligands by NAIPs determines inflammasome specificity. *Nature* **477,** 592–5 (2011).

62. Loo, Y.-M. & Gale, M. Immune Signaling by RIG-I-like Receptors. *Immunity* **34,** 680–92 (2011).

63. Luo, D. Toward a crystal-clear view of the viral RNA sensing and response by RIG-I-like receptors. *RNA Biol.* **11,** 25–32 (2014).

64. Holm, C. K., Paludan, S. R. & Fitzgerald, K. a. DNA recognition in immunity and disease. *Curr. Opin. Immunol.* **25,** 13–18 (2013).

65. Bhat, N. & Fitzgerald, K. A. Recognition of cytosolic DNA by cGAS and other STING-dependent sensors. *Eur. J. Immunol.* **44,** 634–40 (2014).

66. Sun, L., Wu, J., Du, F., Chen, X. & Chen, Z. J. Cyclic GMP-AMP Synthase Is a Cytosolic DNA Sensor That Activates the Type I Interferon Pathway. *Science* **339,** 786–791 (2012).

67. Wu, J. *et al.* Cyclic GMP-AMP Is an Endogenous Second Messenger in Innate Immune Signaling by Cytosolic DNA. *Science* **339,** 1–7 (2012).

68. Hornung, V. & Latz, E. Intracellular DNA recognition. *Nat. Rev. Immunol.* **10,** 123–30 (2010).

69. Sharma, S. & Fitzgerald, K. a. Innate Immune Sensing of DNA. *PLoS Pathog.* **7,** e1001310 (2011).

70. Pestka, S., Krause, C. D. & Walter, M. R. Interferons, interferon-like cytokines, and their receptors. *Immunol. Rev.* **202,** 8–32 (2004).

71. Platanias, L. C. Mechanisms of type-I- and type-II-interferon-mediated signalling. *Nat. Rev. Immunol.* **5,** 375–86 (2005).

72. Pestka, S. The interferons: 50 years after their discovery, there is much more to learn. *J. Biol. Chem.* **282,** 20047–51 (2007).

73. Ivashkiv, L. B. & Donlin, L. T. Regulation of type I interferon responses. *Nat. Rev. Immunol.* **14,** 36–49 (2013).

74. González-Navajas, J. M., Lee, J., David, M. & Raz, E. Immunomodulatory functions of type I interferons. *Nat. Rev. Immunol.* **12,** 125–35 (2012).

75. Kessler, D. S., Levy, D. E. & Darnell, J. E. Two interferon-induced nuclear factors bind a single promoter element in interferon-stimulated genes. *Proc. Natl. Acad. Sci. U. S. A.* **85,** 8521–5 (1988).

76. Platanias, L. C. & Fish, E. N. Signaling pathways activated by interferons. *Exp. Hematol.* **27,** 1583–92 (1999).

77. Aaronson, D. S. & Horvath, C. M. A road map for those who don't know JAK-STAT. *Science* **296,** 1653–5 (2002).

78. De Weerd, N. a *et al.* Structural basis of a unique interferon-β signaling axis mediated via the receptor IFNAR1. *Nat. Immunol.* **14,** 901–907 (2013).

79. Takaoka, A. & Yanai, H. Interferon signalling network in innate defence. *Cell. Microbiol.* **8,** 907–22 (2006).

80. Pestka, S. *et al.* The Interferon Gamma (IFN-y) Receptor : a Paradigm for the Multichain Cytokine Receptor. *Cytokine Growth Factor Rev.* **8,** 189–206 (1997).

81. Bach, E. A., Aguet, M. & Schreiber, R. D. THE IFN γ RECEPTOR : A Paradigm for Cytokine Receptor Signaling. *Annu. Rev. Immunol.* (1997).

82. MacMicking, J. D. Interferon-inducible effector mechanisms in cell-autonomous immunity. *Nat. Rev. Immunol.* **12,** 367–382 (2012).

83. Hertzog, P., Forster, S. & Samarajiwa, S. Systems biology of interferon responses. *J. Interferon Cytokine Res.* **31,** 5–11 (2011).

84. Der, S. D., Zhou, A., Williams, B. R. G. & Silverman, R. H. Identification of genes differentially regulated by interferon alpha, beta, or gamma using oligonucleotide arrays. *Proc. Natl. Acad. Sci.* **95,** 15623–15628 (1998).

85. Isaacs, A. & Lindenmann, J. Virus Interference. I. The Interferon. *Proc. R. Soc. B Biol. Sci.* **147,** 258–267 (1957).

86. Decker, T., Müller, M. & Stockinger, S. The yin and yang of type I interferon activity in bacterial infection. *Nat. Rev. Immunol.* **5,** 675–87 (2005).

87. Schoggins, J. W. *et al.* A diverse range of gene products are effectors of the type I interferon antiviral response. *Nature* **472,** 481–485 (2011).

88. Liu, S.-Y., Sanchez, D. J., Aliyari, R., Lu, S. & Cheng, G. Systematic identification of type I and type II interferon-induced antiviral factors. *Proc. Natl. Acad. Sci.* **109,** 4239–4244 (2012).

89. Li, J. *et al.* A Short Hairpin RNA Screen of Interferon-Stimulated Genes Identifies a Novel Negative Regulator of the Cellular Antiviral Response. *MBio* **18,** e00385–13 (2013).

90. Schoggins, J. W. *et al.* Pan-viral specificity of IFN-induced genes reveals new roles for cGAS in innate immunity. *Nature* **505,** 691–695 (2014).

91. Dittmann, M. *et al.* A Serpin Shapes the Extracellular Environment to Prevent Influenza A Virus Maturation. *Cell* **160,** 631–643 (2015).

92. Zhang, Y., Burke, C. W., Ryman, K. D. & Klimstra, W. B. Identification and characterization of interferon-induced proteins that inhibit alphavirus replication. *J. Virol.* **81,** 11246–55 (2007).

93. Metz, P. *et al.* Identification of type I and type II interferon-induced effectors controlling hepatitis C virus replication. *Hepatology* **56,** 2082–93 (2012).

94. Fusco, D. N. *et al.* A genetic screen identifies interferon-α effector genes required to suppress hepatitis C virus replication. *Gastroenterology* **144,** 1438–49, 1449.e1–9 (2013).

95. Weekes, M. P. *et al.* Quantitative Temporal Viromics: An Approach to Investigate Host-Pathogen Interaction. *Cell* **157,** 1460–1472 (2014).

96. Hornung, V., Hartmann, R., Ablasser, A. & Hopfner, K.-P. OAS proteins and cGAS: unifying concepts in sensing and responding to cytosolic nucleic acids. *Nat. Rev. Immunol.* **14,** 521–8 (2014).

97. Diamond, M. S. & Farzan, M. The broad-spectrum antiviral functions of IFIT and IFITM proteins. *Nat. Rev. Immunol.* **3,** (2012).

98. Seo, J.-Y., Yaneva, R. & Cresswell, P. Viperin: a multifunctional, interferon-inducible protein that regulates virus replication. *Cell Host Microbe* **10,** 534–9 (2011).

99. Skaug, B. & Chen, Z. J. Emerging Role of ISG15 in Antiviral Immunity. *Cell* **143,** 187–90 (2010).

100. Wang, X., Hinson, E. R. & Cresswell, P. The interferon-inducible protein viperin inhibits influenza virus release by perturbing lipid rafts. *Cell Host Microbe* **2,** 96–105 (2007).

101. Jeon, Y. J., Yoo, H. M. & Chung, C. H. ISG15 and immune diseases. *Biochim. Biophys. Acta* **1802,** 485–96 (2010).

102. Kim, B.-H., Shenoy, A. R., Kumar, P., Bradfield, C. J. & MacMicking, J. D. IFN-inducible GTPases in host cell defense. *Cell Host Microbe* **12,** 432–44 (2012).

103. Taylor, G. a *et al.* Pathogen-specific loss of host resistance in mice lacking the IFN-gamma-inducible gene IGTP. *Proc. Natl. Acad. Sci. U. S. A.* **97,** 751–5 (2000).

104. Taylor, G. A., Feng, C. G. & Sher, A. p47 GTPases: regulators of immunity to intracellular pathogens. *Nat. Rev. Immunol.* **4,** 100–9 (2004).

105. MacMicking, J. D. Immune control of phagosomal bacteria by p47 GTPases. *Curr. Opin. Microbiol.* **8,** 74–82 (2005).

106. Haldar, A. K. *et al.* IRG and GBP Host Resistance Factors Target Aberrant, 'Non-self' Vacuoles Characterized by the Missing of 'Self' IRGM Proteins. *PLoS Pathog.* **9,** e1003414 (2013).

107. Bekpen, C. *et al.* The interferon-inducible p47 (IRG) GTPases in vertebrates: loss of the cell autonomous resistance mechanism in the human lineage. *Genome Biol.* **6,** R92 (2005).

108. MacMicking, J. D. IFN-inducible GTPases and immunity to intracellular pathogens. *Trends Immunol.* **25,** 601–9 (2004).

109. Martens, S. & Howard, J. The interferon-inducible GTPases. *Annu. Rev. Cell Dev. Biol.* **22,** 559–89 (2006).

110. Man, S. M. *et al.* The transcription factor IRF1 and guanylate-binding proteins target activation of the AIM2 inflammasome by Francisella infection. *Nat. Immunol.* **16,** 467–475 (2015).

111. Meunier, E. *et al.* Guanylate-binding proteins promote activation of the AIM2 inflammasome during infection with Francisella novicida. *Nat. Immunol.* **16,** 476–484 (2015).

112. Kim, B.-H. *et al.* A family of IFN-gamma-inducible 65-kD GTPases protects against bacterial infection. *Science* **332,** 717–21 (2011).

113. Yamamoto, M. *et al.* A cluster of interferon-γ-inducible p65 GTPases plays a critical role in host defense against Toxoplasma gondii. *Immunity* **37,** 302–13 (2012).

114. Shenoy, A. R. *et al.* GBP5 promotes NLRP3 inflammasome assembly and immunity in mammals. *Science* **336,** 481–5 (2012).

115. Pilla, D. M. *et al.* Guanylate binding proteins promote caspase-11-dependent pyroptosis in response to cytoplasmic LPS. *Proc. Natl. Acad. Sci. U. S. A.* **111,** 6046–51 (2014).

116. Meunier, E. *et al.* Caspase-11 activation requires lysis of pathogen-containing vacuoles by IFN-induced GTPases. *Nature* **509,** 366–70 (2014).

117. Shi, J. *et al.* Inflammatory caspases are innate immune receptors for intracellular LPS. *Nature* **514,** 187–192 (2014).

118. Lee, C. G., Jenkins, N. A., Gilbert, D. J., Copeland, N. G. & O'Brien, W. E. Cloning and analysis of gene regulation of a novel LPS-inducible cDNA. *Immunogenetics* **41,** 263–70 (1995).

119. Degrandi, D., Hoffmann, R., Beuter-Gunia, C. & Pfeffer, K. The proinflammatory cytokine-induced IRG1 protein associates with mitochondria. *J. Interferon Cytokine Res.* **29,** 55–67 (2009).

120. Cho, H. *et al.* Differential innate immune response programs in neuronal subtypes determine susceptibility to infection in the brain by positive-stranded RNA viruses. *Nat. Med.* **19,** 458–64 (2013).

121. Michelucci, A. *et al.* Immune-responsive gene 1 protein links metabolism to immunity by catalyzing itaconic acid production. *Proc. Natl. Acad. Sci. U. S. A.* **110,** 7820–5 (2013).

122. McFadden, B. A. & Purohit, S. Itaconate, an isocitrate lyase-directed inhibitor in Pseudomonas indigofera. *J. Bacteriol.* **131,** 136–44 (1977).

123. Hillier, S. & Charnetzky, W. T. Glyoxylate bypass enzymes in Yersinia species and multiple forms of isocitrate lyase in Yersinia pestis. *J. Bacteriol.* **145,** 452–8 (1981).

124. McKinney, J. D. *et al.* Persistence of Mycobacterium tuberculosis in macrophages and mice requires the glyoxylate shunt enzyme isocitrate lyase. *Nature* **406,** 735–8 (2000).

125. Sasikaran, J., Ziemski, M., Zadora, P. K., Fleig, A. & Berg, I. a. Bacterial itaconate degradation promotes pathogenicity. *Nat. Chem. Biol.* **10,** 371–7 (2014).

126. Li, Y. *et al.* Immune responsive gene 1 (IRG1) promotes endotoxin tolerance by increasing A20 expression in macrophages through reactive oxygen species. *J. Biol. Chem.* **288,** 16225–34 (2013).

127. Hall, C. J. *et al.* Immunoresponsive Gene 1 Augments Bactericidal Activity of Macrophage-Lineage Cells by Regulating β-Oxidation-Dependent Mitochondrial ROS Production. *Cell Metab.* **18,** 265–278 (2013).

128. Stuehr, D. J., Cho, H. J., Kwon, N. S., Weise, M. F. & Nathan, C. F. Purification and characterization of the cytokine-induced macrophage nitric oxide synthase: an FAD- and FMN-containing flavoprotein. *Proc. Natl. Acad. Sci. U. S. A.* **88,** 7773–7 (1991).

129. Gao, J. J. *et al.* Autocrine/paracrine IFN-alphabeta mediates the lipopolysaccharide-induced activation of transcription factor Stat1alpha in mouse macrophages: pivotal role of Stat1alpha in induction of the inducible nitric oxide synthase gene. *J. Immunol.* **161,** 4803–10 (1998).

130. Bogdan, C. Nitric oxide and the immune response. *Nat. Immunol.* **2,** 907–16 (2001).

131. Nathan, C. & Shiloh, M. U. Reactive oxygen and nitrogen intermediates in the relationship between mammalian hosts and microbial pathogens. *Proc. Natl. Acad. Sci. U. S. A.* **97,** 8841–8848 (2000).

132. Trost, M. *et al.* The phagosomal proteome in interferon-gamma-activated macrophages. *Immunity* **30,** 143–54 (2009).

133. Dhariwala, M. O. & Anderson, D. M. Bacterial programming of host responses: coordination between type I interferon and cell death. *Front. Microbiol.* **5,** 545 (2014).

134. Navarini, A. A. *et al.* Increased susceptibility to bacterial superinfection as a consequence of innate antiviral responses. *Proc. Natl. Acad. Sci. U. S. A.* **103,** 15535–9 (2006).

135. Robinson, N. *et al.* Type I interferon induces necroptosis in macrophages during infection with Salmonella enterica serovar Typhimurium. *Nat. Immunol.* **13,** 954–962 (2012).

136. McComb, S. *et al.* Type-I interferon signaling through ISGF3 complex is required for sustained Rip3 activation and necroptosis in macrophages. *Proc. Natl. Acad. Sci. U. S. A.* **111,** 1–8 (2014).

137. Thapa, R. J. *et al.* Interferon-induced RIP1/RIP3-mediated necrosis requires PKR and is licensed by FADD and caspases. *Proc. Natl. Acad. Sci. U. S. A.* **110,** 3109–3118 (2013).

138. Henry, T., Brotcke, A., Weiss, D. S., Thompson, L. J. & Monack, D. M. Type I interferon signaling is required for activation of the inflammasome during Francisella infection. *J. Exp. Med.* **204,** 987–94 (2007).

139. Storek, K. M., Gertsvolf, N. a., Ohlson, M. B. & Monack, D. M. cGAS and Ifi204 Cooperate To Produce Type I IFNs in Response to Francisella Infection. *J. Immunol.* **194,** 3236–3245 (2015).

140. Rathinam, V. A. K. *et al.* TRIF Licenses Caspase-11-Dependent NLRP3 Inflammasome Activation by Gram-Negative Bacteria. *Cell* **18,** 1–14 (2012).

141. Case, C. L. *et al.* Caspase-11 stimulates rapid flagellin-independent pyroptosis in response to Legionella pneumophila. *Proc. Natl. Acad. Sci. U. S. A.* **110,** 1851–1856 (2013).

142. Medzhitov, R. Recognition of microorganisms and activation of the immune response. *Nature* **449,** 819–826 (2007).

143. Chaplin, D. D. Overview of the immune response. *J. Allergy Clin. Immunol.* **125,** S3–23 (2010).

144. Archer, K. a, Ader, F., Kobayashi, K. S., Flavell, R. a & Roy, C. R. Cooperation between multiple microbial pattern recognition systems is important for host protection against the intracellular pathogen Legionella pneumophila. *Infect. Immun.* **78,** 2477–87 (2010).

145. Akamine, M. *et al.* Differential roles of Toll-like receptors 2 and 4 in in vitro responses of macrophages to Legionella pneumophila. *Infect. Immun.* **73,** 352–61 (2005).

146. Archer, K. A. & Roy, C. R. MyD88-dependent responses involving toll-like receptor 2 are important for protection and clearance of Legionella pneumophila in a mouse model of Legionnaires' disease. *Infect. Immun.* **74,** 3325–33 (2006).

147. Fuse, E. T. *et al.* Role of Toll-like receptor 2 in recognition of Legionella pneumophila in a murine pneumonia model. *J. Med. Microbiol.* **56,** 305–12 (2007).

148. Girard, R. *et al.* Lipopolysaccharides from Legionella and Rhizobium stimulate mouse bone marrow granulocytes via Toll-like receptor 2. *J. Cell Sci.* **116,** 293–302 (2003).

149. Newton, C. A., Perkins, I., Widen, R. H., Friedman, H. & Klein, T. W. Role of Toll-like receptor 9 in Legionella pneumophila-induced interleukin-12 p40 production in bone marrow-derived dendritic cells and macrophages from permissive and nonpermissive mice. *Infect. Immun.* **75,** 146–51 (2007).

150. Bhan, U. *et al.* Toll-like receptor 9 regulates the lung macrophage phenotype and host immunity in murine pneumonia caused by Legionella pneumophila. *Infect. Immun.* **76,** 2895–904 (2008).

151. Blanchard, D. K., Djeu, J. Y., Klein, T. W., Friedman, H. & Stewart, W. E. Protective effects of tumor necrosis factor in experimental Legionella pneumophila infections of mice via activation of PMN function. *J. Leukoc. Biol.* **43,** 429–35 (1988).

152. Fujita, M. *et al.* TNF receptor 1 and 2 contribute in different ways to resistance to Legionella pneumophila-induced mortality in mice. *Cytokine* **44,** 298–303 (2008).

153. Hawn, T. R., Smith, K. D., Aderem, A. & Skerrett, S. J. Myeloid differentiation primary response gene (88)- and toll-like receptor 2-deficient mice are susceptible to infection with aerosolized Legionella pneumophila. *J. Infect. Dis.* **193,** 1693–702 (2006).

154. Archer, K. A., Alexopoulou, L., Flavell, R. A. . & Roy, C. R. Multiple MyD88-dependent responses contribute to pulmonary clearance of Legionella pneumophila. *Cell. Microbiol.* **11,** 21–36 (2009).

155. Hawn, T. R. *et al.* Altered inflammatory responses in TLR5-deficient mice infected with Legionella pneumophila. *J. Immunol.* **179,** 6981–7 (2007).

156. Frutuoso, M. S. *et al.* The pattern recognition receptors Nod1 and Nod2 account for neutrophil recruitment to the lungs of mice infected with Legionella pneumophila. *Microbes Infect.* **12,** (2010).

157. Shin, S. *et al.* Type IV secretion-dependent activation of host MAP kinases induces an increased proinflammatory cytokine response to Legionella pneumophila. *PLoS Pathog.* **4,** e1000220 (2008).

158. Diez, E. *et al.* Birc1e is the gene within the Lgn1 locus associated with resistance to Legionella pneumophila. *Nat. Genet.* **33,** 55–60 (2002).

159. Wright, E. K. *et al.* Naip5 affects host susceptibility to the intracellular pathogen Legionella pneumophila. *Curr. Biol.* **13,** 27–36 (2003).

160. Lightfield, K. L. *et al.* Differential Requirements for NAIP5 in Activation of the NLRC4 Inflammasome. *Infect. Immun.* **79,** 1606–14 (2011).

161. Mariathasan, S. *et al.* Differential activation of the inflammasome by caspase-1 adaptors ASC and Ipaf. *Nature* **430,** 213–8 (2004).

162. Pereira, M. S. F., Marques, G. G., DelLama, J. E. & Zamboni, D. S. The Nlrc4 Inflammasome Contributes to Restriction of Pulmonary Infection by Flagellated Legionella spp. that Trigger Pyroptosis. *Front. Microbiol.* **2,** 1–6 (2011).

163. Poyet, J. L. *et al.* Identification of Ipaf, a human caspase-1-activating protein related to Apaf-1. *J. Biol. Chem.* **276,** 28309–13 (2001).

164. Zamboni, D. S. *et al.* The Birc1e cytosolic pattern-recognition receptor contributes to the detection and control of Legionella pneumophila infection. *Nat. Immunol.* **7,** 318–325 (2006).

165. Amer, A. *et al.* Regulation of Legionella phagosome maturation and infection through flagellin and host Ipaf. *J. Biol. Chem.* **281,** 35217–35223 (2006).

166. Fortier, A., de Chastellier, C., Balor, S. & Gros, P. Birc1e/Naip5 rapidly antagonizes modulation of phagosome maturation by Legionella pneumophila. *Cell. Microbiol.* **9,** 910–23 (2007).

167. Molofsky, A. B. *et al.* Cytosolic recognition of flagellin by mouse macrophages restricts Legionella pneumophila infection. *J. Exp. Med.* **203,** 1093 (2006).

168. Ren, T., Zamboni, D. S., Roy, C. R., Dietrich, W. F. & Vance, R. E. Flagellin-deficient Legionella mutants evade caspase-1- and Naip5-mediated macrophage immunity. *PLoS Pathog.* **2,** e18 (2006).

169. Casson, C. N. *et al.* Caspase-11 Activation in Response to Bacterial Secretion Systems that Access the Host Cytosol. *PLoS Pathog.* **9,** e1003400 (2013).

170. Case, C. L., Shin, S. & Roy, C. R. Asc and Ipaf Inflammasomes direct distinct pathways for caspase-1 activation in response to Legionella pneumophila. *Infect. Immun.* **77,** 1981–91 (2009).

171. Aachoui, Y. *et al.* Caspase-11 protects against bacteria that escape the vacuole. *Science* **339,** 975–8 (2013).

172. Akhter, A. *et al.* Caspase-11 promotes the fusion of phagosomes harboring pathogenic bacteria with lysosomes by modulating actin polymerization. *Immunity* **37,** 35–47 (2012).

173. Fontana, M. F. *et al.* Secreted Bacterial effectors that inhibit host protein synthesis are critical for induction of the innate immune response to virulent Legionella pneumophila. *PLoS Pathog.* **7,** e1001289 (2011).

174. Ivanov, S. S. & Roy, C. R. Pathogen signatures activate a ubiquitination pathway that modulates the function of the metabolic checkpoint kinase mTOR. *Nat. Immunol.* **14,** 1219–28 (2013).

175. Barry, K. C., Fontana, M. F., Portman, J. L., Dugan, A. S. & Vance, R. E. IL-1α Signaling Initiates the Inflammatory Response to Virulent Legionella pneumophila In Vivo. *J. Immunol.* **190,** 6329–6339 (2013).

176. Leibundgut-Landmann, S., Weidner, K., Hilbi, H. & Oxenius, A. Nonhematopoietic cells are key players in innate control of bacterial airway infection. *J. Immunol.* **186,** 3130–7 (2011).

177. Horwitz, M. A. & Silverstein, S. C. Interaction of the legionnaires' disease bacterium (Legionella pneumophila) with human phagocytes. II. Antibody promotes binding of L. pneumophila to monocytes but does not inhibit intracellular multiplication. *J. Exp. Med.* **153,** 398–406 (1981).

178. Weinbaum, D. L., Bailey, J., Benner, R. R., Pasculle, A. W. & Dowling, J. N. The contribution of human neutrophils and serum to host defense against Legionella micdadei. *J. Infect. Dis.* **148,** 510–7 (1983).

179. Heath, L. *et al.* Effector mechanisms responsible for gamma interferon-mediated host resistance to Legionella pneumophila lung infection: the role of endogenous nitric oxide differs in susceptible and resistant murine hosts. *Infect. Immun.* **64,** 5151–60 (1996).

180. Shinozawa, Y. *et al.* Role of interferon-gamma in inflammatory responses in murine respiratory infection with Legionella pneumophila. *J. Med. Microbiol.* **51,** 225–30 (2002).

181. Spörri, R., Joller, N., Albers, U., Hilbi, H. & Oxenius, A. MyD88-dependent IFN-gamma production by NK cells is key for control of Legionella pneumophila infection. *J. Immunol.* **176,** 6162 (2006).

182. Ang, D. K. Y. *et al.* Cutting edge: Pulmonary Legionella pneumophila is controlled by plasmacytoid dendritic cells but not type I IFN. *J. Immunol.* **184,** 5429–33 (2010).

183. Opitz, B. *et al.* Legionella pneumophila Induces IFN beta in Lung Epithelial Cells via IPS-1 and IRF3 , Which Also Control Bacterial Replication. *J. Biol. Chem.* **281,** 36173–36179 (2006).

184. Stetson, D. B. & Medzhitov, R. Recognition of cytosolic DNA activates an IRF3-dependent innate immune response. *Immunity* **24,** 93–103 (2006).

185. Lippmann, J. *et al.* Dissection of a type I interferon pathway in controlling bacterial intracellular infection in mice. *Cell. Microbiol.* **13,** 1668–1682 (2011).

186. Vogel, J. P., Andrews, H. L., Wong, S. K. & Isberg, R. R. Conjugative transfer by the virulence system of Legionella pneumophila. *Science* **279,** 873–6 (1998).

187. Creasey, E. a & Isberg, R. R. The protein SdhA maintains the integrity of the Legionella-containing vacuole. *Proc. Natl. Acad. Sci. U. S. A.* **109,** 3481–3486 (2012).

188. Ge, J., Gong, Y.-N., Xu, Y. & Shao, F. Preventing bacterial DNA release and absent in melanoma 2 inflammasome activation by a Legionella effector functioning in membrane trafficking. *Proc. Natl. Acad. Sci.* **109,** 6193–6198 (2012).

189. Monroe, K. M., McWhirter, S. M. & Vance, R. E. Identification of host cytosolic sensors and bacterial factors regulating the type I interferon response to Legionella pneumophila. *PLoS Pathog.* **5,** e1000665 (2009).

190. Ishikawa, H., Ma, Z. & Barber, G. N. STING regulates intracellular DNA-mediated, type I interferon-dependent innate immunity. *Nature* **461,** 788–92 (2009).

191. Sun, W. *et al.* ERIS, an endoplasmic reticulum IFN stimulator, activates innate immune signaling through dimerization. *Proc. Natl. Acad. Sci. U. S. A.* **106,** 8653–8 (2009).

192. Ablasser, A. *et al.* RIG-I-dependent sensing of poly(dA:dT) through the induction of an RNA polymerase III-transcribed RNA intermediate. *Nat. Immunol.* **10,** 1065–72 (2009).

193. Chiu, Y.-H., Macmillan, J. B. & Chen, Z. J. RNA polymerase III detects cytosolic DNA and induces type I interferons through the RIG-I pathway. *Cell* **138,** 576–91 (2009).

194. Takaoka, A. *et al.* DAI (DLM-1/ZBP1) is a cytosolic DNA sensor and an activator of innate immune response. *Nature* **448,** 501–5 (2007).

195. Unterholzner, L. *et al.* IFI16 is an innate immune sensor for intracellular DNA. *Nat. Immunol.* **11,** 997–1004 (2010).

196. Zhang, Z. *et al.* The helicase DDX41 senses intracellular DNA mediated by the adaptor STING in dendritic cells. *Nat. Immunol.* **12,** 959–965 (2011).

197. Lippmann, J. *et al.* IFNbeta responses induced by intracellular bacteria or cytosolic DNA in different human cells do not require ZBP1 (DLM-1/DAI). *Cell. Microbiol.* **10,** 2579–88 (2008).

198. Burdette, D. L. *et al.* STING is a direct innate immune sensor of cyclic di-GMP. *Nature* **478,** 515–8 (2011).

199. Jin, L. *et al.* MPYS is required for IFN response factor 3 activation and type I IFN production in the response of cultured phagocytes to bacterial second messengers cyclic-di-AMP and cyclic-di-GMP. *J. Immunol.* **187,** 2595–601 (2011).

200. Abdul-Sater, A. a *et al.* The overlapping host responses to bacterial cyclic dinucleotides. *Microbes Infect.* **11,** 1–10 (2011).

201. Schiavoni, G. *et al.* Type I IFN protects permissive macrophages from Legionella pneumophila infection through an IFN-gamma-independent pathway. *J. Immunol.* **173,** 1266–75 (2004).

202. Coers, J., Vance, R. E., Fontana, M. F. & Dietrich, W. F. Restriction of Legionella pneumophila growth in macrophages requires the concerted action of cytokine and Naip5/Ipaf signalling pathways. *Cell. Microbiol.* **9,** 2344–2357 (2007).

203. Plumlee, C. R. *et al.* Interferons direct an effective innate response to Legionella pneumophila infection. *J. Biol. Chem.* **284,** 30058–66 (2009).

204. Susa, M., Ticac, B., Rukavina, T., Doric, M. & Marre, R. Legionella pneumophila Infection in Intratracheally Inoculated T Cell-Depleted or -Nondepleted A/J Mice. *J. Immunol.* **160,** 316–321 (1998).

205. Kikuchi, T. *et al.* Involvement of fractalkine/CX3CL1 expression by dendritic cells in the enhancement of host immunity against Legionella pneumophila. *Infect. Immun.* **73,** 5350–7 (2005).

206. Neild, A. L., Roy, C. R. & Haven, N. Legionella Reveal Dendritic Cell Functions that Facilitate Selection of Antigens for MHC Class II Presentation. **18,** 813–823 (2003).

207. Neild, A., Murata, T. & Roy, C. R. Processing and Major Histocompatibility Complex Class II Presentation of Legionella pneumophila Antigens by Infected Macrophages. *Infect. Immun.* **73,** 2336–43 (2005).

208. Brieland, J. K. *et al.* Humoral Immunity and Regulation of Intrapulmonary Growth of Legionella pneumophila in the Immunocompetent Host. *J. Immunol.* (1996).

209. Joller, N., Spörri, R., Hilbi, H. & Oxenius, A. Induction and protective role of antibodies in Legionella pneumophila infection. *Eur. J. Immunol.* **37,** 3414–23 (2007).

210. Joller, N. *et al.* Antibodies protect against intracellular bacteria by Fc receptor-mediated lysosomal targeting. *Proc. Natl. Acad. Sci. U. S. A.* **107,** 20441–6 (2010).

211. Kumar, Y. & Valdivia, R. H. Leading a Sheltered Life: Intracellular Pathogens and Maintenance of Vacuolar Compartments. *Cell Host Microbe* **5,** 593–601 (2009).

212. Randow, F., MacMicking, J. D. & James, L. C. Cellular self-defense: how cell-autonomous immunity protects against pathogens. *Science* **340,** 701–6 (2013).

213. Copenhaver, A. M. *et al.* Alveolar macrophages and neutrophils are the primary reservoirs for Legionella pneumophila and mediate cytosolic surveillance of type IV secretion. *Infect. Immun.* **82,** 4325–36 (2014).

214. Nogueira, C. V *et al.* Rapid pathogen-induced apoptosis: a mechanism used by dendritic cells to limit intracellular replication of Legionella pneumophila. *PLoS Pathog.* **5,** e1000478 (2009).

215. Nash, T. W., Libby, D. M. & Horwitz, M. A. Interaction between the legionnaires' disease bacterium (Legionella pneumophila) and human alveolar macrophages. Influence of antibody, lymphokines, and hydrocortisone. *J. Clin. Invest.* **74,** 771–82 (1984).

216. Hoffmann, C., Finsel, I. & Hilbi, H. Pathogen vacuole purification from legionella-infected amoeba and macrophages. *Methods Mol. Biol.* **954,** 309–21 (2013).

217. Hoffmann, C. *et al.* Functional analysis of novel Rab GTPases identified in the proteome of purified Legionella-containing vacuoles from macrophages. *Cell. Microbiol.* **16,** 1034–1052 (2013).

218. Samarajiwa, S. A., Forster, S., Auchettl, K. & Hertzog, P. J. INTERFEROME: the database of interferon regulated genes. *Nucleic Acids Res.* **37,** D852–7 (2009).

219. Price, C. T. D. & Abu Kwaik, Y. The Transcriptome of Legionella pneumophila-Infected Human Monocyte-Derived Macrophages. *PLoS One* **9,** e114914 (2014).

220. Jäger, J. *et al.* Human lung tissue explants reveal novel interactions during Legionella pneumophila infections. *Infect. Immun.* **82,** 275–85 (2014).

221. Rajagopalan-Levasseur, P., Lecointe, D., Bertrand, G., Fay, M. & Gougerot-Pocidalo, M. A. Differential nitric oxide (NO) production by macrophages from mice and guinea pigs infected with virulent and avirulent Legionella pneumophila serogroup 1. *Clin. Exp. Immunol.* **104,** 48–53 (1996).

222. Brieland, J. K. *et al.* In vivo regulation of replicative Legionella pneumophila lung infection by endogenous tumor necrosis factor alpha and nitric oxide. *Infect. Immun.* **63,** 3253–8 (1995).

223. Miller, B. H. *et al.* Mycobacteria inhibit nitric oxide synthase recruitment to phagosomes during macrophage infection. *Infect. Immun.* **72,** 2872–8 (2004).

224. Davis, A. S. *et al.* Mechanism of inducible nitric oxide synthase exclusion from mycobacterial phagosomes. *PLoS Pathog.* **3,** e186 (2007).

225. Degrandi, D. *et al.* Extensive Characterization of IFN-Induced GTPases mGBP1 to mGBP10 Involved in Host Defense. *J. Immunol.* **179,** 7729–40 (2007).

226. Degrandi, D. *et al.* Murine guanylate binding protein 2 (mGBP2) controls Toxoplasma gondii replication. *Proc. Natl. Acad. Sci. U. S. A.* **110,** 294–9 (2013).

227. Zhao, Y. O., Könen-Waisman, S., Taylor, G. a, Martens, S. & Howard, J. C. Localisation and mislocalisation of the interferon-inducible immunity-related GTPase, Irgm1 (LRG-47) in mouse cells. *PLoS One* **5,** e8648 (2010).

228. Mahmoud, M. E., Ui, F., Salman, D., Nishimura, M. & Nishikawa, Y. Mechanisms of interferon-beta-induced inhibition of Toxoplasma gondii growth in murine macrophages and embryonic fibroblasts: role of immunity-related GTPase M1. *Cell. Microbiol.* **17,** 1069–83 (2015).

229. Heidtman, M., Chen, E. J., Moy, M.-Y. & Isberg, R. R. Large-scale identification of Legionella pneumophila Dot/Icm substrates that modulate host cell vesicle trafficking pathways. *Cell. Microbiol.* **11,** 230–48 (2009).

230. Nakamura, N. *et al.* Endosomes are specialized platforms for bacterial sensing and NOD2 signalling. *Nature* **509,** 240–4 (2014).

231. Sokolovska, A. *et al.* Activation of caspase-1 by the NLRP3 inflammasome regulates the NADPH oxidase NOX2 to control phagosome function. *Nat. Immunol.* **14,** 543–53 (2013).

232. Laguette, N. *et al.* SAMHD1 is the dendritic- and myeloid-cell-specific HIV-1 restriction factor counteracted by Vpx. *Nature* **474,** 654–7 (2011).

233. Ryoo, J. *et al.* The ribonuclease activity of SAMHD1 is required for HIV-1 restriction. *Nat. Med.* **20,** 936–41 (2014).

234. MacMicking, J. D., Taylor, G. A. & McKinney, J. D. Immune control of tuberculosis by IFN-gamma-inducible LRG-47. *Science* **302,** 654–9 (2003).

235. Vidal, S. *et al.* The Ity/Lsh/Bcg locus: natural resistance to infection with intracellular parasites is abrogated by disruption of the Nramp1 gene. *J. Exp. Med.* **182,** 655–66 (1995).

236. Campbell-Valois, F.-X. *et al.* Quantitative proteomics reveals that only a subset of the endoplasmic reticulum contributes to the phagosome. *Mol. Cell. Proteomics* **11,** M111.016378 (2012).

237. Clague, M. J., Urbé, S. & de Lartigue, J. Phosphoinositides and the endocytic pathway. *Exp. Cell Res.* **315,** 1627–31 (2009).

238. Basler, T., Jeckstadt, S., Valentin-weigand, P. & Goethe, R. Mycobacterium paratuberculosis, Mycobacterium smegmatis, and lipopolysaccharide induce different transcriptional and post-transcriptional regulation of the IRG1 gene in murine macrophages. *J. Leukoc. Biol.* **79,** 628–38 (2006).

239. Peirce, M. J. *et al.* Themis2/ICB1 is a signaling scaffold that selectively regulates macrophage Toll-like receptor signaling and cytokine production. *PLoS One* **5,** e11465 (2010).

240. Hsu, P. D., Lander, E. S. & Zhang, F. Development and Applications of CRISPR-Cas9 for Genome Engineering. *Cell* **157,** 1262–1278 (2014).

241. Matsumoto, A., Bessho, H., Uehira, K. & Suda, T. Morphological studies of the association of mitochondria with chlamydial inclusions and the fusion of chlamydial inclusions. *J. Electron Microsc. (Tokyo).* **40,** 356–63 (1991).

242. Sinai, A. P. & Joiner, K. A. The Toxoplasma gondii protein ROP2 mediates host organelle association with the parasitophorous vacuole membrane. *J. Cell Biol.* **154,** 95–108 (2001).

243. Scanlon, M., Leitch, G. J., Visvesvara, G. S. & Shaw, A. P. Relationship between the host cell mitochondria and the parasitophorous vacuole in cells infected with Encephalitozoon microsporidia. *J. Eukaryot. Microbiol.* **51,** 81–7 (2004).

244. Pernas, L. *et al.* Toxoplasma effector MAF1 mediates recruitment of host mitochondria and impacts the host response. *PLoS Biol.* **12,** e1001845 (2014).

245. Chong, A., Lima, C. a, Allan, D. S., Nasrallah, G. K. & Garduño, R. a. The purified and recombinant Legionella pneumophila chaperonin alters mitochondrial trafficking and microfilament organization. *Infect. Immun.* **77,** 4724–39 (2009).

246. Degtyar, E., Zusman, T., Ehrlich, M. & Segal, G. A Legionella effector acquired from protozoa is involved in sphingolipids metabolism and is targeted to the host cell mitochondria. *Cell. Microbiol.* **11,** 1219–1235 (2009).

247. Dolezal, P. *et al.* Legionella pneumophila secretes a mitochondrial carrier protein during infection. *PLoS Pathog.* **8,** e1002459 (2012).

248. West, a P. *et al.* TLR signalling augments macrophage bactericidal activity through mitochondrial ROS. *Nature* **472,** 476–80 (2011).

249. Seth, R. B., Sun, L., Ea, C.-K. & Chen, Z. J. Identification and characterization of MAVS, a mitochondrial antiviral signaling protein that activates NF-kappaB and IRF 3. *Cell* **122,** 669–82 (2005).

250. Weinberg, S. E., Sena, L. a & Chandel, N. S. Mitochondria in the Regulation of Innate and Adaptive Immunity. *Immunity* **42,** 406–417 (2015).

251. West, a P., Shadel, G. S. & Ghosh, S. Mitochondria in innate immune responses. *Nat. Rev. Immunol.* **11,** 389–402 (2011).

252. Zhou, Z. *et al.* TRIM14 is a mitochondrial adaptor that facilitates retinoic acid-inducible gene-I-like receptor-mediated innate immune response. *Proc. Natl. Acad. Sci. U. S. A.* **111,** E245–54 (2014).

253. Zhong, B. *et al.* The adaptor protein MITA links virus-sensing receptors to IRF3 transcription factor activation. *Immunity* **29,** 538–50 (2008).

254. West, a P. *et al.* Mitochondrial DNA stress primes the antiviral innate immune response. *Nature* **520,** 553–557 (2015).

255. White, M. J. *et al.* Apoptotic Caspases Suppress mtDNA-Induced STING-Mediated Type I IFN Production. *Cell* **159,** 1549–1562 (2014).

256. Rongvaux, A. *et al.* Apoptotic Caspases Prevent the Induction of Type I Interferons by Mitochondrial DNA. *Cell* **159,** 1563–1577 (2014).

257. Colombatti, F., Gonzalez, D. H. & Welchen, E. Plant mitochondria under pathogen attack: A sigh of relief or a last breath? *Mitochondrion* **19 Pt B,** 238–44 (2014).

258. Jiang, J.-H., Tong, J. & Gabriel, K. Hijacking mitochondria: bacterial toxins that modulate mitochondrial function. *IUBMB Life* **64,** 397–401 (2012).

259. Stavru, F. & Cossart, P. Listeria infection modulates mitochondrial dynamics. *Commun. Integr. Biol.* **4,** 364–6 (2011).

260. Suzuki, M., Danilchanka, O. & Mekalanos, J. J. Vibrio cholerae T3SS Effector VopE Modulates Mitochondrial Dynamics and Innate Immune Signaling by Targeting Miro GTPases. *Cell Host Microbe* **16,** 581–91 (2014).

261. Pellegrino, M. W. *et al.* Mitochondrial UPR-regulated innate immunity provides resistance to pathogen infection. *Nature* **516,** 414–417 (2014).

262. Cordes, T., Michelucci, A. & Hiller, K. Itaconic Acid: The Surprising Role of an Industrial Compound as a Mammalian Antimicrobial Metabolite. *Annu. Rev. Nutr.* **35,** 1–23 (2015).

263. Calam, C. T., Oxford, A. E. & Raistrick, H. Studies in the biochemistry of micro-organisms: Itaconic acid, a metabolic product of a strain of Aspergillus terreus Thom. *Biochem. J.* **33,** 1488–95 (1939).

264. Strelko, C. L. *et al.* Itaconic Acid Is a Mammalian Metabolite Induced during Macrophage Activation. *J. Am. Chem. Soc.* **133,** 16386–16389 (2011).

265. Sugimoto, M. *et al.* Non-targeted metabolite profiling in activated macrophage secretion. *Metabolomics* **8,** 624–633 (2011).

266. Shin, J. *et al.* H NMR-based Metabolomic Profiling in Mice Infected with Mycobacterium tuberculosis. *J. Proteome Res.* **10,** 2238–2247 (2011).

267. Jha, A. K. *et al.* Network Integration of Parallel Metabolic and Transcriptional Data Reveals Metabolic Modules that Regulate Macrophage Polarization. *Immunity* **42,** 419–430 (2015).

268. Eylert, E. *et al.* Isotopologue profiling of Legionella pneumophila: role of serine and glucose as carbon substrates. *J. Biol. Chem.* **285,** 22232–43 (2010).

269. Wieland, H., Ullrich, S., Lang, F. & Neumeister, B. Intracellular multiplication of Legionella pneumophila depends on host cell amino acid transporter SLC1A5. *Mol. Microbiol.* **55,** 1528–1537 (2005).

270. Price, C. T. D., Al-Quadan, T., Santic, M., Rosenshine, I. & Abu Kwaik, Y. Host Proteasomal Degradation Generates Amino Acids Essential for Intracellular Bacterial Growth. *Science* **334,** 1553–1557 (2011).

271. Manske, C. & Hilbi, H. Metabolism of the vacuolar pathogen Legionella and implications for virulence. *Front. Cell. Infect. Microbiol.* **4,** 125 (2014).

272. Berg, I. a, Filatova, L. V & Ivanovsky, R. N. Inhibition of acetate and propionate assimilation by itaconate via propionyl-CoA carboxylase in isocitrate lyase-negative purple bacterium Rhodospirillum rubrum. *FEMS Microbiol. Lett.* **216,** 49–54 (2002).

273. Huang, C. S. *et al.* Crystal structure of the alpha(6)beta(6) holoenzyme of propionyl-coenzyme A carboxylase. *Nature* **466,** 1001–5 (2010).

274. Chien, M. *et al.* The genomic sequence of the accidental pathogen Legionella pneumophila. *Science* **305,** 1966–8 (2004).

275. Horswill, A. R., Dudding, A. R. & Escalante-Semerena, J. C. Studies of propionate toxicity in Salmonella enterica identify 2-methylcitrate as a potent inhibitor of cell growth. *J. Biol. Chem.* **276,** 19094–101 (2001).

276. Muñoz-Elías, E. J., Upton, A. M., Cherian, J. & McKinney, J. D. Role of the methylcitrate cycle in Mycobacterium tuberculosis metabolism, intracellular growth, and virulence. *Mol. Microbiol.* **60,** 1109–22 (2006).

277. Limenitakis, J. *et al.* The 2-methylcitrate cycle is implicated in the detoxification of propionate in Toxoplasma gondii. *Mol. Microbiol.* **87,** 894–908 (2013).

278. Stone, B. J., Brier, A. & Kwaik, Y. A. The Legionella pneumophila prp locus; required during infection of macrophages and amoebae. *Microb. Pathog.* **27,** 369–376 (1999).

279. Nandakumar, M., Nathan, C. & Rhee, K. Y. Isocitrate lyase mediates broad antibiotic tolerance in Mycobacterium tuberculosis. *Nat. Commun.* **5,** 4306 (2014).

280. Sadosky, A. B., Wiater, L. A. & Shuman, H. A. Identification of Legionella pneumophila genes required for growth within and killing of human macrophages. *Infect. Immun.* **61,** 5361–73 (1993).

281. Mampel, J. *et al.* Planktonic replication is essential for biofilm formation by Legionella pneumophila in a complex medium under static and dynamic flow conditions. *Appl. Environ. Microbiol.* **72,** 2885–95 (2006).

282. Feeley, J. C. *et al.* Charcoal-yeast extract agar: primary isolation medium for Legionella pneumophila. *J. Clin. Microbiol.* **10,** 437–41 (1979).

283. Chen, D.-Q., Huang, S.-S. & Lu, Y.-J. Efficient transformation of Legionella pneumophila by high-voltage electroporation. *Microbiol. Res.* **161,** 246–51 (2006).

284. Müller, U. *et al.* Functional role of type I and type II interferons in antiviral defense. *Science* **264,** 1918–21 (1994).

285. Huang, S. *et al.* Immune response in mice that lack the interferon-gamma receptor. *Science* **259,** 1742–5 (1993).

286. Jung, S. *et al.* In vivo depletion of CD11c+ dendritic cells abrogates priming of CD8+ T cells by exogenous cell-associated antigens. *Immunity* **17,** 211–20 (2002).

287. Churchill, G. A. Fundamentals of experimental design for cDNA microarrays. *Nat. Genet.* **32,** 490–5 (2002).

288. Davey, G. M. *et al.* Priming of CD8 T cell immunity to herpes simplex virus type 1 requires cognate TLR3 expression in vivo. *J. Immunol.* **184,** 2243–6 (2010).

289. Marim, F. M., Silveira, T. N., Lima, D. S. & Zamboni, D. S. A method for generation of bone marrow-derived macrophages from cryopreserved mouse bone marrow cells. *PLoS One* **5,** e15263 (2010).

290. Ritorto, M. S., Cook, K., Tyagi, K., Pedrioli, P. G. A. & Trost, M. Hydrophilic strong anion exchange (hSAX) chromatography for highly orthogonal peptide separation of complex proteomes. *J. Proteome Res.* **12,** 2449–57 (2013).

291. Cox, J. & Mann, M. MaxQuant enables high peptide identification rates, individualized p.p.b.-range mass accuracies and proteome-wide protein quantification. *Nat. Biotechnol.* **26,** 1367–72 (2008).

292. Cox, J. *et al.* MaxLFQ allows accurate proteome-wide label-free quantification by delayed normalization and maximal peptide ratio extraction. *Mol. Cell. Proteomics* **13,** 2513–26 (2014).

293. Reimand, J., Kull, M., Peterson, H., Hansen, J. & Vilo, J. g:Profiler--a web-based toolset for functional profiling of gene lists from large-scale experiments. *Nucleic Acids Res.* **35,** W193–200 (2007).

294. Reimand, J., Arak, T. & Vilo, J. g:Profiler--a web server for functional interpretation of gene lists (2011 update). *Nucleic Acids Res.* **39,** W307–15 (2011).

295. Maere, S., Heymans, K. & Kuiper, M. BiNGO: a Cytoscape plugin to assess overrepresentation of gene ontology categories in biological networks. *Bioinformatics* **21,** 3448–9 (2005).

296. Shannon, P. *et al.* Cytoscape: a software environment for integrated models of biomolecular interaction networks. *Genome Res.* **13,** 2498–504 (2003).

297. Livak, K. J. & Schmittgen, T. D. Analysis of Relative Gene Expression Data Using Real-Time Quantitative PCR and the 2−ΔΔCT Method. *Methods* **25,** 402–8 (2001).

298. Pietzke, M., Zasada, C., Mudrich, S. & Kempa, S. Decoding the dynamics of cellular metabolism and the action of 3-bromopyruvate and 2-deoxyglucose using pulsed stable isotope-resolved metabolomics. *Cancer Metab.* **2,** 9 (2014).

299. Kempa, S. *et al.* An automated GCxGC-TOF-MS protocol for batch-wise extraction and alignment of mass isotopomer matrixes from differential 13C-labelling experiments: a case study for photoautotrophic-mixotrophic grown Chlamydomonas reinhardtii cells. *J. Basic Microbiol.* **49,** 82–91 (2009).

PUBLICATIONS

Naujoks J., Tabeling C., Dill B. D., Hoffmann C., Brown A. S., Kunze M., Kempa S., Peter A., Mollenkopf H.-J., Dorhoi A., Kershaw O., Gruber A. D., Sander L. E., Witzenrath M., Herold S., Hocke A. C., van Driel I., Suttorp N., Bedoui S., Hilbi H., Trost M., Opitz B. Interferons modify bacterial vacuoles to restrict intracellular infection via IRG1. *Under review.*

Peer-reviewed articles

Mueller-Redetzky H. C., Felten M., Hellwig K., Wienhold S. M., **Naujoks J.**, Opitz B., Kershaw O., Gruber A. D., Suttorp N., Witzenrath M. Increasing the inspiratory time and I:E ratio during mechanical ventilation aggravates ventilator-induced lung injury in mice. *Crit. Care* **19,** 23 (2015).

Noe E., Tabeling C., Doehn J.-M., **Naujoks J.**, Opitz B., Hippenstiel S., Witzenrath M., Klopfleisch R. Juvenile megaesophagus in PKCα-deficient mice is associated with an increase in the segment of the distal esophagus lined by smooth muscle cells. *Ann. Anat.* **196,** 365–71 (2014).

Voges M., Bachmann V.**, Naujoks J.**, Kopp K., Hauck C. R.: Extracellular IgC2 constant domains of CEACAMs mediate PI3K sensitivity during uptake of pathogens. *PLoS One* **7,** e39908 (2012).

Lippmann J., Mueller H. C., **Naujoks J.**, Tabeling C., Shin S., Witzenrath M., Hellwig K., Kirschning C. J., Taylor G. A., Barchet W., Bauer S., Suttorp N., Roy C. R., Opitz B. Dissection of a type I interferon pathway in controlling bacterial intracellular infection in mice. *Cell. Microbiol.* **13**, 1668–1682 (2011).

Book chapters

Naujoks J., Opitz B. Innate immunity to Legionella pneumophila infection: focus on type I IFNs. In Parker D (Ed.), Bacterial Activation of Type I Interferons. Springer, 33-42 (2014).

Naujoks J., Opitz B. Bacterial Infections and the DNA Sensing Pathway. In Ishii K, Tang CK (Eds.), Biological DNA Sensor: The Impact of Nucleic Acids on Diseases and Vaccinology. Academic Press, 153-169 (2013).

Oral presentations

03/2015	**19th Symposium "Infection and Immune Defense" of the Study Group "Infection Immunology" of the German Society for Immunology (Burg Rothenfels, Germany)** Type I and II IFNs substantially modify the proteome of bacterial vacuoles and restrict infection through vacuolar IRG1 **(1st prize for best talk)**
10/2014	**Annual Meeting of the German Society for Hygiene and Microbiology (Dresden, Germany)** Comprehensive transcriptome and quantitative proteome analyses of a macrophage-intrinsic type I and II IFN-dependent defense pathway that restricts an intracellular bacterium in the lung

03/2013 **17th Symposium "Infection and Immune Defense" of the Study Group "Infection Immunology" of the German Society for Immunology (Burg Rothenfels, Germany)**
Decoding the interplay of type I and II interferons in innate immune defense against *Legionella pneumophila* **(sponsorship award for best talk)**

03/2011 **15th Symposium "Infection and Immune Defense" of the Study Group "Infection Immunology" of the German Society for Immunology (Burg Rothenfels, Germany)**
Dissection of a type I interferon pathway in controlling bacterial intracellular infection in mice

11/2010 **Autumn Meeting of the Section "Cell Biology" of the German Respiratory Society (Berlin, Germany)**
Dissection of a type I interferon pathway in controlling bacterial intracellular infection in mice

Poster presentations

09/2014 **44th Annual Meeting of the German Society for Immunology (Bonn, Germany)**
Comprehensive transcriptome and quantitative proteome analyses of a macrophage-intrinsic type I and II IFN-dependent defense pathway that restricts an intracellular bacterium in the lung **(1st prize for best poster)**

05/2013 **Keystone Symposium „The Innate Immune Response in the Pathogenesis of Infectious Disease" (Ouro Preto, Brazil)**
Decoding the interplay of type I and II interferons in innate immune defense against *Legionella pneumophila* **(Participation supported by GlaxoSmithKline Travel Grant)**

10/2012 **Annual Meeting of the German Society for Hygiene and Microbiology (Hamburg, Germany)**
Decoding the interplay of type I and II interferons in innate immune defense against *Legionella pneumophila*

09/2012 **International Conference of the SFB-TR84 and Leopoldina „Innate immunity of the lung – Improving pneumonia outcome" (Berlin, Germany)**
Decoding the role of type I and II interferons in *Legionella pneumophila* infection

05/2011 **Toll2011 Meeting - Decoding Innate Immunity (Riva del Garda, Italy)**
Dissection of a type I interferon pathway in controlling *Legionella pneumophila* lung infection